Smarter Charging

Modeling optimal EV charging in solar parking lots for reducing peak demand, considering uncertainty in solar power forecasting and EV energy demand

Y. D. Snow

Smarter Charging

Modeling optimal EV charging in solar parking lots for reducing peak demand, considering uncertainty in solar power forecasting and EV energy demand
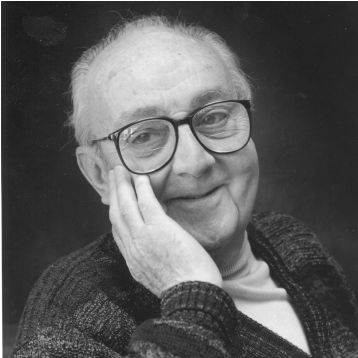
by

Y. D. Snow

to obtain the degree of Master of Science
at the Delft University of Technology,
to be defended publicly on Thursday, August 29th, 2019.

TUDelft

Preface

"All models are wrong ...

... but some are useful."

George Box

Smart charging offers the potential for electric vehicles to use renewable energy more efficiently, lowering costs and improving the stability of the electricity grid. Many computer models have been developed to simulate the behavior of smart charging. Yet these models often assume that future information is known perfectly, including when vehicles will begin charging and how much solar energy will be available at that time. In reality, this information is subject to uncertainty, meaning the performance of smart charging may be worse than predicted by these models. This report details the development of an improved model which considers future uncertainty in smart charging behavior. It is determined that uncertainty does decrease the effectiveness of smart charging, but with strategies that are able to robustly consider this uncertainty smart charging can still offer tremendous benefits over traditional uncoordinated charging.

This thesis has been the culmination of a great deal of work, and it would have been utterly impossible without the help of many people. To Ad van Wijk, thank you for providing me with guidance and supervision throughout this project. I would also like to thank René van Swaaij and Zofia Lukszo for taking time out of their busy schedules to sit with Ad on my thesis defense committee.

To Rishabh, thank you for your constant support, for your helpful suggestions, and for your invaluable input through several rounds of drafts and rewrites. To Samira, thank you for your unending patience and constructive criticism in working with me to formulate the optimization problem which forms the backbone of this report. To Tomás, thank you for meeting with me to discuss my research. And to Hayes and Christopher from Massport, thank you for providing me with the airport parking data which serves as a critical input to my model. I am also compelled to thank my family for their love and cynicism throughout this process. And finally, thank you to Katharina for the endless support, without which I am sure I would never have been able to finish this thesis.

Over the past year, I have spent an enormous amount of time on this project, with the goal of developing a detailed and versatile model. I have spent many long days struggling with MATLAB or optimization or a seemingly never-ending ocean of previous research. On those days, the wise words of George Box have brought me a great deal of reassurance.

I won't pretend that my model is not wrong. It is. All models, of course, are wrong. But I hope that this model is also useful. I hope that in some way I have contributed to the ever-growing body of scientific knowledge surrounding electric vehicles and smart energy systems. I hope that future researchers will be able to use the model I have developed and the results I have discovered, bringing us just a bit closer to a more sustainable future. And even if this thesis is never read again, and my conclusions are never considered by any future author, I am thankful for the opportunity I have had to write this thesis, and I am thankful for everything that I have learned along the way. In that way this model has been useful, at least to me.

Y. D. Snow
Delft, August 2019

Contents

List of Figures

List of Tables

List of Acronyms

ABA	Activity Based Approach	MILP	Mixed Integer Linear Programming
ABM	Activity Based Model	MLD	Mixed Logical Dynamical
AC	Alternating Current	MPC	Model Predictive Control
AOI	Angle of Incidence	NMOT	Nominal Mean Operating Temperature
BESS	Battery Energy Storage System		
BEV	Battery Electric Vehicle	PHEV	Plug-in Hybrid Electric Vehicle
BIPV	Building Integrated Photovoltaic	POA	Plane of Array
CI	Carbon Intensity	PSO	Particle Swarm Optimization
CO_2	Carbon Dioxide	PV	Photovoltaic
DC	Direct Current	RMSE	Root Mean Squared Error
DHI	Diffuse Horizontal Irradiance	RT	Real Time
DNI	Direct Normal Irradiance	SDE	*Stimulering Duurzame Energieproductie*, stimulation of sustainable energy production
DSO	Distribution System Operator		
DUOATS	Direct Use of Observed Activity Travel Schedules		
		SOC	State of Charge
ESS	Energy Storage System	STC	Standard Test Conidtions
EV	Electric Vehicle	STSM	Summary Travel Statistics Model
EVSE	Electric Vehicle Supply Equipment	THD	Total Harmonic Distortion
GHI	Global Horizontal Irradiance	TMY	Typical Meteorological Year
LCOE	Levelized Cost of Energy	TSO	Transmission System Operator
LED	Light Emitting Diode	UBIS	User Battery Interaction Style
LP	Linear Programming	V2G	Vehicle to Grid
MBE	Mean Bias Error	VOAMM	Vehicle Ownership and Annual Mileage Model
MCM	Markov Chain Model		

<div align="right">

1

</div>

Introduction

This thesis will examine solar parking lots, which can be used to charge electric vehicles using renewable energy. Through smart charging, vehicle electricity demand can be coordinated in order to reduce the peak demand for electricity. Solar parking lots and smart charging have already been extensively researched, but these systems involve a great deal of uncertainty. The exact values for future solar power generation are always uncertain, and the energy demand from electric vehicles which have not yet begun charging are often unknown. In this thesis, smart charging strategies will be developed which allow for peak demand to be reduced, despite these uncertainties. The effectiveness of these strategies is then tested through the use of simulations of a solar parking lot. Previous research on the subject of smart charging for peak reduction has typically assumed that solar power production and electric vehicle charging demand are known perfectly in advance, making this thesis the first work to research smart charging for reducing the peak electricity demand in solar parking lots when considering this forecasting uncertainty.

This chapter provides an overview of the entire thesis. In Section 1.1, the motivation behind this research is described. Then, Section 1.2 will describe the goals of this research, and Section 1.3 will define the central research question based on these goals. Finally, Section 1.4 will provide an outline of the entire report.

1.1. Motivation for the Research

Countless research has already demonstrated the need for the world to transition away from fossil fuels towards renewable sources of energy. During this energy transition, solar panels and electric vehicles will play increasingly critical roles. Solar panels allow for the generation of clean, sustainable electricity. Electric vehicles, meanwhile, allow for us to work towards decarbonizing the transportation sector, reducing our dependence on fossil fuels. Due to strong government incentives and rapidly falling prices, both of these technologies are growing exponentially. Although solar power and electric vehicles are currently small players on a global scale, both will inevitably play a major role in our future energy systems.

Unsurprisingly, these two key technologies are often combined. By placing solar canopies over parking spaces, solar energy can be generated and used to charge electric vehicles. These solar parking lots allow for land which would otherwise be only used for parking to generate clean sustainable energy. At the same time, these systems allow for electric vehicles to be charged using locally generated solar power. Solar parking lots can offer a number of benefits to all the parties involved. The parking lot owner generates low-cost renewable energy which can be used to charge the vehicles. The vehicle owners gain the opportunity to drive using green energy while having their parked cars protected from the elements during charging. And society benefits from decreased emissions and increased renewable energy.

Despite their advantages, there are downsides to these technologies. Solar power can be unreliable and unpredictable, leading to increasing variability in our electricity supply. If the sun stops shining, fossil fuel plants may need to quickly ramp up their generation, which can be expensive and polluting. But there can also be problems if there is too much sun. High solar power production can lead to overgeneration, which is also problematic for the electricity grid. At the same time, electric vehicles require an enormous amount of electricity. If a large number of vehicles plug in at the same time, the combined load can result in a large peak in electricity demand. This peak demand can again require fossil fuel powered peaking plants to ramp up production. If the peak demand is too large, the stability of the entire electricity grid can be threatened. On a

local level, these peaks in demand can also create issues for distribution networks, leading to under-voltages and harmonics in the power lines along with damage to transformers and other equipment.

Both of these problems have a single solution: smart charging. At times when large amounts of excess solar energy is available, electric vehicles can be charged. When the sun isn't shining, charging can be delayed to avoid large spikes in demand. By intelligently scheduling vehicle charging in this way, the variability in solar energy and the power demand from electric vehicles can both be reduced. Because of these advantages, smart charging to reduce the peak electricity demand has been the subject of a large amount of research. Computer models have been developed with the goal of evaluating the effectiveness of different smart charging strategies under various conditions. Pilot projects have begun to examine the feasibility of smart charging in real world conditions. Although the initial results have been quite promising, there are problems with some of the methods used. Many computer models of smart charging systems make unrealistic or oversimplified assumptions about the electric vehicles which will be charging. If these models are not accurate, then the conclusions which are drawn and the recommendations which are made may be flawed.

A further problem, is the presence of uncertainty in smart charging systems. During smart charging, it is important to know how much solar power will be available. In addition, future vehicle charging demands must be anticipated, including when the cars will arrive, how much energy they will need, and when they plan on departing. Yet these quantities can never be predicted with absolute certainty. Solar generation forecasts are frequently mistaken, and vehicle arrivals are typically unscheduled. Because of this uncertainty, smart charging strategies may perform worse than expected. Yet previous literature on smart charging often assumes that this information is known in advance with total accuracy. When designing an optimal strategy, it is critical that uncertainty of both solar generation and vehicle behavior is taken into account.

1.2. Research Goals

These problems can fundamentally be broken down into two major questions. First, how can computer models for solar parking lots with smart charging realistically model the system they are designed to represent? And second, how does forecasting uncertainty affect the performance of this system? These two questions form the foundation for this this research, defining the two research goals presented here.

1.2.1. Develop a Useful Model for Solar Parking Lots

The first goal of this thesis is to develop a useful model for simulating smart charging in a solar parking lot. This model should be sufficiently realistic and detailed that the conclusions which are drawn can be applied to real-world situations. In developing this model, it is therefore important that the simulated system behavior is as close as possible to the true system behavior. This thesis will consider two locations where smart charging may be used: at the parking lot for an office or business park, and at the long-term parking facility for an airport. The behavior of the solar parking lot at both locations will be modeled using real-world data and and modeling practices from the literature, justifying any assumptions that needed to be made. The details of this model are described in Chapter 3. This model then serves as a tool to answer the second main question of this thesis.

1.2.2. Investigate the Effect of Uncertainty on Smart Charging

The second goal for this thesis is to consider the effect of uncertainty when smart charging is implemented in a solar parking lot. This requires a realistic understanding of the uncertainties which are inherent to this system. Forecasting error for solar power generation will be simulated. Electric vehicle parking behavior, such as the arrival and departure times, as well as the starting state of charge and the battery capacity, are assumed to be unknown before arrival. Smart charging strategies are then developed which seek to minimize the peak electricity demand despite these uncertainties. Different strategies will be considered for both the solar and the vehicle uncertainties, as detailed in Chapter 4. The performance of these strategies will then be analyzed, and the effectiveness of smart charging in an uncertain system will be evaluated.

1.3. Research Question

These two goals can be combined into the following research question:

How can smart electric vehicle charging be used to minimize the peak electricity demand at a workplace or airport solar parking lot, considering uncertainty in solar power forecasting and electric vehicle charging demand?

1.4. Thesis Outline

After the introduction to this thesis, Chapter 2 will provide some background on the previous work which has been carried out. A review will be made of the literature regarding solar parking lots, electric vehicle charging strategies, and smart charging, including previous smart charging projects and ways in which smart charging strategies can consider uncertainty.

Then, Chapter 3 will discuss the details of the computer model which is used to simulate the solar parking lot. The model is built in MATLAB, and realistically simulates the solar modules, electric vehicles, vehicle charging equipment, fixed storage battery, and lighting. The model uses real-world data with standard practices from literature to combine the individual components into a single model.

Next, Chapter 4 will describe the control strategies which are employed in this report. These strategies are responsible for the charging and discharging of vehicle batteries, the management of energy in the fixed storage battery, and the power which is sent to the electricity grid. As a base scenario, uncoordinated charging is described. Mixed Integer Linear Programming (MILP) is then used to implement smart charging, with the intention of minimizing peak demand. The optimization problem is first defined assuming that perfect information is available, then expanded to take into account uncertainty with solar generation and vehicle behavior.

Chapter 5 will then present and analyze the results of the computer simulations. This includes a discussion of the preferred system topology, such as the fixed battery storage capacity and the choice between AC and DC vehicle charging. The chapter also reports on the impact of uncertainty on the peak electricity demand for a solar parking lot engaged in smart charging. The effectiveness of different charging strategies is described.

Finally, Chapter 6 will summarize the conclusions of this report, including some key observations of the simulation results. In addition, possible shortcomings of this thesis will be addressed, and recommendations will be given for future work which can build on the findings of this report.

<div style="text-align: right">

2

</div>

<div style="text-align: right">

Background

</div>

Solar parking lots, peak demand reduction, and smart charging for electric vehicles are already the subject of extensive research. This chapter will provide background information on the work which has been carried out. Section 2.1 discusses the literature on solar parking lots including solar power, electric vehicles, vehicle charging, and the combination of these elements through systems like the proposed PowerParking project. Section 2.2 then describes the work which has been done with smart charging, including its theoretical advantages, previous smart charging projects, computer models of smart charging, and smart charging control strategies, including those which deal with forecasting uncertainty.

2.1. Solar Parking Lots

Solar parking lots are systems where surface parking lots are covered by canopies containing solar panels as part of the roof. The power which is generated can then be used to charge electric vehicles. Each component of the solar parking lot will be discussed separately in this section.

2.1.1. Solar Power

Solar power is sustainable, abundant, and will undeniably play a large role in the energy transition. In 2018, installed peak solar capacity in the Netherlands increased by 46%, from 2.9 GW to 4.2 GW [1]. Despite this rapid growth, solar provides only a small fraction of the total Dutch electricity production, accounting for just 1.8% of total generation in 2018. In order to meet the goals for greenhouse gas emissions, this number will need to grow substantially. As part of the Dutch Energy Agreement in 2013, a sharp increase was proposed for all types of renewable energy, including solar and wind, with the share of renewables planned to rise from 4.5% in 2013 to 15.9% in 2023 [2]. The rise of solar energy in the Netherlands mirrors a global trend, with worldwide installed solar capacity increasing by 25% in 2018 over 2017 [3]. In the Netherlands and around the globe, this growth in solar power is driven by falling prices.

In some locations, solar power is becoming increasingly cost-competitive with fossil fuels, as seen in Figure 2.1 [1]. For large scale solar photovoltaic (PV) projects, the global levelized cost of energy (LCOE) was $43 per MWh in 2018. This is lower than conventional energy such as coal or natural gas, and represents a price drop of 88% in just the past ten years. Different methodologies will yield different average costs for solar power, and prices are dependent on a variety of factors including the size and location of the solar power plant. More conservative estimates suggest that the global unsubsidized LCOE for utility-scale solar PV projects was $85 per MWh, although this price still represents a 77% decrease since 2010 [3]. Although prices have fallen substantially, solar power in the Netherlands remains relatively expensive.

Renewable energy in the Netherlands is subsidized through the SDE+ scheme (*Stimulering Duurzame Energieproduction*, stimulation of sustainable energy production). In 2017, the budget for SDE+ subsidies was €12 billion, of which 43% went to solar power projects with a peak power greater than 15 kW [1]. The SDE+ contribution compensates generators of renewable electricity for the difference between the cost price and the market value of the electricity they produce [4]. This means that the SDE+ contribution combined with the market price for electricity should equal the cost of the renewable energy, which is known in the SDE+ system as the "base amount." In spring of 2019, the base amount for solar systems between 15 kW and 1 MW ranged from €0.090–0.101 per kWh. In order for these systems to be profitable, their LCOE cannot be

higher than this base amount, which is equivalent to €90-101 per MWh. This cost is higher than the global average of $43 per MWh, in part due to the poor solar conditions in the Netherlands, but there is reason to believe that the cost could go down. Northern Germany has similar solar conditions to the Netherlands, with a total annual Global Horizontal Irradiance (GHI) of 950 kWh per m^2. Due to a more mature solar market, however, the LCOE of utility-scale solar installations in northern Germany was only €50.8–67.7 per MWh in 2018, with costs steadily decreasing over time [5]. As the Dutch solar industry matures, prices may decrease to be more in line with those in Germany.

Selected Historical Mean Unsubsidized LCoE Values ($/MWh)
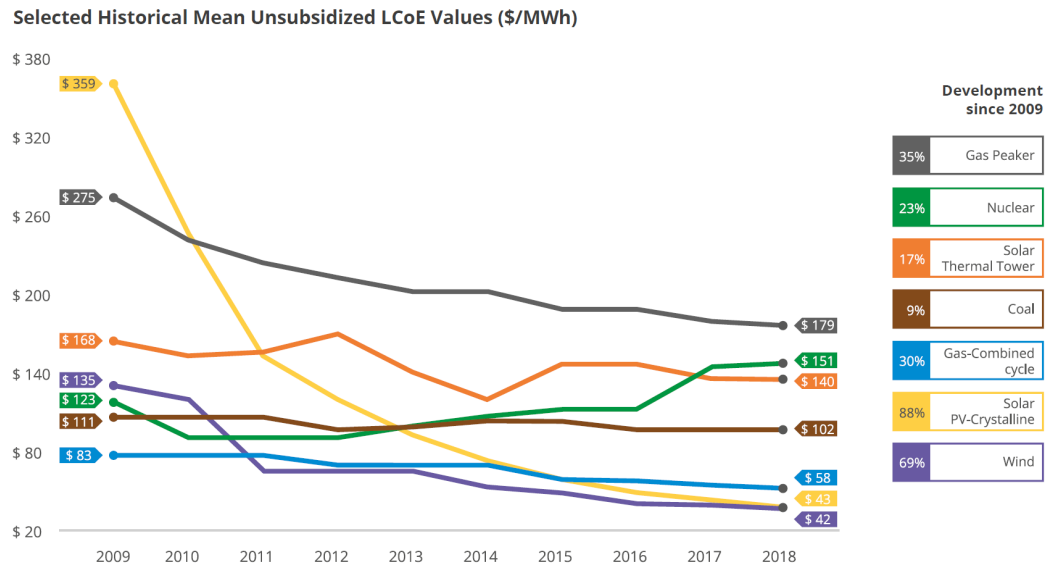
Figure 2.1: Global Levelized Cost of Electricity (LCOE) for various electricity sources [1]

The future of solar energy in the Netherlands is still uncertain. In 2019, the SDE+ budget will be reduced from €12 billion to €10 billion. In 2020 an even bigger change will occur, with the SDE+ system being replaced by the SDE++ system. The new system will shift from subsidizing renewable electricity production to greenhouse gas emission reduction [6]. This means that in addition to providing subsidies for sustainable energy, the scheme will also incentivize technologies such as renewable heat production, hydrogen for industrial processes, and carbon capture and storage (CCS). The precise details of this scheme have yet to be determined, but there are some concerns in the Dutch solar industry that these changes may weaken the competitiveness of solar power projects [1].

Although solar power offers a number of benefits, it also presents a number of challenges. PV power is variable and uncertain, and can lead to overgeneration and congestion. These issues will require the power system to adapt as solar power becomes more common in the future [7]. In the Netherlands, the variable and uncertain generation from sources like solar and wind power will require the electricity grid in the future to be much more flexible. Peaking power plants will be required to rapidly ramp up and down their production in to ensure that the electricity supply and demand remain balanced [7]. This flexible capacity is especially important at times of peak demand, when renewable sources may not be available, as shown by the load duration curves in Figure 2.2.

Load duration curves demonstrate the number of hours that the total electricity demand in the Netherlands is above a certain level. The residual load subtracts wind and solar power generation from the total load, representing the demand that must be met by other sources. In 2015, only 8% of the total load was provided by wind and solar power, resulting in a relatively small difference between the total and residual load duration curves [7]. In 2050, it is assumed that 80% of all electricity will come from wind and solar power. This is in line with the EU target of reducing cutting greenhouse gas emissions 80% below 1990 levels by 2050 [2]. As shown in Figure 2.2, the peak residual load is barely below the peak total load, indicating at times of high demand renewable energy may not provide very much power. By 2050, the share of the total load covered by renewable energy will be less than 20% for 2600 hours per year. This unreliability is one issue in power systems that rely heavily on variable renewable energy.

In addition to not always providing enough power, variable renewable sources can also provide too much,

resulting in generation which is higher than the total demand and a residual load that is below zero. This problem is known as overgeneration. As seen in Figure 2.2, by 2050 overgeneration will occur for over 3200 hours per year, resulting in 16%–17% of total renewable production which must be exported or curtailed. But even when there is sufficient demand for renewable energy, it may still be wasted due to congestion.

(a) Load duration curve, 2015

(b) Load duration curve, 2050
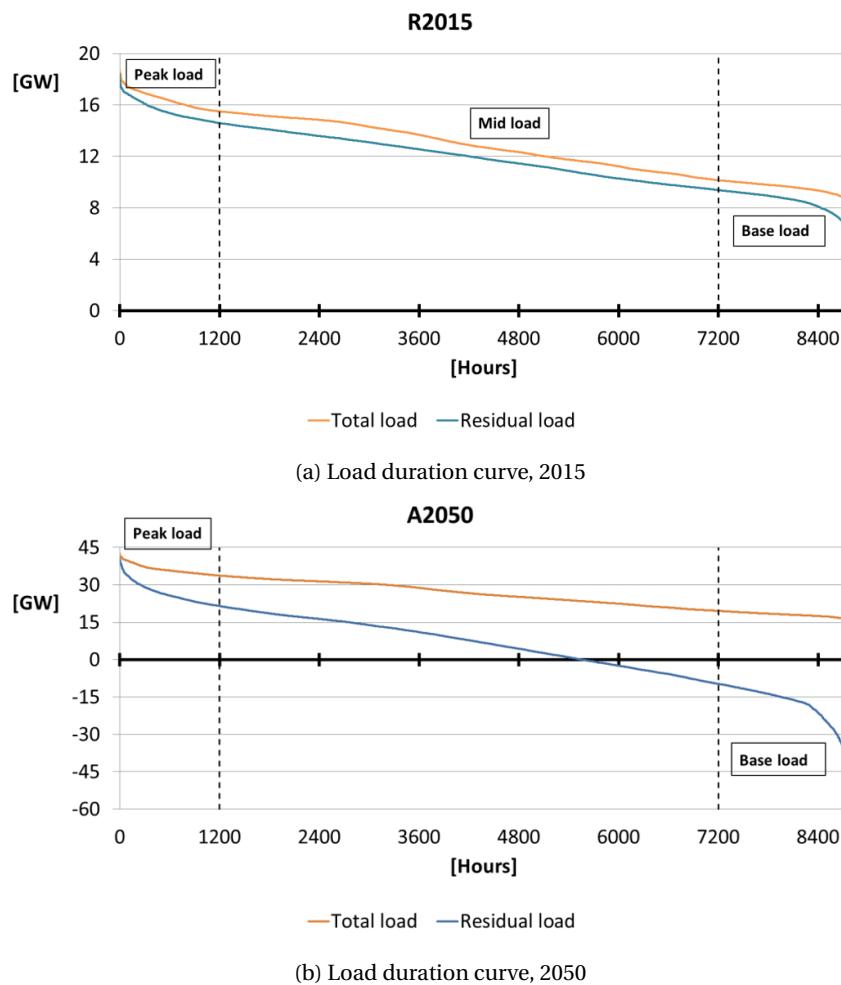
Figure 2.2: Duration curves of total and residual load in the Netherlands [7]

Congestion occurs when components like transformers or cables are overloaded and unable to transport electricity to where it is needed. This can be a serious problem for solar power, which is often connected to the local distribution system, unlike conventional power plants which are typically connected directly to the high-voltage transmission system. Liander, one of the Distribution System Operators (DSOs) in the Netherlands, estimates that by 2030 8% of their distribution transformers and 9% of their substation transformers could become overloaded [7]. Connecting all the new solar power systems while preventing overloads and avoiding congestion will require significant investments from grid operators. Enabling local consumption of renewable energy and encouraging consumers to use the solar power they generate rather than feeding it into the grid can help prevent this congestion. But solar power generation is only part of the problem. Congestion is also exacerbated by the increased electrification of household loads, through technologies like heat pumps and electric vehicles.

2.1.2. Electric Vehicles

The adoption of electric vehicles (EVs) will be crucial in the transition away from fossil fuels. Globally, road transportation accounts for 17% of all emissions of carbon dioxide, or CO_2 [8]. Critics often complain that EVs are still charged using fossil fuels, meaning that they are still indirectly responsible for CO_2 emissions. EVs, however, are much more efficient than conventional cars, emitting 50% less CO_2 than gasoline cars and

40% less than diesel cars on a Well-to-Wheel basis [9]. Naturally, the emissions of EVs are strongly dependent on the carbon intensity of the electricity grid in the time and place where they are being charged. When assuming the average European carbon intensity of 521g CO_2 per kWh, carbon emissions over the lifetime of an EV will be 20–27% lower when compared to similar-sized conventional cars [10]. This benefit is because the European electricity grid has a carbon intensity below that of natural gas (595 g CO_2 per kWh). If EVs were charged only using electricity generated by coal power (1029 g CO_2 per kWh), they would have lifetime emissions which are slightly higher than conventional vehicles. Fortunately, as the electricity grid becomes more sustainable, emissions due to EV charging will go down. With the current European electricity mix, 55%–65% all EV emissions occur during charging. This means that if EVs were charged using exclusively green energy, their lifetime emissions could be 66%–70% lower than conventional vehicles. As electricity generation grows more sustainable, EVs become a greener choice.

Just like solar power, EVs are becoming increasingly affordable over time. Alternatively, EVs of the same price are consistently improving, as seen in Figure 2.3 [11]. For EVs in the Netherlands costing less than €40,000, the estimated range in 2013 was only 125 km. By 2020, the range is expected to be around 300 km [11]. As consumer options improve, the number of electric vehicles will continue to grow. In 2017, over one million new electric vehicles were sold worldwide, an increase of 54% compared to the previous year, with more than half of the growth taking place in China [9]. This exponential growth is likely to continue. By 2030, the number of EVs worldwide is anticipated to be around 130 million.
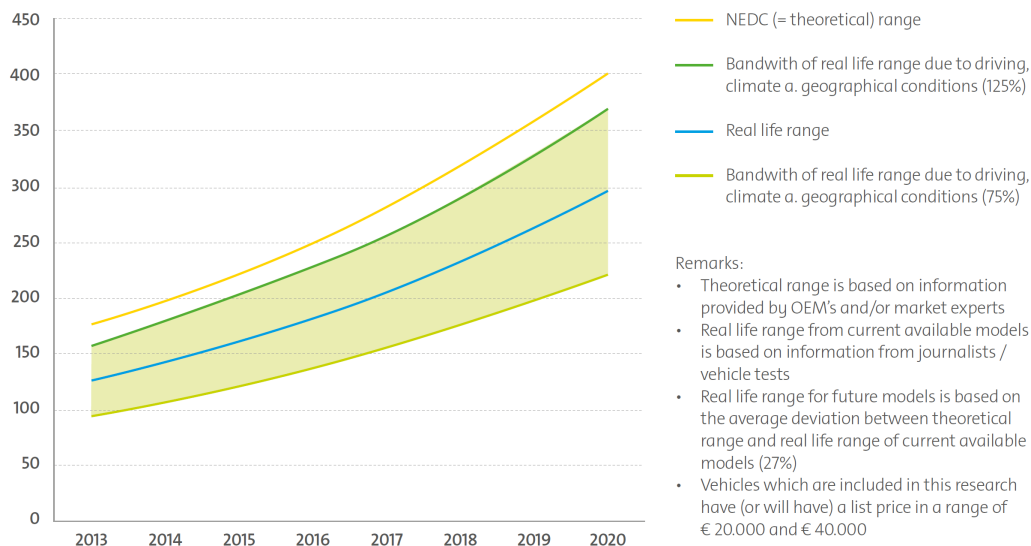
Figure 2.3: The increase in range (in km) for affordable EVs over time [11]

In the Netherlands, EVs are becoming increasingly popular, driven heavily by government policy. The Netherlands set the goal of reducing greenhouse gas emissions in the transport sector by 17% below 1990 levels by 2030, and 60% by 2050 [2]. Such a strong reduction is not possible with only improved efficiencies in gasoline powered vehicles, and can only be achieved with electric vehicles powered by batteries or fuel cells, which are charged using renewable energy [12]. The Dutch government is therefore working to incentivize the adoption of EVs. In 2015, the government worked with the Formule-E team to create a path towards a more electric future, publishing a report titled "*Maak Elektrisch Rijden Groot*" (Make Electric Driving Great) [11]. The report examined the current state of Dutch electric driving, and provided a number of recommendations to increase the market share of EVs.

The Dutch efforts appear to have been successful, as seen in Figure 2.4. As of the end of 2017, there were over 120,000 EVs on Dutch roads, accounting for 1.6% of the entire fleet. This figure puts the Netherlands behind only Norway among European countries [13]. The Dutch government has set aggressive goals for electrification. The Coalition Agreement of October 10, 2017 set the target of having 100% of all new cars be emission free by 2030, with the ambition to ultimately switch the fleet over to entirely zero emission vehicles [14]. If all new sales are zero emission by 2035, the entire Dutch fleet should be able to drive emission free by 2050 [2, 11]. The Netherlands is also seeking complete electrification of public transportation, with the goal of

100% of all public bus sales to be electric by 2025, and 100% of public bus stock to be electric by 2030 [9]. This transition has already begun. In April 2018, 100 battery powered electric buses were delivered to Schiphol for use in and around the airport, giving it the largest electric bus fleet in Europe [15]. The plan is to completely electrify the fleet with 258 buses by 2021.
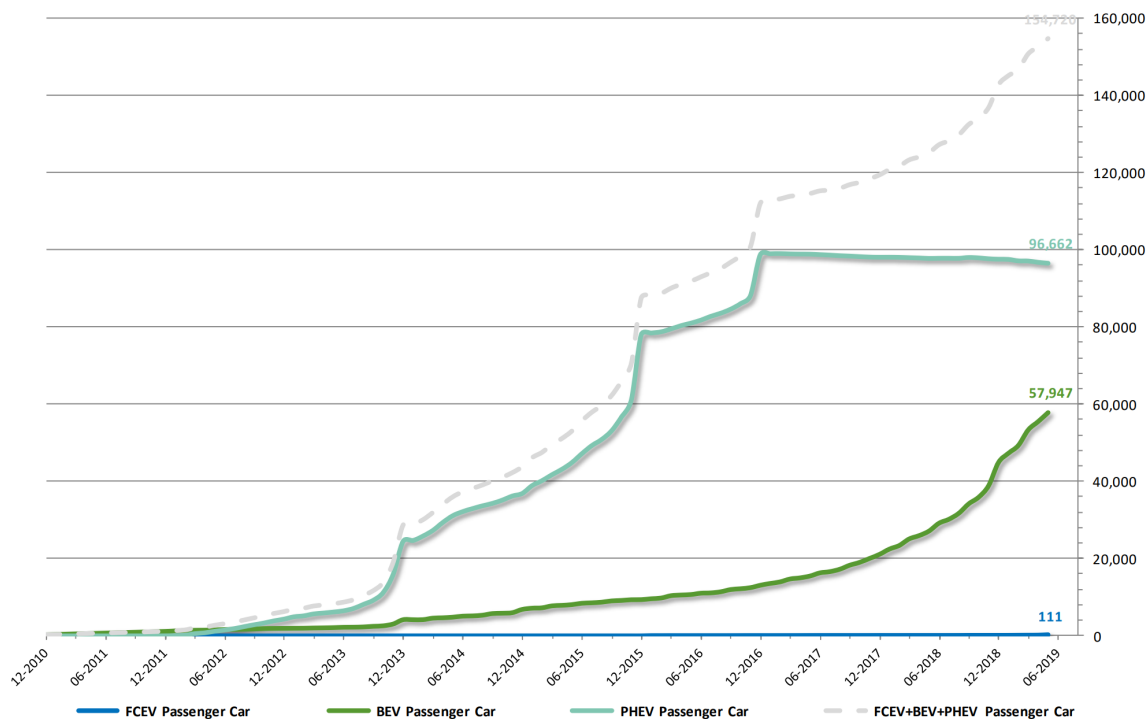
Figure 2.4: Total EV registrations in the Netherlands over time [16]

The state of electric vehicle adoption in the Netherlands is changing extremely rapidly. The removal of a tax incentive in 2017 caused sales of plug-in hybrid electric vehicles (PHEVs) to stop almost entirely, as can be observed in Figure 2.4 [16]. During 2017, the total EV sales were therefore substantially lower than they had been in previous years, with a market share of only 2.6% [9]. This was concerning, considering the Dutch target of having 10% of all newly registered vehicles be electric by just 2020 [13]. Fortunately, the status of EVs seems to be improving. Although PHEVs have remained unpopular, battery electric vehicle (BEV) sales are growing rapidly. Total registrations for BEVs increased from roughly 21,000 at the end of 2017 to nearly 58,000 vehicles by May 2019 [16]. The adoption rate has been accelerating in recent years. By 2018, the market share of EVs was up to 6.5%, and in the first five months of 2019 it reached 8.4%, suggesting that the Netherlands may well succeed in reaching their goal of a 10% market share in 2020. With each passing year electric vehicles are getting less expensive and more widespread.

2.1.3. Electric Vehicle Charging

As the share of EVs grows, so will the energy demand for charging these vehicles. This charging will be supported by an extensive network of electric vehicle chargers, or Electric Vehicle Supply Equipment (EVSE), a network which is already in development. Globally in 2017, there were already almost 3 million private chargers at homes and workplaces, with an additional 430,000 public chargers, of which roughly a quarter are fast charging [9]. This number has been increasing rapidly over recent years, in conjunction with the increased popularity of EVs. The increasing electricity demand due to EV charging can lead to issues like congestion, which will be discussed in Section 2.2.

The availability of good charging infrastructure is an important consideration in the decision to purchase an EV. This can create a chicken-and-egg problem, as buyers may be hesitant to purchase an electric vehicle if there is not sufficient charging infrastructure, but infrastructure is less likely to be built if there is no demand [9]. In order to get around this problem, the Netherlands has has invested heavily in public charging infrastructure. In Amsterdam, there are 5.5 charging points per 1,000 inhabitants—the highest density of any

city in Europe. This infrastructure is supported with grants, as there is currently no cost-effective business case for building charging infrastructure [17]. As of 2017, the Netherlands had the highest number of public EVSE per EV in the world, with roughly one public charging station for every four EVs in the country, as can be seen in Figure 2.5 [9].
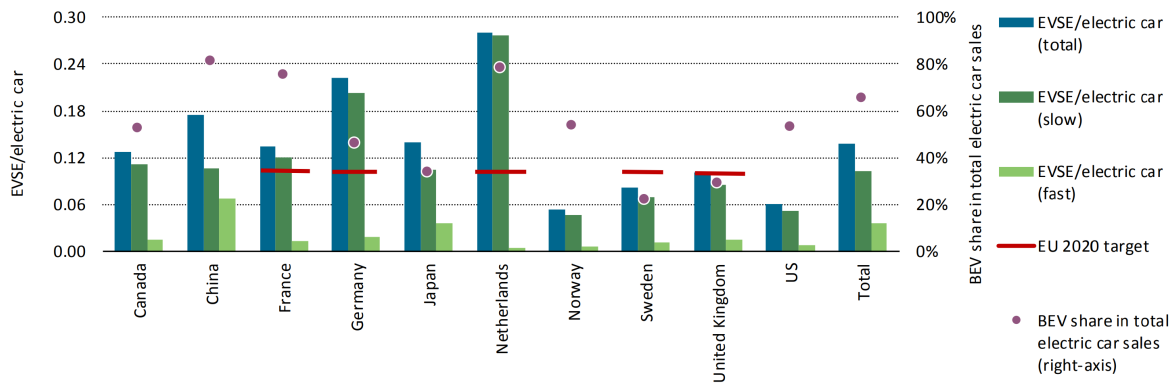
Figure 2.5: Ratio of public Electric Vehicle Supply Equipment (EVSE) to EVs [9]

Almost all publicly available chargers are slow chargers, especially in Europe, and slow charging is the most common means of charging individually owned EVs due to the lower cost and greater convenience when compared with fast charging. Slow charging can occur at public charging stations, at work, or most commonly at home. 90% of EV owners in Norway and Sweden charge their vehicle at home on a daily or weekly basis, while only 20%–40% charge at work [9]. This preference for home charging may be the reason for Norway's relatively limited public charging infrastructure, although it has the largest marker share of EVs in the world as seen in Figure 2.5. This suggests that public charging infrastructure, while important, may not be necessary in enabling the adoption of EVs.

Fast charging is more popular in China and Japan, although it still makes up the minority of all charging events [9]. Fast charging can supply DC power at a high voltage in order to rapidly recharge a vehicle battery. This can help enable long distance travel, reducing range anxiety which is one of the greatest concerns for potential EV owners. Manufacturers are continuously seeking higher and higher charging rates for DC fast charging. Tesla recently announced that the maximum power for their Supercharging network will increase from 120 kW to 250 kW [18]. In Germany, BMW and Porsche are testing ultra-fast charging up to 450 kW, enabling a vehicle to charge from 10% to 80% SOC in just 15 minutes [19]. Many electric vehicles, however, are limited to a lower charge rate. The Nissan Leaf, for example, has a maximum charging power of 50 kW [20]. It remains to be seen what role DC fast charging will play in the future of EV charging.

In the field of EV charging, increasing attention is being given to bidirectional charging. Bidirectional charging, or Vehicle to Grid (V2G), is a system where EVs are able to discharge their batteries, powering the electricity grid [21]. By sending power to the distribution network, V2G allows for EVs to provide ancillary services to electricity grid operators. This could provide additional income for the owners while stabilizing and allowing more flexibility in the grid. By allowing EVs to charge their batteries when renewable energy is more abundant, and return the energy to the grid when it is needed, V2G could make the electricity grid more sustainable [12]. Vehicles could also be used to benefit the grid with other ancillary services, for example by reducing harmonics in transmission lines or regulating the system frequency. As vehicles are only in use a small fraction of the time (4% in the USA), storage capacity in vehicles would likely be more than enough to serve as short term storage even in power systems with very high penetration of variable renewable sources of electricity [22]. Tapping into this unused potential could be more economical than paying for dedicated storage, since the batteries would not need to be manufactured and installed for this purpose specifically.

Although Vehicle-to-Grid is typically considered to be synonymous with bidirectional charging, it has sometimes been used to describe an aggregator who combines a number of EVs and controls their charging demand in response to the electricity market price [23]. This "Unidirectional V2G" allows the aggregator to sell the reduction in capacity to the system operator, allowing for them to provide auxiliary services like frequency regulation. "Unidirectional V2G" is something of a misnomer, as there is no energy being sent from the vehicle to the grid. These unidirectional charging strategies are also occasionally referred to as "V1G",

with uncoordinated charging then being referred to as "V0G" [24]. Although often used, these names are somewhat meaningless. In order to avoid confusion, V2G in this report will refer exclusively to charging strategies where energy is discharged from EV batteries, and unidirectional strategies will instead fall under the broader umbrella of smart charging. It is also worth noting that some studies specify how the power from the vehicles is used, with terms such as V2V (vehicle-to-vehicle), V2B (vehicle-to-battery), and V2X (vehicle-to-everything). For simplicity, all bidirectional charging in this report will be considered as V2G.

Despite the possible benefits, there are concerns regarding the potential use of V2G. One of the biggest concerns for EV drivers is that extensive charging and discharging can reduce the cycle life and storage capacity of the battery. This phenomenon is known as battery degradation. Battery degradation is most dependent on energy throughput and the depth of discharge for the battery. Some reports have found that with proper control strategies, the effect of V2G on battery performance can be negligible [25]. Other researchers, however, have found that V2G services can dramatically shorten the battery lifetime for both Battery Electric Vehicles (BEVs) and Plug-in Hybrid Electric Vehicles (PHEVs), accelerating the frequency of battery replacement. One study found that vehicles which provide bulk energy services, regularly discharging large amounts of energy to the grid, would require their batteries to be replaced annually [26]. If the vehicles provided only ancillary services, the frequency of battery replacement could be reduced to once every two or three years. The battery degradation could be minimized by using a lower energy throughput and limiting the allowed depth of discharge. Nonetheless, battery degradation can be a serious problem for vehicles if V2G becomes common. In addition to concerns about battery degradation, bidirectional charging will require significant quantities of energy to be injected into the distribution grid. Doing so will likely require increased communication between the EVs and the electricity grid operators, as well as changes to the system infrastructure [21]. Bidirectional charging is still the subject of academic research, and is generally considered only as part of demonstration projects.

Another barrier to V2G is the charging equipment which is required. V2G can be performed using AC chargers, but this requires additional hardware to be installed in the vehicle [27]. Many manufacturers believe that this hardware will reduce charging efficiency and increase costs. As a result, it is preferable to consider DC equipment for V2G. This may be problematic in Europe. Currently, all DC bidirectional charging is tested using CHAdeMO chargers, which are the industry standard for DC charging in Japan. In Europe, DC charging uses the CCS standard, which has been opposed to V2G in the past, and as of 2018 there were no planned V2G trials using CCS chargers. In order for V2G to be viable in Europe, V2G hardware must be developed and tested using the CCS standard.

Currently very few vehicles are capable of bidirectional charging, due to either software or hardware restrictions, although this is changing rapidly. The Nissan leaf is one of the only commercially available passenger BEVs which is compatible with V2G [27]. Other manufacturers, such as Honda [28], BMW [29], and Volkswagen [30] are looking into the potential of V2G in small-scale research projects. Although V2G has a greater potential with larger batteries, PHEVs are also considered for V2G. The Mitsubishi Outlander is the most popular PHEV in the Netherlands, and is being tested in multiple V2G pilot projects around the country, including Amsterdam and Zaandam [31, 32]. In Denmark, the GridMotion demonstration project will include bidirectional charging with Peugot iOn or Citroen C-ZERO vehicles [33, 34]. But not all EV manufacturers view V2G as a priority. Most notably, Tesla has no current plans to develop V2G, although they have experimented with bidirectional charging in the past [35]. Given the increasing attention to V2G, it is important to consider how bidirectional charging can play a role in smart EV charging projects.

2.1.4. Combining Solar Power and Electric Vehicles

With such rapid development in solar power and electric vehicles, it is only natural that the two technologies would be combined into solar parking lots. In a solar parking lot, solar panels are mounted in canopies over the parking spaces [36]. These parking lots offer a number of advantages for the parking lot operator and for the drivers. The solar panels can provide shade to vehicles parked underneath, protecting the vehicles from the elements, preventing sun damage, and keeping the internal temperature in the vehicle down [37]. Renewable energy from the solar panels can then be use to power nearby buildings or charge EVs. Charging EVs using local solar power is known as Solar to Vehicle (S2V) charging, first described under that name by Birnie (2009) [38]. These systems enable renewable energy to be used where it is generated, reducing transmission losses and allowing for vehicles to drive more sustainably.

One of the biggest advantages of solar parking lots is that ample space is already available, especially in urban areas where parking lots already occupy an enormous amount of land. This is especially beneficial in places like the Netherlands where land is more limited. Considering only rooftop photovoltaic (PV) systems,

there are 892 km^2 of suitable roof space in the Netherlands. If this entire area was covered in solar panels, the energy generated would be equivalent to half of all Dutch electricity demand [39]. Meanwhile, in Amsterdam alone an estimated 1.6 million m^2 are devoted to surface parking lots [40]. To illustrate how ubiquitous parking lots are in many Dutch cities, Figure 2.6 highlights in green all the surface parking in a section of Delft which includes part of the TU Delft campus. In many regions, parking can occupy a substantial area, covering approximately 4.97% of all urban land in the Upper Great Lakes region of the United States [41]. In Los Angeles County, 14% of all land is devoted to parking [42]. As the amount of solar power in the Netherlands increases, solar parking lots offer an opportunity for land to be used more efficiently.
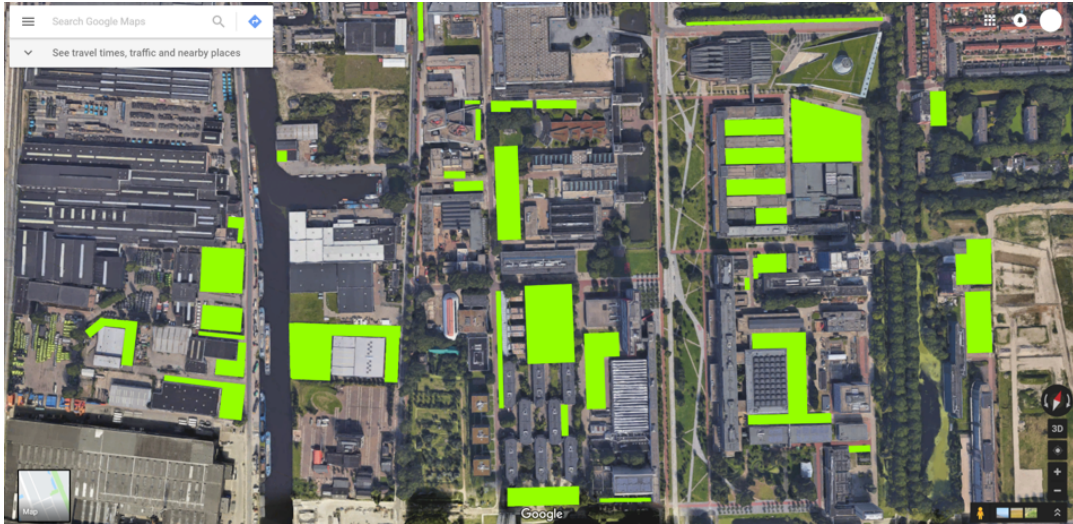
Figure 2.6: Surface parking lots in part of Delft, demonstrating the potential of solar parking lots

The solar canopies which cover the parking spaces can be built in a variety of different configurations. The different canopy designs can be distinguished according to the position and number of columns, and the angle for the roof [43]. Solar canopies can be built over a single row of cars, over a double row, or over multiple rows and aisles. For the sake of space efficiency, this report will consider solar canopies which are built over two rows of cars. The possible designs for the frames are shown in Figure 2.7 [43].
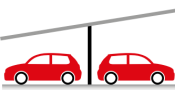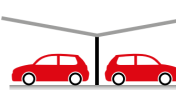
Figure 2.7: Possible frame designs for a solar canopy [43]

Monopitch designs have the advantage of a higher overall yield if the modules can be oriented facing south. Duopitch designs produce more energy if the panels are not tilted to face south, and have a slightly higher generation than monopitch in the mornings and evenings. Although modules in the northern hemi-

sphere are typically oriented south, the choice of azimuth for solar canopies is often limited by the geometry of the parking lot. Ultimately, the difference in generation between monopitch and duopitch is relatively small, regardless of the azimuth, and the choice is often made considering the visual impact rather than the energy yield. The choice of a V-frame or a T-frame will not affect the energy yield, and is decided based on other factors. A T-frame may be preferred aesthetically, but will require a greater amount of steel to support the larger overhang, making the V-frame the most cost-effective solution. One final design consideration is the tilt angle of the solar modules. A typical solar installation will have an optimal tilt angle of roughly the latitude [44]. Solar canopies, however, typically have a much lower tilt angle of 5–10° [43]. Higher tilt angles would be worse aesthetically, and would lead to higher wind loads, resulting in the need for deeper foundations and more expensive supporting structures. When designing a solar canopy, it is therefore important to balance the performance, cost, and aesthetics of the design.

Solar parking lots are an example of building integrated photovoltaic (BIPV) systems, an alternative to conventional PV systems. Although solar parking lots are integrated into canopies over parking spaces, BIPV systems can also be integrated into walls or rooftops, generating electricity while providing aesthetic and architectural benefits [36]. A variety of systems have been investigated, including facades, skylights, and curtain walls, using photovoltaic glass rather than conventional glass. These systems off additional advantages, such as absorbing infrared and ultraviolet rays to help maintain a more comfortable building temperature. Being integrated into a wall, however, prevents the modules from being oriented at their optimal orientation, and can lead to heating issues. These issues, along with perceived higher prices, have led to these types of BIPV systems representing only a small share of the PV market.

Another common idea for reducing land use is building PV modules into the surface of roads, parking lots, or bike paths, taking advantage of these flat spaces for energy generation. In the Netherlands, a solar bike path was built as a test project at Krommenie in the province of North Holland [45]. Despite the potential of this project, there are still a number of drawbacks to solar roads. Because they are installed in the ground, the solar modules cannot be oriented at the optimal tilt angle to capture sunlight, and the lack of convective cooling can lead to overheating of the cells, lowering their efficiency. Panels are shaded by pedestrians and bikes passing over the modules, and soiled by the dirt they leave behind. Finally, in order to make the roadway safely drivable an anti-skid coating is required, which depending on the angle of incidence can absorb 27%–55% of the incident irradiance. These factors combined result in a benchmark annual energy production of only 85–90 kWh/m^2 for Dutch solar bike paths, an efficiency of below 10%. Although solar roadways may have some niche applications, the higher price and lower efficiency suggest that they are not suitable for large scale energy generation if alternative locations are available.

(a) Wonderland Eurasia, Ankara [46]   (b) Intel campus, Folsom [47]   (c) Fastned EV charging station [48]
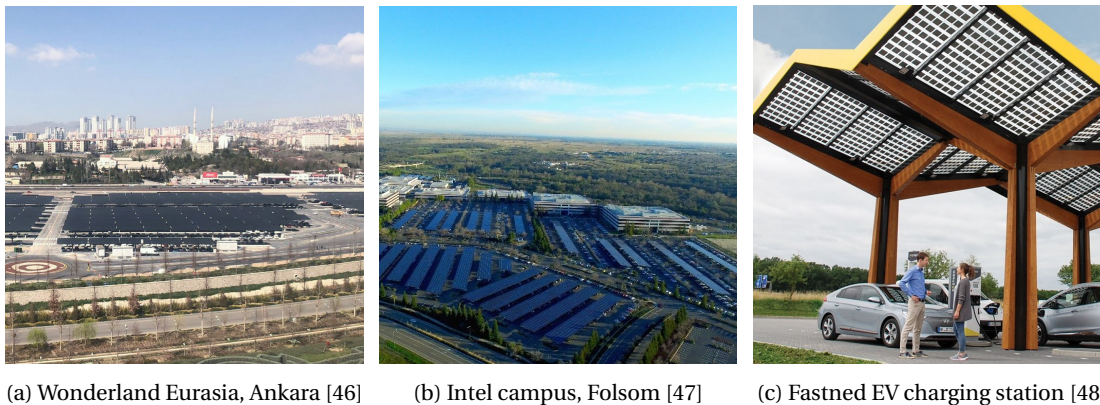
Figure 2.8: Images of different solar parking systems around the world

In part due to corporate commitments to sustainability, many solar parking lots have been built in recent years, with some examples shown in Figure 2.8. Some installations are quite large, operating on the megawatt scale. With a capacity of 10.2 MW, the world's largest solar parking lot covers 1.3 million square meters of parking at an amusement park in Ankara, Turkey [46]. At their offices in Folsom, California, Intel installed 8.7 MW of solar power over 3000 parking spaces, giving them the largest private solar parking lot in the United States [47]. In the United States, the government of Maryland implemented a grant program to support solar parking lots including EV charging. The largest project, at the new headquarters of the McCormick company in Baltimore, included 20 EV charging stations under a solar roof with a capacity of 744 kW [49]. Smaller solar

parking lots, including some with EV charging, are common as well. The Dutch company Fastned, which operates fast electric vehicle charging stations, has built solar panels into the roof over their car charging spaces [48].

Ultimately, solar parking lots can financially benefit parking lot operators, as the cost for the solar electricity is quite low after an initial investment, reducing the expense of charging EVs. By charging vehicle owners for the electricity they consume, and by selling the excess solar power, solar parking lots can be quite profitable. One proposed system in Lisbon found a payback time of 14 years [50]. A similar analysis for solar EV charging in the United States found a payback time of 14 years in Columbus, Ohio, and 15 years in Los Angeles, California [51]. Due to their numerous advantages, solar parking lots are likely to become increasingly common as solar prices continue to decrease and EVs become more widely used.

2.1.5. The PowerParking Project

In future energy systems, these technologies will all be combined. It is therefore important to investigate the intelligent integration of solar parking lots, electric vehicle charging, V2G, and energy storage. In order to research these systems under real-world conditions, the PowerParking project was developed. The goal of PowerParking is to develop a public-private collaboration which provides an innovative, decentralized, and integrated energy system for large parking areas. This could lead to greater production of renewable energy, improved energy efficiency, increased stability in the grid due to storage and smart grids, and the stimulation of electric transportation [52]. PowerParking seeks to carry out a project involving a solar parking lot connected to electric vehicle chargers and energy storage as part of an intelligent microgrid. The proposed project locations are in the long-term parking area at Lelystad Airport, and at a parking lot for the nearby Lelystad Airport Business Park. The energy produced will be used locally, primarily to charge parked electric vehicles. Surplus energy can be stored in fixed battery storage, or used to power the nearby airport[1]. A rendering of the PowerParking project is shown in in Figure 2.9.

Figure 2.9: The PowerParking project, with EVs charging under solar canopies [52]

The PowerParking project plans to include 100–125 parking spaces each at Lelystad Airport and Lelystad Airport Business Park. All the parking spaces will be covered with solar canopies, totaling 500 kW peak capacity. All the parking spaces will be suitable for EV charging, with bidirectional charging possible for 52 parking spaces at the airport and 8 at the business park. Both locations will also include DC fast charging, LED lighting, and 250 kWh of fixed battery storage. The solar panels will produce 450,000 kWh of renewable electricity per year, equivalent to reducing CO_2 emissions by 750 tons annually compared to the carbon intensity of the Dutch electricity grid. As part of the PowerParking project, a DC microgrid will be implemented. Typically, our

---

[1]The current plans for the PowerParking project have been scaled back from the original more ambitious design, but that original design nonetheless serves as a strong template for smart solar parking lots. It is therefore the original PowerParking project which is discussed in this section.

electricity networks are operated using Alternating Current (AC). However, there are some situations where Direct Current (DC) has advantages. Solar power is generated in the form of DC, and many loads such as LED lights and lithium-ion batteries consume power in the form of DC. This means that if a DC microgrid is not implemented, power could be generated in the form of DC by the solar panels, converted to AC, converted back to DC to be stored in the fixed storage battery, converted back to AC for the EV charging equipment, and finally converted back to DC power by the vehicle in order to charge the battery. This is highly inefficient [53]. The use of a DC microgrid could significantly reduce conversion losses.

DC power can be incorporated into a solar parking lot in two possible topologies [53]. The first involves the construction of a full DC microgrid. All incoming AC power would be converted to DC, and all loads, including the EV chargers, would run on entirely DC power. The alternative is a hybrid AC-DC network. A low-voltage DC bus would connect some elements, such as the fixed battery storage, solar panels, and LED lighting. It is also possible for the EV charging equipment to run on DC power, although slow chargers typically use AC. Any AC chargers or other loads could be connected to both the DC bus and the electricity grid. Both systems have advantages and disadvantages. The full DC network would require the least conversion between AC and DC, but it would be more technically complicated and more expensive to implement. For this reason, a hybrid AC-DC network is planned for PowerParking in Lelystad.

The choice of Lelystad as a location offers a number of advantages for PowerParking [52]. Firstly, this area is currently under development, meaning that the project can be built into the infrastructure from the beginning, rather than attempting to retrofit older construction. Furthermore, Lelystad is located in Flevoland, which has the ambitious goal of becoming energy neutral by 2020 excluding transportation, and by 2030 including transportation. This is a hugely challenging goal, especially given the growing demand for power in the Flevoland due to the growing population and increasing development. Because of the large area requirements of renewable electricity, and the high costs of electricity networks, the government is interested in building energy systems as an integrated part of future development. Finally, the parent company of Lelystad Airport is the Schiphol Group. Schiphol Airport has plans for expansion, and has expressed interest in projects like PowerParking at their own facilities. However, due to a number of uncertain factors it is not desirable to carry out such an experimental and innovative project at the busiest airport in the Netherlands. Lelystad therefore serves as a good pilot location.

To the author's knowledge, there is currently no example of an integrated, decentralized energy system with generation, storage, and bidirectional smart charging in a large-scale business environment. Although there are projects with many of these individual elements, no project combines all these technologies at a large scale. Large solar parking lots may have some unidirectional EV chargers, but the solar energy is usually primarily intended to power nearby buildings, rather than a local microgrid [46, 47]. Smart charging projects will be discussed in Section 2.2.3, but most of these systems are small pilot projects, often lacking one or more of the elements studied at PowerParking.

The goal of PowerParking is to develop a framework for integrating all these technologies in a way that adds value for all the parties involved and is feasible, scalable, and reproducible. Feasible in this context means that the pilot project demonstrates the technical feasibility of such a system, as well as economic feasibility without subsidies, enabling a system that supports electric mobility for everyone. Scalable means that the project is able to be easily expanded as necessary. Lelystad Airport is planned to initially have 3,500 parking spaces, with another 1,600 at the business park. Ideally, it would be possible to add more solar docks, EV charging points, and battery storage without complicated or expensive renovations of the infrastructure which has already been built. Finally, the project should be reproducible, allowing the lessons which are learned to be applied at other parking locations. Some suggested further locations are Schiphol Airport (60,000 parking spaces currently, with an expansion of 11,000 planned), Keukenhof (8,000 spaces, including 1,000 for buses) and Q park (5,800 parking facilities with 800,000 parking spaces).

TU Delft is a partner in the PowerParking project, being involved with developing, testing, monitoring, and evaluation of the parking infrastructure. This includes the system integration of the solar canopy, the charging and discharging of vehicles, energy storage, matching energy demand, and measurement and analysis of data in order to further develop the business case [54]. As part of this role, TU Delft will be responsible for the construction of a small-scale model in the Green Village. This model will be used to test the monitoring system, the individual components, and the integrated system as a whole. The goal of this experiment is to be in line with the vision of the PowerParking project, including modular design, bidirectional charging, solar panels, and a DC microgrid. Components will be identical to those which will be used at Lelystad, providing insight into the project. The Green Village model will allow for the system to be tested under real-world conditions to see how it may behave at Lelystad. For example, it is possible to investigate the system

performance if a component fails, or if it is unexpectedly cloudy [55]. The results of tests at the Green Village will be used in the design of the system in Lelystad. Despite the benefits of the Green Village model, however, there are still many limitations to its utility.

There are some questions which cannot be practically answered using a small-scale model. In order to evaluate the system at a larger scale, considering a wide range of scenarios, a computer model of the parking lot is developed. The computer model can be simulated to analyze different design choices and control strategies. This report will cover the development of the model, the implementation of various control strategies, and the results of the simulation.

2.2. Smart Charging

Although there are benefits to the PowerParking project and solar parking lots, the system can only reach its full potential when combined with smart charging.

2.2.1. The Challenges of Uncoordinated Vehicle Charging

Electric vehicles will play a significant role in future energy systems. Although they offer many benefits over the current system, they also present significant challenges. When a vehicle begins charging the moment it is plugged in, without consideration for electricity demand or price, it is known as uncoordinated charging or dumb charging. Uncoordinated charging of electric vehicles can lead to increased demand for electricity, especially at peak times. This can lead to higher electricity costs, greater carbon emissions, increased grid congestion, and overloading of transformers and other infrastructure in distribution networks. In order to make widespread EV adoption a reality, these challenges will need to be addressed.

As the market share of EVs increases, so does the electricity consumption. In 2017, EVs consumed 54 TWh of electricity worldwide, equivalent to 0.2% of global electricity consumption [9]. In Norway, with the highest penetration rate of EVs worldwide, the electricity used for vehicle charging is 0.78% of total demand. At the household level, this demand could be enormous. In 2017, the average Dutch household consumed 2,980 kWh of electricity. If we consider an electric vehicle with typical efficiencies and driving behavior, the annual charging demand for the vehicle would be 2,431 kWh [17]. This means that the addition of an electric vehicle could almost double annual electricity consumption for a typical Dutch household.

Table 2.1: Impact of uncoordinated charging on peak grid load [21]

Location	EV penetration [%]	Peak load increase [%]
Los Angeles	5	3.03
California	10	17
United Kingdom	10	17.9
Portugal	11	14
Western Australia	17	37
Los Angeles	20	12.47
United Kingdom	20	35.8
California	20	43
Netherlands	30	54
Belgium	30	56
Western Australia	31	74
New York	50	10

Not only will the total demand for electricity grow, but at high levels of EV penetration uncoordinated charging can lead to significant increases in peak electricity demand for the grid, as seen in Table 2.1 [21]. Even at modest levels of EV penetration, the increase in peak demand for electricity can be significant. One study found that an EV penetration level of 30 % in the Netherlands would lead to a 54% increase in peak load [56]. In Western Australia, a similar penetration level of 31% would lead to a 74% increase [57]. The increase in peak electricity demand due to uncoordinated charging can lead to serious issues with the electricity grid.

Solar power alone is not able to solve the problem of increased peak demand. EVs are most commonly charged when people arrive at home in the evening, a time when electricity demand is already at its peak and when solar energy will be quite low [17]. Energy storage with batteries or other technologies could allow for energy during the day to be stored and used to charge EVs in the evening, but seasonal fluctuations would still

pose a problem [58]. Using solar power to charge EVs would lead to an excess of solar generation during the summer and a shortage during the winter. Battery storage is unable to solve this problem because it cannot handle seasonal variations, so an electricity grid with controllable generation is required to keep the system balanced.

Electricity generation must always be carefully controlled to match the demand. The conventional approach is to increase or decrease the generation, which involves turning on or off power plants. This can lead to issues, in particular during peak hours [59]. These high peak loads, combined with the problems already presented by the variability of solar energy, will put a serious strain on transmission and distribution networks. The grid may become dangerously congested, and in the worst-case scenario, blackouts may even occur. Electric vehicle charging demand will contribute significantly to congestion in the future, especially in dense urban areas [7]. Grid operators all across Europe will need to upgrade their infrastructure in order to accommodate EV charging and avoid congestion. In the Netherlands alone, network operators estimate that they will spend €20–71 billion preparing for the energy transition [2]. In addition to ensuring that transmission and distribution capacity are available, it is also important to guarantee that sufficient generation capacity is available at times of peak demand.

At times of peak demand, generation capacity is often provided by natural gas peaking plants. These plants are rarely used, and the levelized cost of electricity from these plants can therefore be quite high. As seen in Figure 2.1, a gas peaking plant will have an average LCOE of $179 per MWh, compared to only $58 per MWh for a conventional combined cycle gas plant. Reducing the demand at peak times can therefore have a substantial impact on electricity prices. These demand peaks also affect the environmental friendliness of the electricity, although the relationship between carbon emissions and electricity demand is complicated.
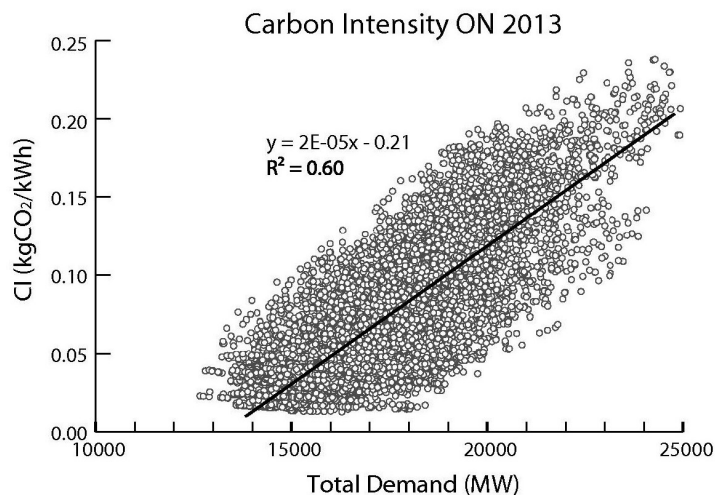
Figure 2.10: Total electricity demand vs. Carbon Intensity (CI) in Ontario [60]

As shown in Figure 2.10, the carbon intensity of electricity production is strongly correlated with the electricity demand in Ontario [60]. This is because Ontario relies on carbon-free hydropower and nuclear electricity to supply the base load, with natural gas power used during times of higher demand. The relationship between carbon emissions and electricity demand thus depends mainly on the types of power which are used. In New Zealand by contrast, less than 20% of electricity is generated with fossil fuels, with most power coming from hydropower and geothermal energy. Because the fossil fuels are mainly used to generate base load power, there is no correlation between demand and carbon intensity, although New Zealand is largely an exception in this regard [61]. In many power systems, coal is used to provide base load power while natural gas is used to run peaking plants at times of high demand. Because electricity from coal is more carbon intensive than natural gas, in these locations the marginal emissions rate actually decreases at times when the electricity demand is higher. This is true in Portugal [62] and many regions of the United States [63]. In the Netherlands, coal power is being phased out entirely, to be replaced with renewable sources such as wind and solar power [14]. In this future energy system, natural gas will be used to generate electricity only when the supply from renewables is insufficient. Renewable sources are quite variable so the carbon intensity of electricity will be dependent on the weather, but it will also be greater at times of high electricity demand as it currently is in Ontario. This provides another incentive to reduce the electricity demand at peak times.

Uncoordinated EV charging presents problems for the stability, cost, and sustainability of electricity networks from a large-scale perspective. But this charging behavior can also cause issues on the local level. The increase of peak demand due to EV charging can lead to under-voltages due to the higher power demand as well as current and voltage harmonics due to the nonlinear power electronic equipment in EV battery chargers [64]. If EVs are charged using fast charging, the peak power demand will be higher and the voltage drops will be greater when compared to slow charging [65]. Under-voltages are especially problematic at charging stations which are relatively far from the service transformer [64]. At high levels of EV penetration, these voltage drops could violate the recommended limits, especially in secondary wires.

EV chargers can also lead to current and voltage harmonics, which reduce the power quality, lead to increased power losses, and shorten the lifespan of components such as cables and transformers [66]. In order to have a reasonable transformer life expectancy, it is recommended that the total harmonic distortion (THD) in EV chargers is maintained below 25%–30%. The International Electrotechnical Commission (IEC) standard 1000-3-4 recommends a current THD of less than 20% [67]. In addition to harmonics and under-voltages, uncoordinated charging can create issues at the local level through increased transformer loading.

If the demand due to EV charging exceeds the transformers rated capacity, the transformer may become overloaded, increasing system losses and decreasing the transformer's lifespan [64]. Simulations have demonstrated that for high levels of PHEVs in residential distribution networks, the load due to vehicle charging will result in some transformers exceeding their rated capacity for part of the year [68, 69]. Transformers are often loaded beyond their rated capacity for short intervals, and this overloading is often permissible the temperature of the device remains low and the transformer overloading time is relatively short. Overloading beyond these limits can lead to increased hot-spot temperatures, resulting in the evolution of free gas from insulation and insulating fluid, reduced mechanical strength or deformation of conductors and structural insulation, and high internal pressures resulting in leaking gaskets or loss of oil [70]. These issues can shorten the lifetime of a transformer.

There are three main overloading types which are considered for transformers: planned overloading, long-term emergency loading, and short-term emergency loading [70]. Planned overloading is typically restricted to transformers that do not carry a continuous load, and may result in the hot-spot temperature rising from the standard 65 °C to operate in the 120 °C – 130 °C range. Long-term emergency loading is due to the prolonged outage of some other element in the power system which leads to a transformer being overloaded from hours up to months. The hot-spot temperature may reach 120 °C – 140 °C, and the risk to the transformer is greater than for planned loading. Short-term emergency loading is due to unlikely events which lead to serious disturbances and hot-spot temperatures as high as 180 °C. Although the duration is shorter than long-term emergency loading, with events of half an hour or less, the higher temperatures mean that the risk of failure is greatest for short-term emergency loading, which can typically occur only once or twice over the typical lifetime of the transformer. Uncoordinated charging can lead to these types of short-term spikes in demand, severely shortening the lifetime of a transformer in the distribution system.

Uncoordinated charging of EVs will lead to higher electricity demand, especially at peak times. This demand can lead to congestion, more expensive and polluting power, issues with local power quality, and damage to infrastructure such as transformers. These concerns over uncoordinated charging have led researchers to seek techniques to minimize the peak demand due to EV charging.

2.2.2. The Benefits of Smart Charging

In order to avoid problems due to uncoordinated charging, the peak electricity demand can be reduced, a process known as peak shaving. Often, the total energy used is not decreased, but instead demand is shifted to off-peak times, known as valley filling [59]. Peak shaving and valley filling can offer a number of benefits, including improved power quality, lower energy losses, decreased costs, more efficient integration of renewable energy, and higher reliability. Peak shaving can be achieved using three main strategies:

1. Energy Storage Systems (ESS), where energy storage technologies including Battery Energy Storage Systems (BESS) are charged during off-peak hours and used to power the grid at peak times

2. Demand Response (DR), where electricity consumers are incentivized to reduce their consumption at peak times

3. Vehicle-to-Grid (V2G) schemes, where EVs can discharge their battery at times of peak demand

In the system modeled in this report, all three strategies are combined in an effort to reduce the peak load as much as possible. As part of PowerParking and similar systems, fixed battery storage is combined with

demand response from charging EVs, by shifting the charging rate and time of the vehicles. Some EVs are also capable of providing V2G services. The use of BESS for peak shaving can be seen in Figure 2.11 [59].
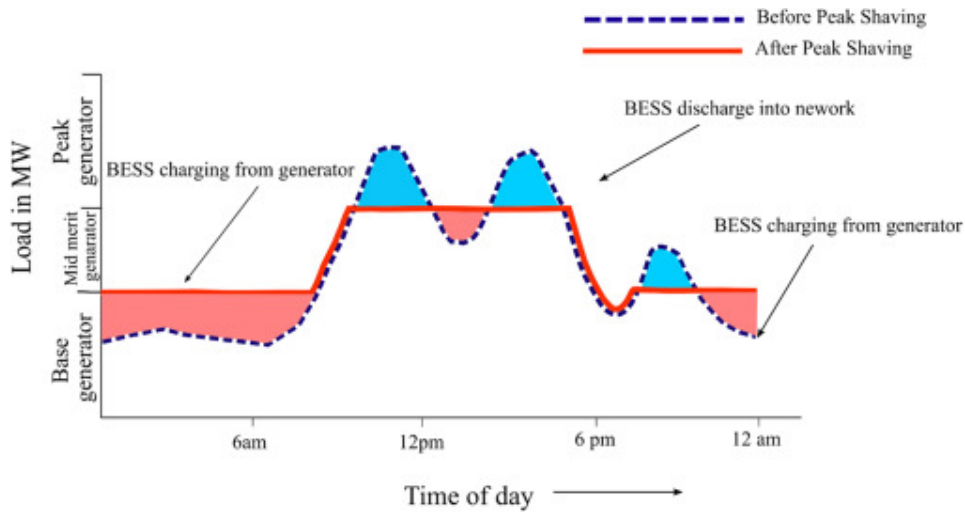
Figure 2.11: An demonstration of peak shaving using battery energy storage systems (BESS) [59]

Demand response can be implemented using a wide variety of controllable loads. In the Netherlands, the market for DR is expected to grow with the increasing use of renewable energy, and could include industry, horticulture, cooling, and transport. By allowing demand response to trade on the intraday market, the potential market is estimated to be 489 GWh per year, with a net gain of €11 million [71]. The Dutch government recognizes that there is a great potential benefit in grid tariffs that depend on the load in real-time, thereby incentivizing consumers to use electricity in a way that is more efficient and flexible [2]. Furthermore, demand response could help grid operators avoid costly infrastructure upgrades.

(a) Total investments, 2023–2030

(b) Total investments, 2031–2050
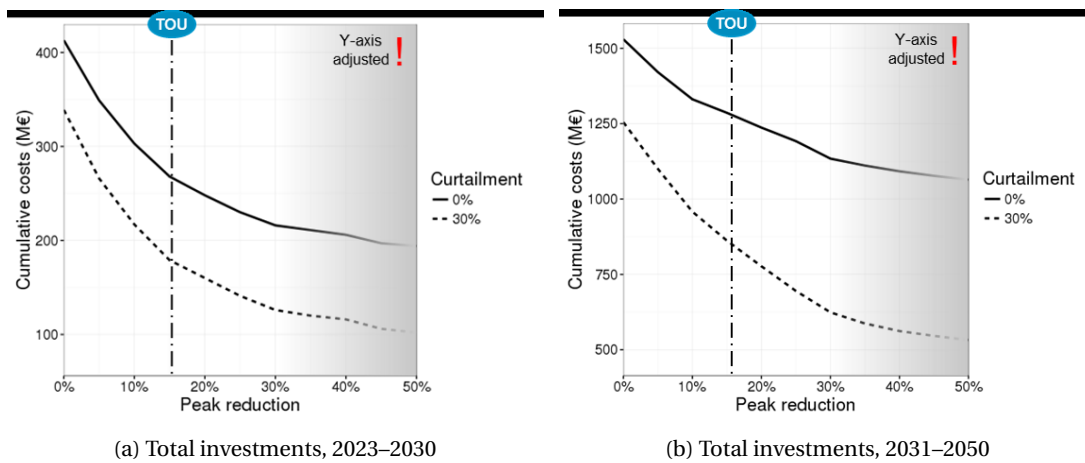
Figure 2.12: Cost of cumulative grid investment costs for Liander vs. reduction in peak demand [7]

Flexibility could reduce the required investments in electricity networks by hundreds of millions of euros, as seen in Figure 2.12. This figure shows the expected cumulative costs for electricity grid investments by Liander, a Dutch DSO [7]. By 2050, the Dutch power system will need to support 56 GW of solar power capacity and a 74% penetration rate of EVs. In order to avoid congestion, major upgrades will be needed for infrastructure like transformers and cables. Some investments could be avoided by curtailing solar power at key times. Alternatively, the peak demand can be reduced, allowing existing infrastructure to be used more efficiently. As seen in Figure 2.12, reducing the peak demand by 20% without any curtailment could be more cost-effective than curtailing 30% of solar generation. Time of Use (TOU) pricing is one suggested option to reduce the peak demand, but many other techniques are possible. One kind of demand response problem that demonstrates a great deal of potential for peak shaving is coordinated smart EV charging.

In contrast to uncoordinated charging, smart charging alters the rate, rate of change, timing, and direction of electric vehicle charging in a coordinated and intelligent way. Smart charging can include V2G technologies, but with or without bidirectional charging it could help balance generation and demand of electricity in future energy systems [72]. Smart charging covers a range of possible goals, including: reducing the impact of EV charging on peak grid loading; minimizing voltage deviations, line currents, power losses and load surges in transformers; balancing the load and voltage profile; reducing the cost of electricity; maximizing the use of renewable energy; and increasing the system stability, power quality, and reliability [21].

Properly implemented, smart charging can solve the problems of high peak grid demand that results from uncoordinated charging and provide value to many parties [17]. EV drivers can better determine when they should charge their vehicles, and may be financially rewarded for their flexibility. Grid operators can use the flexibility provided by smart charging to reduce congestion and imbalance in electricity networks. This may enable them to avoid costly infrastructure upgrades. Charge point operators can optimize the use of their charging points, by for example distributing the available power to the cars present based on the drivers' preferences. In order for smart charging to be effective, these stakeholders must work together along with other partners like municipalities and EV manufacturers.

Smart charging also helps the parking lot operators. This peak shaving can also offer financial benefits by preventing damage to equipment like transformers and cables, extending their lifespan. Reducing peak consumption could also lead to parking lot operators charging less from the grid and more from renewable energy. This will likely lead to a higher self-consumption of renewable sources of energy, although that is not the explicit goal. In addition, by reducing their peak demand parking lot operators are able to reduce the size of their grid connection. If demand in the parking lot grows, smart charging will allow the parking lot operator to delay or avoid altogether the need to upgrade their infrastructure.

The grid connection can play a significant role in the cost of electric vehicle charging infrastructure. There are two main aspects to this cost [73]. First, there is an upfront cost to connect to the electricity network. This cost includes the installation of new infrastructure such as cables, electrical panels, and transformers, to ensure sufficient capacity for the charging equipment. In order to reduce the project cost, charging station operators can seek to reduce the capacity needed to minimize these installations. Second, there are recurring costs for the electricity connection. In addition to paying for the electricity consumed, many facilities pay demand charges, which consider the peak electricity demand. These charges will be dependent on the utility, but in the United States, consumers will often pay these charges if their peak demand is above a certain threshold, typically 20–50kW. These charges can range from \$3–\$40 per kW, meaning that the demand charges can cost thousands of dollars per month without even considering the cost for electricity itself. These demand charges can increase the monthly fee by up to a factor of four.

In the Netherlands, both the upfront and recurring costs for the electricity connection contribute significantly to the cost of a charging station. For a single charging pole with two plugs, the initial grid connection cost is estimated to be €750, which is 23% of all one-time costs [74]. This cost is rising, having increased by 15% since 2013 even as total upfront costs have fallen by by 30%. As electric vehicles become more common, the cost of charging infrastructure is expected to continue decreasing, but this connection cost is likely to continue rising. The electricity connection also plays a role in recurring costs, with the grid connection for a single charger estimate to cost €190 per year, which is 37% of costs excluding electricity (€510). The cost of electricity will of course be dependent on how busy the charger is, but with an average demand the grid connection will represent 20% of annual costs including energy (€943) [74]. For operators of EV charging stations, even a small reduction in the electricity capacity can lead to large savings. The use of smart charging to reduce peak demand in parking lots is therefore the subject of considerable interest.

2.2.3. The Current State of Smart Charging

Smart charging projects have already been implemented around the globe, typically in the form of demonstration projects. These projects investigate the potential of smart charging under real world conditions. Most smart charging projects are relatively recent, and relatively small. In Toronto, the ChargeTO pilot project was the first project involving residential smart-charging, using a set of 30 EVs in 2015. The project found that by curtailing the charging load when the vehicles charged overnight, they were able to shed 70–80% of charging load at peak times while still ensuring that all the vehicles were fully charged by their desired departure time [75]. Vehicle to Grid (V2G) is also commonly investigated as part of these pilot projects. In the largest project to date, Nissan is planning a large-scale V2G demonstrator project with 1000 charging stations across the UK for commercial fleet drivers of their Leaf [76]. Nissan has long been a leader in bidirectional charging, with V2G pilots involving the Leaf being deployed in Denmark [77], Italy [78], and the United States [79]. The

pilot project in Denmark consisted of 10 Nissan Leafs, each with a battery of 24 kWh, providing frequency containment reserves as part of a commercial V2G hub. Field results showed that EVs are able to operate in aggregated mode to support the grid with fast frequency regulation [80]. Vehicle availability, especially on weekdays, played an important role in the bidding process, as vehicles were not always present during working hours.

In the Netherlands, there have been a wide range of projects involving smart charging. The FlexPower project in Amsterdam, a collaboration between between the municipality, Nuon, Liander, and ElaadNL, consisted of 200 charging points where vehicles are charged faster when there is lower demand for electricity, and slower when demand is high. These stations are already in operation and available to consumers, as seen in Figure 2.13 [13]. At the Amsterdam Arena, which has a very high peak demand for electricity during sports events and gigs, energy storage and V2G are being investigated as a way to meet this peak demand [81]. And consumers are now able to use Jedlix, a program from Eneco which enables drivers to save money by allowing the company to control their charging rate based on the grid demand, availability of sustainable energy, and electricity price [82]. Unlike most other smart charging projects, Jedlix controls the charging rate via software on the car itself, rather than through the charging equipment. This allows for smart charging without the use of dedicated infrastructure.

Figure 2.13: An EV driver charging her car at a FlexPower charging station in Amsterdam [13]

Some Dutch smart charging projects also consider V2G, such as LomboXnet in the Lombok neighborhood of Utrecht. This system involved two EVs charging from a 31 kW PV installation, with V2G being used to increase self-consumption of renewable energy and decrease peak electricity demand for the vehicles [83]. The project found that smart charging including V2G could increase self consumption from 49% to 87% and decrease the demand peaks by 67%. Despite these benefits, the annual energy throughput increased by a factor of 3–4 compared to a uncoordinated charging without V2G. Since energy throughput is the strongest indicator for battery degradation, this suggests that V2G may cause the batteries to degrade at a rate much higher than they otherwise would, incurring additional costs to the EV owner. The project used predictions for renewable energy production and charging demand, and found that accurate forecasts were necessary to achieve good results [84]. After the successful pilot program, the project is planning on expanding to 70 vehicles across five districts in the Utrecht region [13].

Consumers who have had the opportunity to try smart charging generally appreciate the ability to contribute to the stability of the electricity grid and the integration of renewable energies, while being rewarded financially for their flexibility [85]. One common concern for drivers is the longer charging times, which may require more planning about when they would need to use their vehicle. In commercial smart charging, it is therefore important that the EV owners are not inconvenienced. The required financial rewards for smart charging are still uncertain. The ChargeTO project found that the majority of consumers considered adequate

compensation for smart charging to be \$10 per month or higher, with a quarter considering \$25 per month to be their required rate [75]. Other surveys, however, have found that despite the claims of consumers, willingness to engage in smart charging was not related to the level of financial compensation [86].

Despite potential benefits, there are many barriers which impede the development of smart charging on an institutional level. Typically, these barriers involve regulatory, financial, or coordination issues [17]. For drivers charging at home, there is often no incentive to store excess solar energy in a vehicle battery, as net-metering rules mean that the energy can be sold to the grid and then purchased back later at no additional cost. There are also issues of double taxation. A vehicle owner who charges their car with 10 kWh and sells 3 kWh back to the grid may need to pay taxes on that 3 kWh both when buying and selling. The parliament of the European Union (EU) recognizes these barriers, noting in a recent directive that smart charging and V2G are hindered by legal and commercial barriers such as "disproportionate fees for internally consumed electricity, obligations to feed self-generated electricity to the energy system, and administrative burdens, such as the need for consumers who self-generate electricity and sell it to the system to comply with the requirements for suppliers [87]." The directive recommends that member states implement laws which remove these barriers, enabling EV charging to provide flexibility to the electricity market.

From the perspective of the grid operator, such as the transmission system operator (TSO) or distribution system operator (DSO), there are regulatory uncertainties which limit the use of smart charging. While smart charging could be theoretically deployed to prevent congestion, it cannot be currently legally used to permanently avoid grid upgrades [17]. Grid operators are still obliged to improve transmission infrastructure as quickly as possible, meaning that preventing congestion via smart charging may provide little financial benefit to them. This may be resolved in the future, as the recent EU directive instructs DSOs to make use of demand response when possible as an alternative to expanding the electricity grid [87]. Doing so could stimulate the adoption of electric transport by benefiting drivers and create much-needed flexibility in the electricity grid, enabling the more rapid and efficient adoption of renewable sources of energy.

Even if these regulatory issues are solved, however, the adoption of smart charging may still be hindered by risk-averse behavior from consumers [88]. Although smart charging could lead to lower prices if consumers adjust their charging behavior, drivers tend to prefer certainty in pricing over variable pricing, even if there is a good chance that the variable price will decrease their cost. There are also barriers from the perspective of the charging point operator [17]. The operator may profit by using the charge point as much as possible, by having a higher number of cars parked for a shorter time. This means that the operator may wish to prevent smart charging which delays charging or sells energy to the grid, unless they are adequately compensated for this lost revenue. In addition, vehicle charging is more flexible if the charging station has a higher higher-capacity grid connection, allowing for smart charging to be more effective. Because these connections are more expensive, charging point operators typically install lower-capacity connections at public or semi-public charging points. It remains to be seen if a business case develops for smart charging, which would help to overcome these barriers.

2.2.4. Modeling Smart Charging

Although smart charging promises a wide range of benefits, it is often difficult to test in the real world. For this reason, computer models are often used to simulate the charging behavior of EVs in order to understand the impact of different scenarios and strategies [89, 90]. This behavior can be used to determine the behavior of an energy system with coordinated or uncoordinated charging. Models for EV charging behavior can be used for various purposes, and are therefore implemented in various different ways.

There are two different dimensions must be considered when determining the kind of model which will be built. These dimensions are the required time resolution and the extent to which individual vehicles can be aggregated together [89]. These choices will depend on the system being analyzed, with different kinds of analysis calling for different modeling decisions. These two dimensions, and some examples of systems with different modeling requirements, are shown in Figure 2.14 [89].

The first dimension is the time resolution. Vehicle Ownership and Annual Mileage Models (VOAMMs), consider only behavior over longer periods of time, such as a year. VOAMMs are suitable for analyses of annual energy requirements, but are not sufficient for studying charging patterns or the impact of charging behaviors on the electricity grid. These subjects require a higher temporal resolution. Short period modeling is therefore used, which analyzes behavior at a time resolution of an hour or less. These models can be used to analyze issues such as CO_2 emissions for EVs, based on the changing carbon intensity of electricity generation over the course of the day. Short period modeling is also used when analyzing the impact of EV charging on the electricity grid, and how that impact is affected by smart charging.
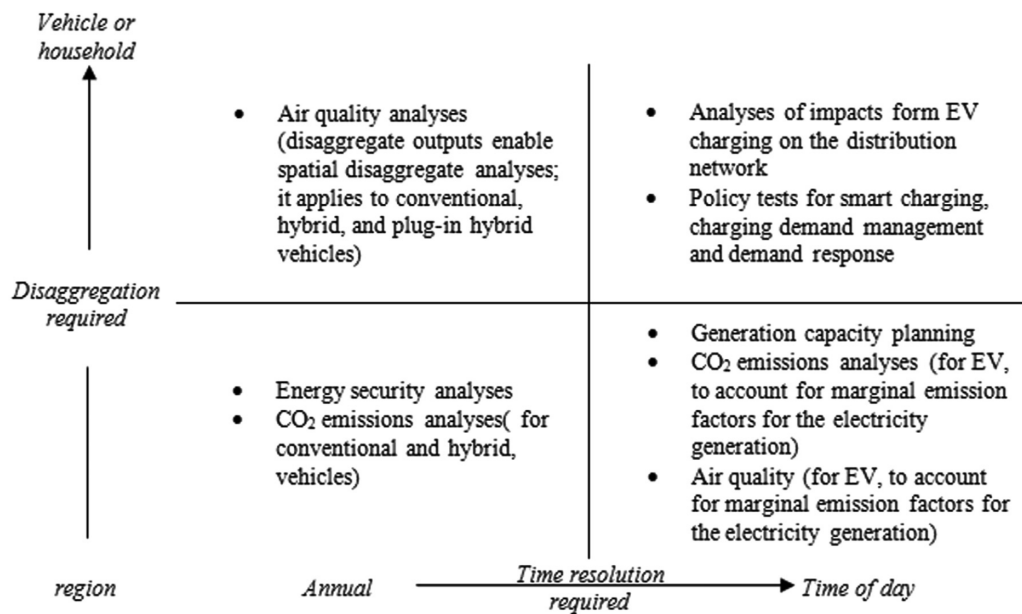
Figure 2.14: Aggregation levels and time resolutions required by different EV models [89]

The second dimension is the level of vehicle aggregation. Some models consider the charging behavior of each vehicle individually [91, 92]. Others aggregate vehicles together, considering only the combined impact of all vehicles [93, 94]. When considering the behavior of individual vehicles, a common technique is the Summary Travel Statistics Model (STSM), in which information about (conventional) vehicle use, such as typical distance driven or times at which the EV is parked at home, is used to create vehicle use patterns. STSMs can be used to generate charging profiles, which are useful for applications such as capacity planning, but the models are not detailed enough to analyze the effect of different smart charging strategies or the impact of charging on the power grid [89]. An alternative approach which can consider more complex vehicle patterns over the course of the day is the Markov Chain Model (MCM). These models generate EV patterns based on a Markov chain, in which an individual vehicle moves between driving and parking in commercial, industrial, or residential areas [95]. The probabilities of transition from one state to another are based on real-world traffic data. Although they are more suitable than STSMs for modeling smart charging, MCMs are still not commonly used.

When modeling smart charging strategies, Activity Based Approaches (ABAs) are typically favored. These approaches analyze travel using patterns of behavior which vary from driver to driver. In pure Activity Based Models (ABMs), a set of desired traveling activities are generated for agents, such as locations where the agents would like to arrive and depart at certain times [96]. Traveling and charging behavior is then chosen assuming that the agents are seeking to maximize their own utility. These models have the advantage that they allow for an interdependence between smart charging incentives and driving behavior. This is important because drivers may change their driving and charging behavior based on these incentives, and if models do not consider these interactions, they may not properly examine the impact of different charging scenarios [97]. Despite their advantages, ABMs are more complex to model, and rarely implemented in the literature [89].

The more common form of ABA is the Direct Use of Observed Activity-Travel Schedules (DUOATSs), where observed vehicles patterns are used to model EV use. With this approach, non-electric vehicle driving patterns are used to simulate EV behavior. This is a common approach, but it may fail to account for the fact that driving behavior may be different for EVs compared to conventional vehicles. As seen in Figure 2.15, a substantial fraction of drivers would need to change their driving behavior if they switched from a conventional vehicle to an EV [98]. That study of Seattle drivers found that only 50% of one-car households and 80% of two-car households would be able to have 99% of their driving needs met through an electric vehicle with a range of 100 miles (160 km) that is charged daily. Consequently, drivers can be expected to change their behavior if they begin driving an EV. It is therefore important to be cautious when using driving statistics for conventional vehicles in models of EVs.

Unlike BEVs, PHEVs do not experience the same limitations on driving range. Nevertheless, different pricing structures for charging at different locations or times may lead to some drivers adapting their travel patterns in order to minimize their charging costs [89]. This means that DOUATS models are often not suitable for modeling smart charging systems where the driving behavior is expected to change based on the pricing incentives for smart charging. Despite its limitations, the DUOATS approach is often used in models including those analyzing the impact of smart charging and demand response. For example, a study using driving data from the United States Department of Transportation's National Household Travel Survey (NHTS) found that PHEVs would significantly increase the peak load in the electric grid when they begin charging during evening hours, but that this load could be nearly eliminated if vehicles delayed charging as much as possible, so that they only finish charging right before departing in the morning [99]. Another study used the same NHTS data to generate a Monte Carlo simulation based on the charging probability at each time of day [93]. They found that the Monte Carlo simulation accurately matched empirical data from a PHEV demonstration project in Texas. DOUATS modeling is considered to be usable under circumstances where it is reasonable to assume that driving behavior of conventional vehicles will be similar to that of EVs, or where driving behavior is taken from EVs specifically. In this report, DOUATS modeling will be used, with real-world driving data used to generate vehicle patterns for a Monte Carlo simulation. Driving data will be taken from EVs whenever possible, and from comparable conventional vehicles when suitable EV data is lacking.

(a) Single vehicle households   (b) Double vehicle households
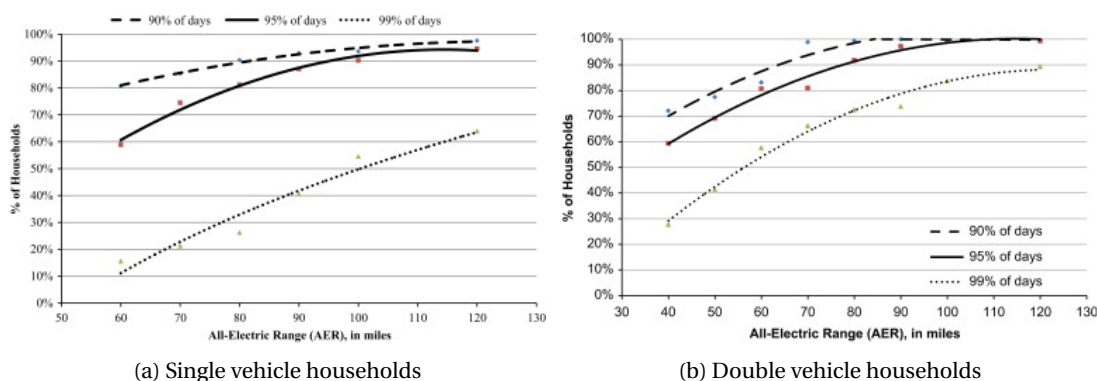
Figure 2.15: Vehicle range vs. usability, given conventional driving behavior [98]

2.2.5. Smart Charging Strategies

Smart charging encompasses a wide range of possible behaviors and strategies. There are a number of possible goals for smart charging, including minimizing peak loads, maximizing use of renewable energy, or minimizing costs for either drivers or parking lot operators [37]. Although these goals are overlapping, it is desirable to state the desired outcome, in a manner which allows different objectives to be compared quantitatively. In this report, the goal will be for the parking lot operator to reduce the total demand for electricity at peak times.

Charging strategies seeking to reduce peak demand can involve coordinated or uncoordinated charging of EVs. One possibility for uncoordinated charging is delay charging, in which vehicle charging is delayed past a certain time of day, typically after the evening peak demand is over. A similar option is off-peak charging, where vehicles are prevented from charging during times of high demand, such as the morning and evening peak hours, but are allowed to charge freely the remainder of the day [21]. Although these strategies may serve to shift some of the charging demand, they are still uncoordinated and do not take into account future loads. These strategies therefore will not lead to the optimal reduction in peak demand.

Under some implementations, these strategies can actually increase the peak load. For example, delay charging can be incentivized by instituting lower electricity tariffs during off-peak nighttime hours such as after 22:00. The lower tariffs may then lead to electricity demand spiking dramatically at the time when the low-tariff period begins [96]. This new peak demand may be greater than the original, meaning that delay charging could cause greater stress on the grid than fully uncoordinated charging. Off-peak charging can suffer from the same problem. If a no-charge window is implemented from 13:00–19:00, drivers will simultaneously begin charging their vehicles after the window is over. This can result in a higher peak load than scenarios with no limitations on charging [99]. Another study found that with uncoordinated vehicle charging, a simulated electricity grid began to experience unacceptable levels of congestion at a 10% penetration

rate of EVs. If a dual-tariff policy were adopted, where the price of electricity is different at day and at night, that number could be increased to only 14% [100]. The dual-tariff policy was not able to avoid congestion due to the creation of a new peak in electricity demand at the time when the lower rate period begun. Using fully coordinated smart charging, congestion could be avoided up to a 52% penetration of EVs without any upgrades to the electricity network. The same level of penetration with uncoordinated charging led to unacceptably high peak loads, as seen in Figure 2.16 [100].
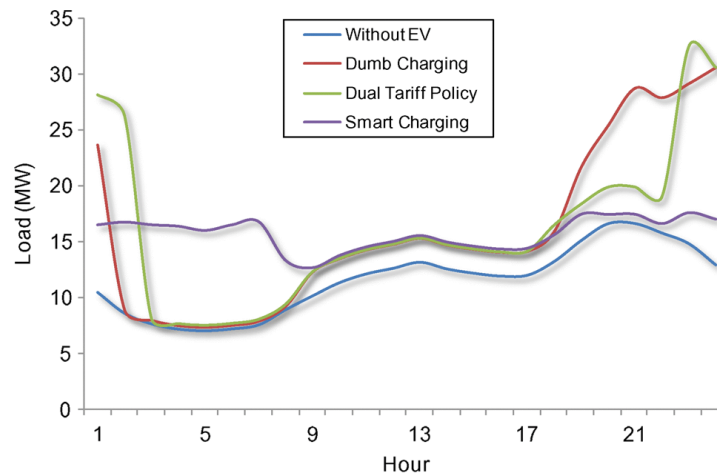
Figure 2.16: Load on electricity network with different charging strategies [100]

Uncoordinated charging, regardless of incentives, is unsuitable to reduce peak electricity demand. Coordinated smart charging is necessary in order for peak shaving to achieve its full potential. Yet even coordinated charging may be insufficient to achieve optimal peak shaving if future information is not taken into account. A smart charging strategy known as Real-Time (RT) charging was tested as part of the LomboXnet project [83]. In this strategy, the difference between the PV generation and the uncontrollable loads is calculated at each time step. If there is more PV power than electricity demand, EVs are charged using that excess. EVs extract power from the grid only when there is not enough energy in the battery to make an upcoming trip. The RT strategy can be combined with V2G, where energy is extracted from the vehicle batteries in order to cover the uncontrollable loads when PV power is insufficient. RT strategies, with or without V2G, do not consider future loads or generation, and are therefore not nearly as effective at reducing the peak demand. RT control was able to reduce peak loading by 27% without V2G and 43% with V2G. A linear programming algorithm which considered future energy and loads, however, was able to reduce peak loads by 67%, even considering solar forecasting uncertainty. In order to reduce the peak demand by the greatest margin, smart charging should consider future PV generation, charging demand, and uncontrollable loads.

A similar real-time algorithm can be employed to encourage EV users to use a greater portion of solar energy. In this control strategy, EV drivers would not be guaranteed to receive power from an EV charging station when they plug in, with the charging station. Instead, power delivered to EVs would be limited by the charging infrastructure. In this system, the speed at which EVs are charged will be dependent on the driver's Solar Friendliness Index, which is the proportion of energy used by the driver that comes from solar power [101]. This system would encourage people to charge at times when solar power is available, increasing utilization of renewable energy. Despite this benefit, the control strategy could artificially prevent some EVs from being charged before they need to depart, which could be frustrating to the drivers.

In order to determine the best control strategy while considering the limitations of the system, EV charging is often formulated as an optimization problem. The target of an optimization problem is finding a set of variables which minimizes an objective function subject to a set of constraints. These problems can be differentiated by the objective function which is optimized, the variables which are considered, and the constraints which are implemented. When considering demand response programs such as smart EV charging, there are a number of possible objective functions [90]. Some common objective functions which are considered include minimizing electricity cost, maximizing social welfare, and minimizing power consumption. The optimal energy to charge EVs at each time step can be solved using linear programming (LP). If charging is unidirectional, the problem can often be expressed without integer variables or non-linear constraints. If a linear objective function is chosen, the problem can be formulated as LP, where the decision variables

determine the amount of energy charged to each vehicle, and the constraints consider the requirements and limitations of the vehicles. Linear programming can be used with variety of possible objective functions, such as minimizing the total electricity cost [102], maximizing the power which can be delivered without violating electricity network limits [103] or minimizing the peak demand [104, 105].

Although many smart charging optimization problems use only continuous variables when unidirectional charging is considered, this is not sufficient to consider bidirectional charging. In the event that the charging and discharging rates or efficiencies are not the same, binary variables must be introduced which represent whether a vehicle is charging or discharging [104, 106]. This transforms the problem from Linear Programming (LP) to Mixed Integer Linear Programming (MILP). In these formulations, the power delivered to or from the vehicle battery is still considered to be a continuous variable. Some charging models do consider control strategies in which the vehicle charger is considered to be binary, either on or off based on the desired power regulation [107]. This strategy, however, may lead to issues with power quality due to the rapid changes in power consumption, so continuous charging power is usually preferred.

In both LP and MILP, it is assumed that the constraints are linear functions of the decision variables. This assumption is often not strictly the case. For example, the maximum charging power for a vehicle battery decreases as the battery approaches being fully charged. This change in maximum charging power as a function of stored energy results in the introduction of nonlinear constraints [108]. There are a number of possible strategies to solve nonlinear constrained optimization problems. One common approach is Particle Swarm Optimization (PSO) [109]. In PSO, a set of random solutions is modeled as a swarm of particles with a set of positions and velocities. The objective function is then evaluated for each particle, and the particles with the best value of the function are found. The position and velocity of each particle is updated as a function of it's misfit and the misfit of its neighbor in such a way that over time the swarm will tend towards the global optimum. A similar approach is known as Krill Herd optimization, which can also be used to reduce peak grid demand and reduce EV charging costs [110].

Another approach for solving nonlinear optimization problems is through the use of a genetic algorithm. A set of possible solutions is used to generate new solutions in a process that mimics natural selection. Over time, the set of solutions will evolve towards the optimum. This approach was used to find a charging strategy that maximizes the use of solar energy in a solar parking lot [50]. There are other nonlinear optimization approaches, such as the Maximum Sensitivities Selection approach, which minimizes system losses during EV charging by finding the sensitivity of the entire system to each EV charger. By prioritizing the EVs with the lowest sensitivities, overall system losses can be minimized [111]. This is able to reduce system losses while maintaining the grid demand below a maximum level. Ultimately, algorithms such as these can have a high computational cost and limited problem size [112]. It is therefore desirable to seek linear formulations for these optimization problems.

2.2.6. Smart Charging with Uncertainty

When formulating the EV charging schedule as an optimization problem, it is necessary to know future simulation inputs. This includes the value of future PV generation, uncontrollable loads, and EV arrivals and departures. In much of the research on smart charging, it is assumed that all of these factors are known accurately in advance [50, 104, 113]. In reality, this is often not the case. Optimization algorithms must be updated to account for this problem.

For PV generation and uncontrollable loads, the most simple approach is to use nominal optimization. In this strategy, the optimization algorithm is solved using the predicted values, and then executed using the actual results. This approach should work well if forecasting errors are small. A nominal optimization control strategy was used in the simulation of LomboXnet, with the assumption that the absolute error in PV forecasting was less than 10% of generated values [83]. It was found that this strategy was required solar errors to be below 20%, an unrealistically low value. Solar forecasting errors in the Netherlands will likely be closer to 40%–60%, as will be discussed in Section 3.1.5.

There are more advanced algorithms which allow for errors and uncertainty to be included in optimization problems, even when continuing to use LP or MILP techniques. One possible approach uses stochastic programming, which seeks to minimize the expected value of the objective function, considering a a set of inputs with errors given by known distribution functions. The expected value is found by considering a set of possible errors, determining the value of the objective function for each error, and finding the average of these values weighted by their likelihoods. This approach can be used to minimize power losses during smart charging of EVs with uncertain electricity demand, using quadratic programming [94]. Similar techniques can be used to minimize the variance of the total demand when charging known EVs while simultaneously

powering other uncertain electrical loads [102]. Although these studies were able to minimize their respective objective functions, there are drawbacks to the use of stochastic programming.

Stochastic programming can consider a range of possible uncertain scenarios, but the optimization problem considers only the expected value, and can therefore allow for high peak demand in the worst-case scenario. In order to ensure the minimum peak demand under uncertainty, robust optimization can be used. Robust optimization guarantees stability and performance over a range of possible uncertainties [114]. This can lead to improved worst-case scenario performance when compared to both nominal and stochastic optimization. Robust optimization has been used to schedule the charging of fuel-cell vehicles, considering the possible uncertainty in PV generation [115]. When seeking to minimize peak grid demand under all possible scenarios, robust optimization may enable the lowest peak load despite the uncertainty.

In order to be truly robust, however, the smart charging model must consider uncertainty in the charging demand of EVs, including the arrival time, departure time, battery capacity, and initial state of charge (SOC). Previous literature dealing with uncertainty has often not considered the demand for individual EVs [94, 102] or assumed that all this information is known in advance [83, 115]. These studies thereby assume that the unexpected arrival of EVs will not lead to a decrease in performance. This assumption is flawed. If vehicles with a high demand for electricity arrive unexpectedly at an inconvenient time, the peak electricity demand could increase significantly.

One approach to handle uncertain EV behavior is through the use of fuzzy logic. Fuzzy logic, in contrast to binary logic, uses variables with a value ranging between 0 and 1. Fuzzy logic can be used to establish a control strategy which works in complex, nonlinear systems, allowing for the mathematical formulation of general rules such as "when electricity is cheap, EVs should be charged faster." [116] Fuzzy logic can be used to establish a control strategy for EV charging which results in lower electricity costs and higher use of renewable energy. Fuzzy logic can also be used to enable EVs to support the electricity grid through improved frequency control [117]. Fuzzy logic can also be used to account for the uncertainty in EV behavior by transforming uncertain objectives and constraints into satisfaction functions of fuzzy constraints. Probabilistic models can be used to estimate arrival times, departure times, and initial SOCs, allowing for an optimization problem to be clearly defined even under uncertainty. When seeking to minimize charging cost, fuzzy optimization was able to handle this uncertainty robustly, achieving higher profits than the deterministic approach which did not consider uncertainty [118]. This study, however, did not compare the performance to an approach which considered uncertainty using non-deterministic approaches such as stochastic or robust optimization. Fuzzy logic also has a number of drawbacks [112]. Fuzzy logic controllers are only suitable for systems with a limited number of EVs. As the number of vehicles grows, the rule table becomes more complicated and the algorithm becomes less efficient. Furthermore, tuning the parameters of the fuzzy logic controller can be difficult to do accurately, and a poorly tuned controller will lead to sub-optimal results.

When using non-fuzzy logic, it is possible to determine an optimal charging strategy for EVs through a decentralized, or local, optimization scheme. In this approach, the optimal behavior is determined only for vehicles which have already arrived, rather than being planned ahead by a centralized controller. As vehicles arrive and depart, the optimal solution can be recalculated and updated, without forecasting or predicting future EV arrivals. When minimizing the total cost of charging, this solution was found to perform nearly as well as the optimal strategy with perfect information [119]. The performance of this technique improves with a larger number of EVs and with a smaller fraction of EVs which engaging in V2G. A similar technique was used to minimize peak electricity demand through peak shaving and valley filling with smart charging of EVs [120]. The study found that the peak shaving behavior was close to the optimal performance under some circumstances.

Decentralized optimization performs best when the EV properties are relatively homogeneous. These strategies have been proven to be optimal if all arrival times, departure times, and battery requirements are identical for each vehicle [121]. In cases where vehicle behavior is non-homogeneous, increasing variability and uncertainty can reduce performance. Many studies on decentralized optimization underestimate the possible uncertainty in EV charging demands. For example, reference [119] considers vehicles only with a battery of 16 kWh, charging stations of up to 5 kW, and charging durations of at least four hours. This means that all vehicles had some amount of flexibility in their charging behavior. It was also assumed that vehicles arrived uniformly throughout the day, without any significant spikes in arrivals at one time, which is clearly unrealistic. Reference [120] considers only PHEVs with a battery capacity of 10 kWh, and again assumes that all arrivals are uniform within a certain time window. This study found that peak shaving strategies performed best when arrival and departure times are all the same, with the peak load increasing as the charging duration becomes more variable. The peak load deviates significantly from the optimum if the arrival time range

for the vehicles is allowed to range from 20:00 until 5:00 the next day, for vehicles departing at 9:00. This estimation of arrival uncertainty was deemed "unlikely", despite the fact that no charging events of less than four hours were considered. As will be demonstrated in Section 3.2.1, charging events of less than four hours are quite common both in workplace and airport parking. This means that many charging events will be relatively inflexible.

The performance of smart charging algorithms decreases as PV forecasting and future EV charging behavior becomes more uncertain. The existing literature frequently underestimates this uncertainty, with respect to both PV generation and EV charging. More commonly, uncertainty is ignored altogether. This will lead to simulations overestimating the potential of smart charging, promising benefits which may not be attainable. In order to evaluate the potential of smart charging to reduce peak demand, detailed models are needed which consider realistic errors in solar forecasting and the inherent variability and unpredictability in EV charging behavior. Different smart charging algorithms can then be investigated. By constructing such a model, smart charging can be investigated under real-world conditions.

3

System Modeling

In order to use computer simulations to analyze a solar parking lot, it is important to develop a realistic model of this system. A computer model was therefore built which includes solar panels, battery storage, EV charging, lighting, and a connection to the electricity grid. This system is shown in Figure 3.1. In order to obtain meaningful results, care was taken to ensure that each component was modeled accurately, using a combination of real-world data and modeling practices from the literature.
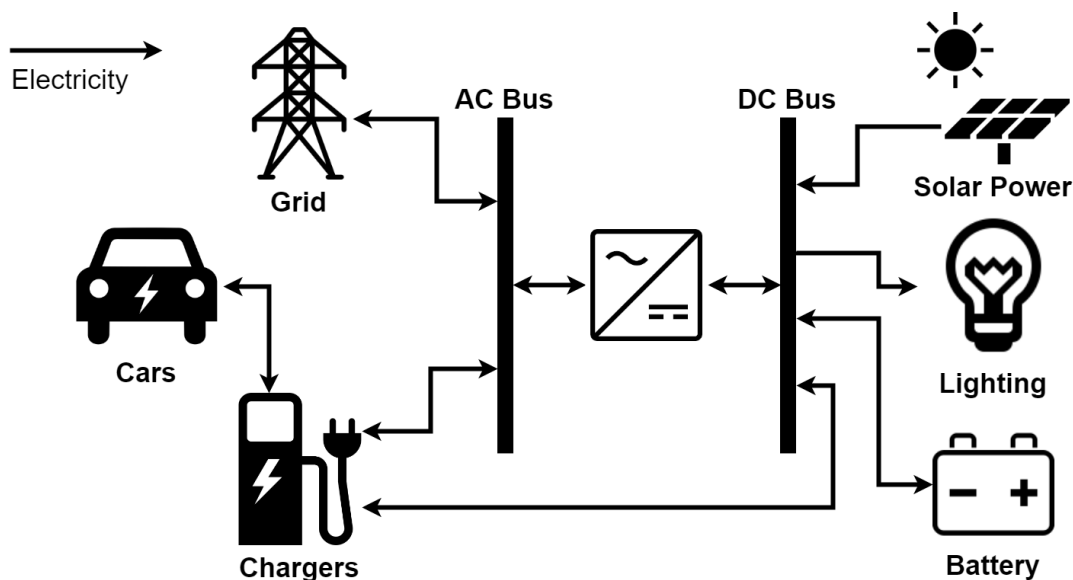
Figure 3.1: Diagram of the smart solar parking lot

In the system, energy is generated with a solar array built into a canopy mounted over the parking spaces. The solar panels are connected to a DC bus, which is also connected to fixed battery storage, some DC Electric Vehicle (EV) chargers, and the lighting system. The DC grid is also connected bidirectionally to the main AC electricity grid, which is connected to AC EV chargers.

This system was modeled using MATLAB, with values for solar generation, EV behavior, and lighting requirements created at discrete time steps of 15 minutes. This time resolution was chosen because charging demand and solar power generation are assumed to be reasonably static within such a short window, allowing for the model to balance accuracy and computational efficiency.

In total, 40 parking spaces were considered in this simulation. The number 40 was chosen as the size in order to strike a balance. If the simulated system were too small, then a single vehicle charging could substantially impact the peak demand, and the results might not be generalizable to larger systems. If the system were too large, computation time could be problematic. Considering these different concerns, 40 parking spaces was found to be a good size for this model. Note smart charging in a larger system can be

expected to reduce the peak demand at least as much as in this smaller system, since it could be broken down into several parking lots of 40 vehicles each.

The model was designed to realistically represent each component of the system. In this chapter, each component will be discussed individually. In Section 3.1, the solar energy generation will be discussed. Section 3.2 will then discuss the parking and charging behavior of EVs. Section 3.3 will discuss the EV chargers. Section 3.4 will discuss the fixed battery storage. Finally, Section 3.5 will discuss the other loads and losses which consume energy in the model. These components are combined to simulate the system as a whole. The overall system behavior will be dependant on the charging strategy being employed, which will be discussed in Chapter 4.

3.1. Solar Energy

Solar energy is clearly a critical component in solar parking lots. A realistic model of solar energy generation is therefore crucial.

3.1.1. System Design

The Photovoltaic (PV) modules which were simulated are Canadian Solar 60 cell CS6K-300 modules, with a nominal maximum power of 300 W, corresponding to an efficiency of 18.33% [122]. These modules were chosen because of their relatively high efficiency and good performance at low irradiance levels. In addition, having modules with 60 cells instead of a larger 72 cell module enables the panels to be installed with less cost and difficulty. The specifications of these modules are shown in Table 3.1 [122].

Table 3.1: Specifications for CanadianSolar CS6K-300 Solar Modules [122]

Specification	Value		Unit
	STC	NMOT	
Nominal max power (Pmax)	300	222	W
Optimal operating voltage (Vmp)	32.5	30.0	V
Optimal operating current (Imp)	9.24	7.40	A
Open circuit voltage (Voc)	39.7	37.2	V
Short circuit current (Isc)	9.83	7.93	A
Module Efficiency	18.33	16.95	%
Cell type	Mono-crystalline Si		
Cell arrangement	60 (6×10), 6 inch cells		
Dimensions	$1650 \times 992 \times 35$		mm
Weight	18.2		kg
Nominal module operating temperature (NMOT)	42 ± 3		°C
Temperature coefficient (Pmax)	-0.39		% / °C
Temperature coefficient (Voc)	-0.29		% / °C
Temperature coefficient (Isc)	+0.05		% / °C

The module placement and orientation is based on the design for the PowerParking project. The panels are all elevated with the lower edge 2.6 meters above the ground, oriented facing due south with a tilt angle of 13°. The solar canopies use a monopitch design, meaning that all panels are oriented in the same direction. This allows for the system to maximize energy generation.

The topology of the solar power installation is shown in Fig 3.2. The design for the system is based on the proposal for the PowerParking project at Lelystad Airport and Lelystad Airport Business park. The solar panels with power optimizers are collected into canopies, with each canopy covering four parking spaces, as seen in Fig. 3.2a. Each canopy contains 40 PV modules in a 5 by 8 grid. Since each solar module has a nominal power of 300 W, each canopy has a nominal power of 12 kW.

Because the PV system is connected to a DC microgrid, the solar canopies are not connected directly to an inverter. Instead, each module is connected to a module level DC-DC converter, sometimes referred to as a power optimizer, shown in Fig. 3.2b. The power optimizers adjust the DC output voltage of each module, ensuring that the module is operating at its maximum power point in a process known as maximum power point tracking (MPPT). If the solar modules were connected in series without power optimizers, each mod-

ule would need to operate at the same current. In this case, the power output of this string of solar modules would be limited by the module with the lowest output current. Shading, soiling, degradation, or module mismatch losses could then significantly reduce overall power generation [123]. With power optimizers, each module can operate at a different current, with the output current of the DC-DC converters remaining constant, reducing these losses. In addition, the optimizers can operate at a DC voltage close to the voltage of the solar modules, allowing them to be more efficient than micro-inverters, which must boost the input voltage to a much higher level so that it can be converted to AC power [44]. Commercial power optimizers from companies like SolarEdge can operate with an efficiency greater than 98%, and can operate as either buck or buck-boost converters depending on the model [124]. Power optimizers are frequently included in commercial installations, as their improved performance and higher-efficiency MPPT can increase the overall system yield.

(a) A single solar canopy with four parking spaces

(b) Solar module with power optimizer

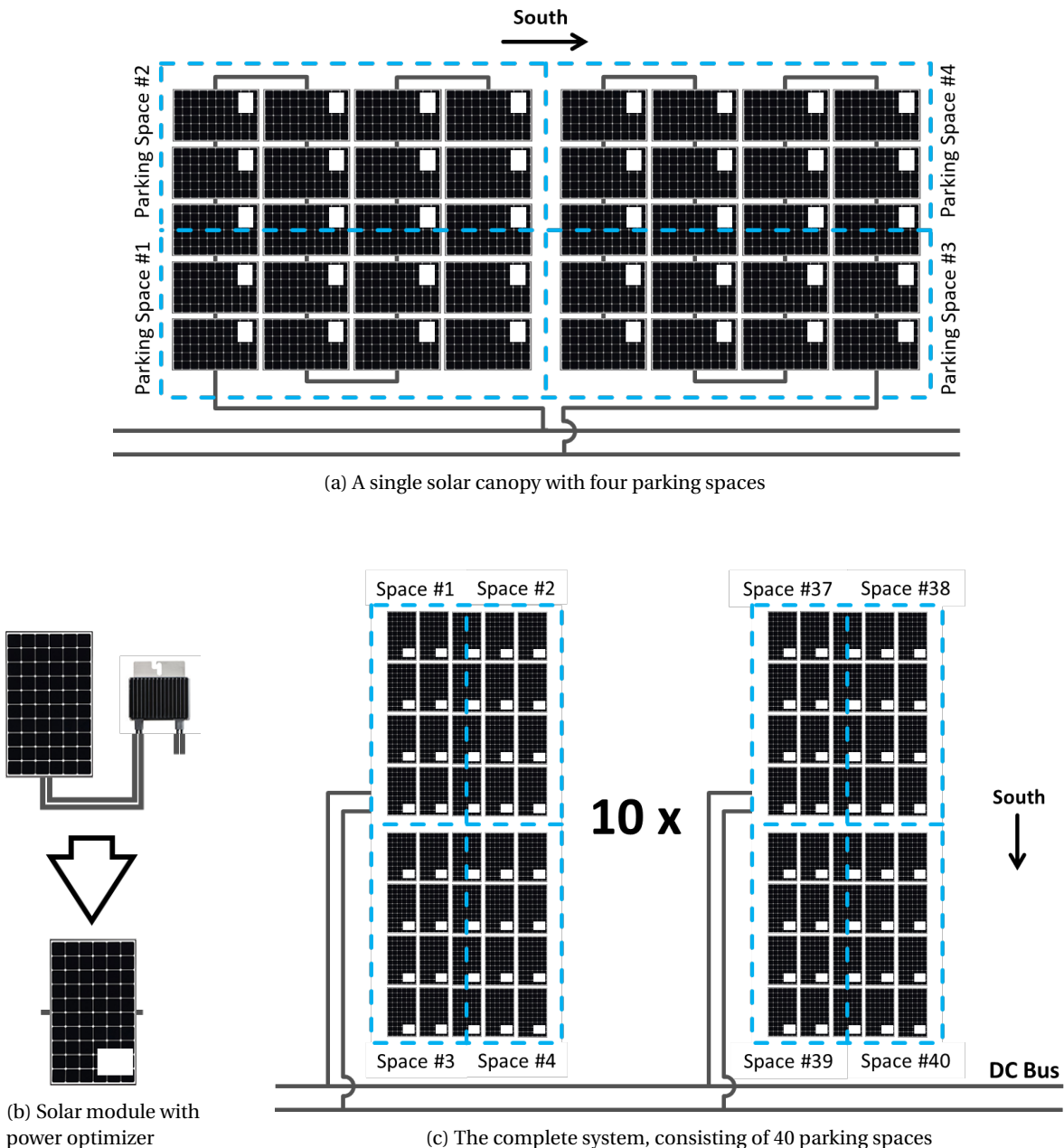(c) The complete system, consisting of 40 parking spaces

Figure 3.2: Diagrams showing the topology of the solar system in the parking lot

In order to reach a higher voltage, reducing resistive losses, the power optimizers in each canopy are

connected in series as seen in Fig. 3.2a. The solar canopies are then connected to each other in parallel, as seen in Fig. 3.2c. The connection of the canopies in series prevents the DC bus voltage from becoming dangerously high. In addition, this will prevent the system voltage from being affected if solar canopies are added or removed. In total, 10 canopies are considered in this system, covering a total of 40 parking spaces, with a nominal power of 120 kW. The canopies are connected to a DC bus, which connects further to the battery and lighting, and a central inverter to convert power from DC to AC. Because of the high peak power level in the system, multiple inverter units will be needed. The Canadian Solar CSI-66KTL-GS was selected due to its high efficiency and rated output power [125]. The specifications of this inverter are shown in Table 3.2. The inverters are rated to a CEC efficiency of 98.4%, with a peak efficiency of 98.8%. The rated and maximum output power for the inverter is 66 kW, so two of these inverters connected together would be able to output up to 132 kW of power, ensuring that if necessary all the solar power could be converted from AC to DC. Each inverter is also rated to a DC input power of 90 kW, giving the system a safety factor of 50%.

Table 3.2: Specifications for the Canadian Solar CSI-66KTL-GS Inverter [125]

Specification	Value	Unit
Inverter type	Grid-tie string inverter	
Grid connection type	3 phase / PE	
Peak efficiency	98.8	%
CEC weighted efficiency	98.4	%
Dimensions	$630 \times 1034 \times 354$	mm
Weight	78	kg
DC max input power	90	kW
AC max / rated output power	66	kW

The system is modular, and can be expanded without great difficulty. If more solar canopies are needed, they can be built alongside the old ones, and connected to the DC bus in parallel. This allows the system to scale easily according to the needs of the parking lot operator. Note that if the system is expanded too much, the current in the cables of the DC bus may exceed the rated capacity, and they may need to be replaced with higher capacity ones. Additional inverters may also be required if more power must be converted to AC.

3.1.2. Weather Data

Weather data is required to simulate solar power output. This requires the solar irradiance, including Direct Normal Irradiance (DNI), Diffuse Horizontal Irradiance (DHI), and Global Horizontal Irradiance (GHI). In addition, data on temperature, humidity, air pressure, and wind speed can be used to create a more accurate model.

In order to obtain highly accurate models for solar power, weather data was used from the Cabauw weather station of KNMI (*Koninklijk Nederlands Meteorologisch Instituut*, Royal Dutch Meteorological Institute), located in the province of Utrecht roughly 70 km southwest of Lelystad airport. [126]. This dataset includes weather data including DHI, DNI, GHI, dry bulb temperature, relative humidity, air pressure, and wind speed, recorded at one minute intervals since in 2005.

The weather data from Cabauw was used to create a Typical Meteorological Year (TMY), according to the procedures developed by the National Renewable Energy Laboratory (NREL) [127]. TMY data enables the simulation of the typical solar energy output for a PV installation. A TMY dataset is composed of 12 typical meteorological months, which are concatenated together. The data for each month is taken directly from historical data for that month in a previous year, without modification. This ensures that short term fluctuations and variations are considered. In the case of this report, data from 2009–2018 was used to construct the TMY dataset. For each month of the year, the weather in that month is compared across all the years. The month which has the most typical values for irradiance, temperature, and wind velocity is used. The exact manner in which the month is chosen is described by the User Manual for TMY3 Datasets [127]. For example, January 2014 was the most typical January in all the years examined. The data from January 2014 was therefore used in this model.

The weather data from Cabauw is has been gap-filled and validated by KNMI for temperature, pressure, windspeed, and humidity. For the irradiance data, some gaps were occasionally present. In this case, the months with missing irradiance data were not eligible to be chosen as the typical month in the TMY3 dataset.

However, the complete days from those months were still used to determine what a typical month looks like. For example, if 1–3 February 2012 was missing data from the weather data, 2012 would not be a candidate for the dataset for the month of February. However, 4–29 February 2012 would still be used to determine which February was the most typical. Once the weather dataset was created, the expected solar power output in a typical year was simulated.

3.1.3. Solar System Simulation

Solar power output is dependent on a number of factors, and can be modeled with a high degree of accuracy by various different software packages. This model uses PVLib [128]. This tool is developed as a toolbox addition to MATLAB by Sandia National Labs and is validated, open source, and able to model a number of different system topologies.

The first step in calculating solar energy is determining the position of the sun. This is a function of the location and the time. However, the apparent position is also a function of atmospheric refraction, which is dependant on temperature and pressure. This data was used to calculate the sun azimuth and altitude at each minute, using the *pvl_ephemeris* function. The altitude was then used to calculate the air mass, which represents the amount of air which absorbs solar radiation as it travels through the atmosphere. The relative airmass was calculated using the method the method described by Kasten and Young in 1989, which is the default method in PVLib [129]. Using the tilt and azimuth of the solar array, and the zenith and azimuth of the sun, the angle of incidence on the solar array was calculated. This was done using the equation:

$$\cos(\text{AOI}) = \cos(a_M)\cos(a_S)\cos(A_M - A_S) + \sin(a_M)\sin(a_S) \tag{3.1.1}$$

where A_M and A_S are the azimuth of the solar module and sun respectively, and a_M and a_S are the altitude of the module and sun respectively [44].

The solar radiation which is incident on the modules can be broken into three main components: beam radiation, which comes from direct sunlight; diffuse radiation, which comes from the rest of the sky excluding direct sunlight; and ground reflected radiation, which is the sunlight that reflects onto the panels from the ground in front of them. Beam radiation is a function of DNI, along with the Angle of Incidence (AOI), which is the angle at which the sunlight reaches the solar panels:

$$E_{\text{beam}} = \text{DNI} \cdot \cos(\text{AOI}) \tag{3.1.2}$$

Next, the diffuse radiation, E_{diffuse} is calculated. This is the radiation which is incident on the Plane of Array (POA) for the solar panels. POA diffuse radiation is only a fraction of the DHI, because the tilt of the modules themselves blocks out some of the diffuse radiation. Calculating the POA diffuse radiation requires knowledge of where in the sky the diffuse radiation originates. There are a number of solar radiation models, and the one chosen was first described by Perez et al. in 1990 [130]. In an empirical test of the most common models, Perez 1990 was found to have the highest overall accuracy [131]. The model depends on the apparent solar position, which takes into account distortion of light through the atmosphere as a function of air pressure and temperature. In addition, the model considers the array orientation and tilt, the DHI, the DNI, and the time of year.

The ground reflected radiation is dependent on the module orientation and the GHI, along with the albedo of the ground. The albedo is the fraction of incident light which is reflected by a surface, with an albedo of 1 being completely reflective and an albedo of 0 reflecting nothing. Asphalt, which is a typical material for parking lots, has an albedo around 0.1 (in comparison to grass which is approximately 0.2 and concrete which is approximately 0.3) [132]. The ground reflected radiation is given by:

$$E_{\text{ground}} = \text{GHI} \cdot \alpha \cdot 0.5(1 - \cos(\theta_M)) \tag{3.1.3}$$

Where GHI is the global horizontal irradiance, α is the albedo, and θ_M is the module tilt angle [44]. The total irradiance which is incident on the solar panel is then given by:

$$E_{\text{total}} = E_{\text{beam}} + E_{\text{diffuse}} + E_{\text{ground}} \tag{3.1.4}$$

The efficiency of solar modules depends on the cell temperature, with power decreasing by 0.39% per degree as seen in Table 3.1. The cell temperature was calculated using the Photovoltaic Array Performance Model developed by Sandia National Laboratories [133], which considers the module parameters, illumination, ambient temperature, and wind speed. Using this model, the cell temperatures were modeled for each

time interval. Given the temperature of the cells, a new IV curve was calculated based on the temperature, the irradiance, and the module parameters. This was done using the five-parameter De Soto model [134], which is more accurate than the four-parameter model [135]. This model assumes a single-diode equivalent circuit for a solar cell, and allows for the calculation of the voltage and current and the maximum power point to be calculated at each time step. The single-diode model is frequently used in the modeling of photovoltaic systems, as it offers a good compromise between accuracy and simplicity [136]. The equivalent circuit for the single-diode model can be seen in Figure 3.3 [134].
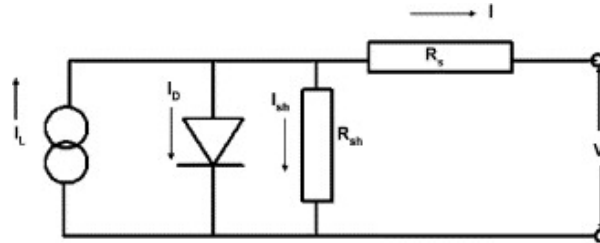
Figure 3.3: Single diode equivalent circuit for a solar cell [134]

The simulation must further consider that some of the incident light is reflected due to soiling on the panels. The amount of energy lost due to soiling is heavily dependent on the location, and is a factor of rainfall, air pollution, and the surrounding environment [137]. Although the Netherlands has a relatively low level of air pollution and a high annual rainfall, a conservative value of 2% is taken for soiling losses. Note that the light which is blocked by soiling does not contribute to energy generation, but nonetheless warms the panels.

Further losses were then considered. Resistive losses in the system are dependant on the system topology and therefore difficult to calculate without an exact knowledge of the configuration. For simplicity, these losses were assumed to be a constant 3%. Furthermore, MPPT and DC-DC conversion losses in the power optimizers were assumed to be 2%, based on typical literature values [44] and values from manufacturers of power optimizers [124]. It is assumed that there are no surrounding buildings or trees which would shade the panels, and because there is only a single row of solar canopies the modules are not able to cast a shadow on each other. Therefore, shading losses were not considered.

3.1.4. Solar Power Output
The net daily generation, along with the average daily generation for each month and the year as a whole, can be seen in Figure 3.4.
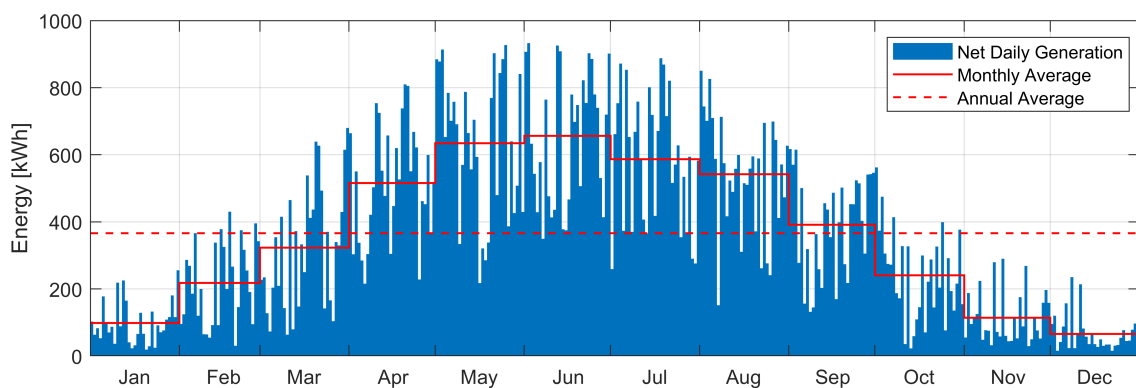
Figure 3.4: Net solar energy generation on each day of the year, as well as monthly and annual averages

Over the course of a year, the system generates 133,625 kWh, which is an average of 366 kWh per day. Since the system has a nominal power of 120 kW, this production is equivalent to 3.05 sun hours per day. This corresponds to a capacity factor of 12.7%, which is typical for the Netherlands [44]. Naturally, the solar power

output is very dependant on the season. During June the system had an average daily output of 657 kWh, a capacity factor of 22.8%. During December, on the other hand, the average daily output was only 65 kWh per day, or 2.3%. Thus, generation during the sunniest month is ten times higher than it is during the least sunny month.

The average system efficiency is 16.9%, which is quite close to the Nominal Module Operating Temperature (NMOT) efficiency of 16.95%. Compared the nominal efficiency of 18.33% for the PV modules, the performance ratio of the system is 0.92. This high value for the performance ratio can be explained by a few factors. First, because the modules are connected to a DC microgrid, inverter losses are not considered as part of the PV system. Furthermore, the use of power optimizers on each module instead of a centralized maximum power point tracker means that MPPT losses are quite low. In addition, modules were specifically chosen which have a relatively high power output under low irradiance, which reduces irradiance losses and gives the system a higher average efficiency in a cloudy location like the Netherlands. And finally, the open-backed mounting system in the solar canopies, combined with the high wind speeds and low air temperatures, means that the cell temperatures in the system are almost always below the nominal operating module temperature of 45° C, which reduces the temperature losses.

Weather data was recorded at one minute intervals, and the power generation for the typical meteorological year was calculated at that same resolution. Because the simulation has a time step of 15 minutes, the minutely PV data was integrated to give the average power over each 15 minute interval. For the purpose of the simulation, generation is assumed to be constant within each time interval.

3.1.5. Forecasting Solar Energy

When considering the accuracy of a solar forecast, two metrics were used: The Root Mean Square Error (RMSE), and the Mean Bias Error (MBE). These metrics are commonly used in literature in order to quantify the errors in solar forecasting [138, 139]. The RMSE is the square root of the mean of the square of the errors, and is analogous to the standard deviation. The RMSE is therefore observable in the spread of forecasting errors, with a larger RMSE corresponding to greater over- and underestimations. The MBE is simply the average of the errors, and is analogous to the mean. A negative MBE means that most forecasts are below the true generation, whereas a positive MBE means that forecasts are typically greater than the real results.

(a) Root Mean Square Error (RMSE)   (b) Mean Bias Error (MBE)
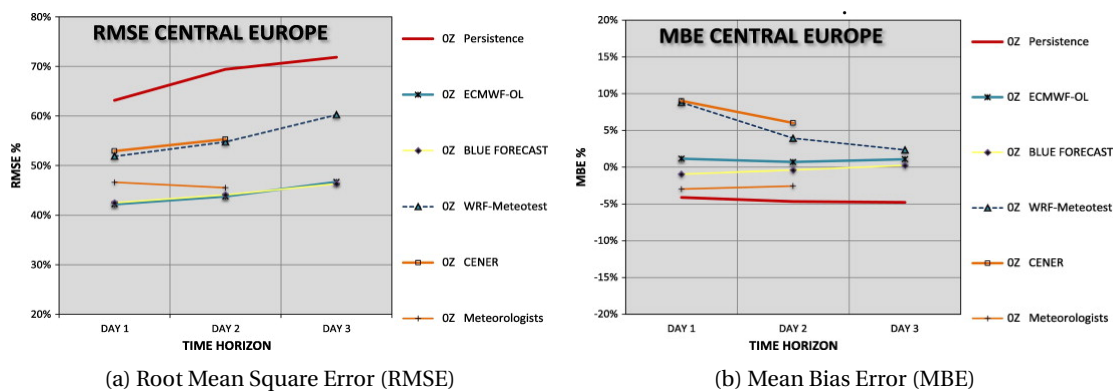
Figure 3.5: Typical errors in central Europe for solar forecasts made at midnight for the upcoming day [139]

Figure 3.5 demonstrates the accuracy of solar irradiance forecasting in central Europe [139]. In Germany, Austria, and Switzerland, forecasts one day ahead which are made at midnight typically have an RMSE of 40%–60% and an MBE of -5% – 10%. These quantities are given as a percentage of the average daily generation. In this simulation, solar uncertainty was therefore typically assumed to have an RMSE of 50% and an MBE of 0%, although a range of values was investigated.

In order to demonstrate the impact of different forecasting errors, Figure 3.6 compares the forecasted values of total daily generation with the true values. The forecasted values are taken from simulated forecasts of the following 24 hours, starting at midnight, which are generated using the process described below. As can be observed, a higher value of the RMSE results in a wider range of errors, with more days where the forecasted generation is high but the actual generation is low and vice versa. MBE, on the other hand, does not affect the spread of the forecasting errors. Instead, it affects the expected difference between the forecasted and actual generation. When the MBE is positive, forecasted generation is on average higher than actual generation, as

evidenced by the fact that most days are above the diagonal black lines. When the MBE is negative, on the other hand, forecasted generation is on average below the actual generation, with most days sitting below the diagonal line.

(a) 20% RMSE, 0% MBE   (b) 40% RMSE, 0% MBE   (c) 60% RMSE, 0% MBE

(d) 50% RMSE, -10% MBE   (e) 50% RMSE, 0% MBE   (f) 50% RMSE, 10% MBE
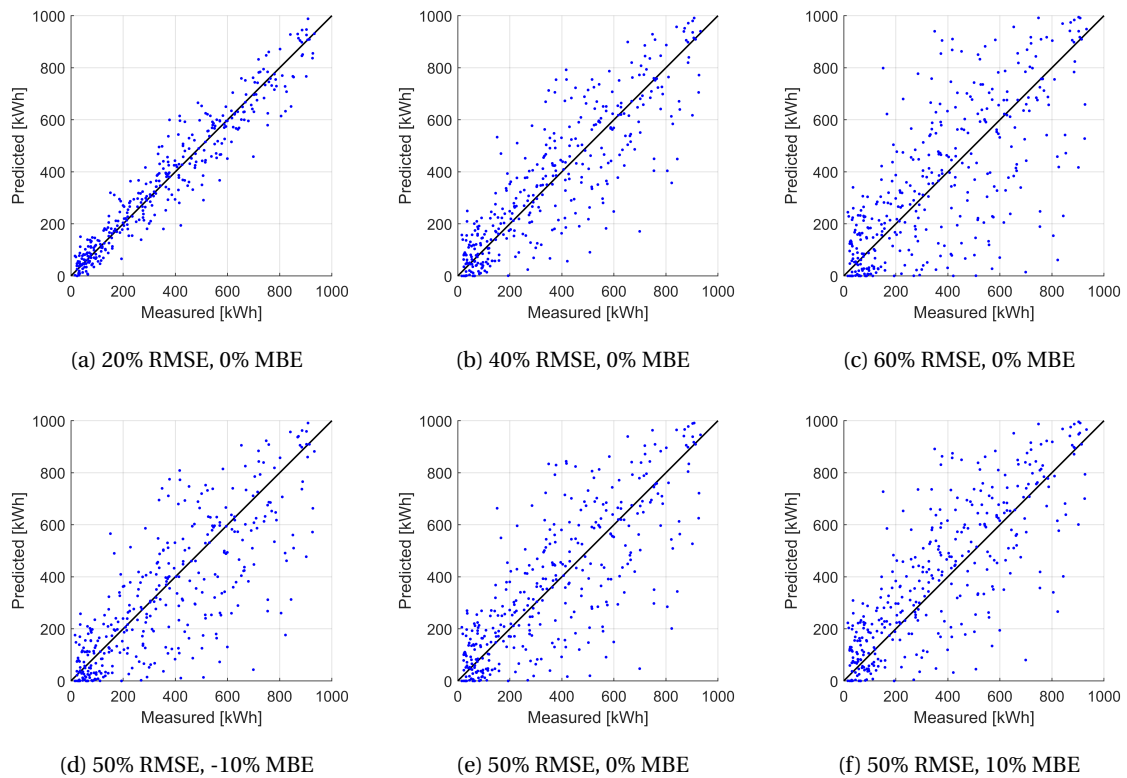
Figure 3.6: Forecast vs. reality for net daily generation with different forecasting errors

In order to simulate the system behavior under uncertainty, it is important to accurately generate forecasts of solar energy in a way which realistically resembles real-world solar forecasting errors. Much of the forecast which was generated was dependant on the value for clear sky generation. This represents that energy which would have been generated under ideal, cloudless conditions, and is a function of the time, date, and location. The clear sky generation, compared to the actual generation, is shown in Figure 3.7. To illustrate the changing clear sky generation over the course of the year, the 15th day of each month is presented.
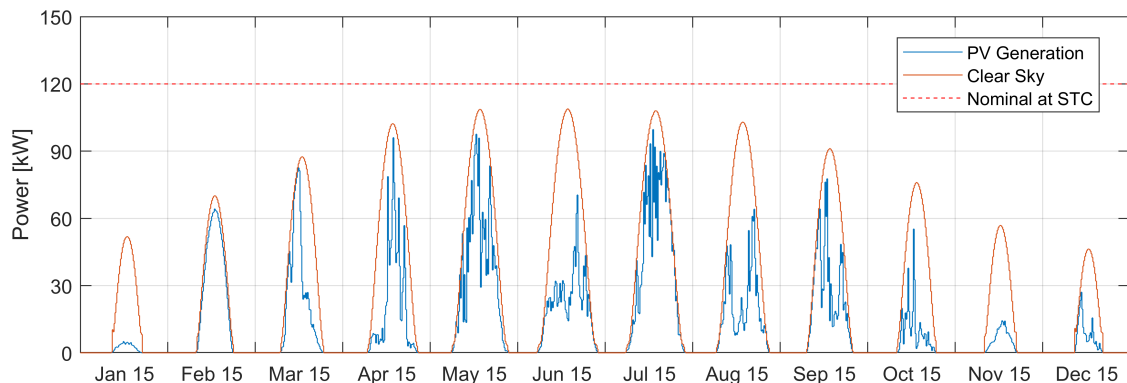
Figure 3.7: Clear sky and actual irradiance over the course of the year

The clear sky values for clear sky DHI, DNI, and GHI were generated using the method given in [140]. This

method relies on the Linke Turbidity Coefficient, which is used to determine atmospheric transmittance, the amount of light which can pass through the atmosphere. The transmittance depends on factors such as air mass and humidity. For the purposes of this simulation, the clear sky generation was intended to describe the maximum possible energy generation at a given moment. Therefore, a constant value of 2.5 was chosen for the Linke Turbidity coefficient. Lower values of the coefficient correspond to a higher level of irradiance, and 2.5 was the minimum value of the course of the year for this location. This value appears to consistently represent the maximum theoretical generation over the course of the year. Once the clear sky irradiance was known, it was used to simulate the clear sky generation using the same methods described previously to simulate solar power generation.

Based on the clear sky generation, simulated forecasts of future solar power generation were made. To illustrate these forecasts, some some example days are shown in Figure 3.8. These foreasts have an RMSE of 50% and an MBE of 0%.
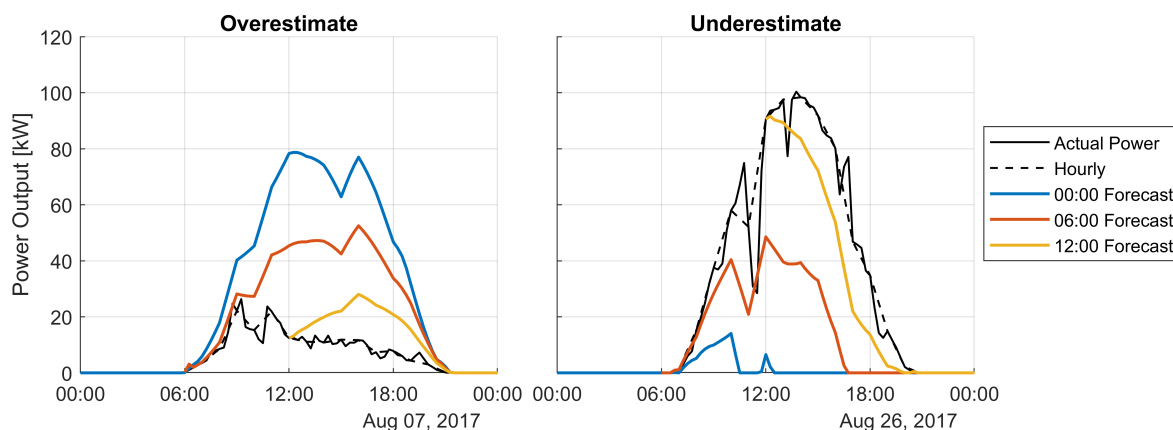
Figure 3.8: Solar generation forecasts made at different times of day, compared to the true generation

Three forecasts, made at at at midnight, 6 AM, and noon, are compared with the actual power which is generated. As can be observed, the forecasting errors are greater in the further future. This means that the predicted generation at 3 PM is most accurate with the forecast made at noon, less so with the forecast made at 6 AM, and most inaccurate with the forecast made at midnight. It is possible for forecasts to significantly over- or underestimate the generation over the course of a day, although forecasts are correct on average over the course of a year.

Because weather data is not accurately available at 15 minute intervals very far in advance, it was assumed that the forecast was given hourly. In order to base the forecast off of hourly data, values exactly on the hour were considered for the forecast, with the intermediate time steps interpolated linearly. Because forecasts are based only on hourly predictions, whereas the control strategy updates every 15 minutes, it is possible that variations within an hour can lead to larger errors at individual time steps.

Solar forecasts were then generated by adding normally distributed random errors to the hourly values of PV generation. The errors generated were proportional to the clear sky generation values, and mean and standard deviation for the normally distributed errors were chosen based on the desired accuracy of the forecasts. When considering the error, it is necessary to consider both the errors at each time step and the net error over the course of the day. For this reason, two errors were introduced at each time step: daily errors, which are the same at every time step throughout the day, and hourly errors, which are independently generated for each hour and linearly interpolated to 15 minute intervals. Both kinds of error are normally distributed and proportional to the clear sky generation. The magnitude of the errors was scaled linearly based on the time until the predicted value, so that forecasts are less accurate in the further future. It was found that the hourly errors should have a standard deviation 20% of the daily error in order to mostly closely remember the errors in literature [138]. Forecasts were then truncated so that they are always between zero and the clear sky generation. It was also assumed that the generation forecast at the present time step is always accurate, because the system generation can be monitored in real time.

Once the forecasts were simulated, the forecasting errors were quantified in order to develop a charging strategy which is able to reduce the peak demand despite this uncertainty. The forecasting error at each time

step was calculated as a fraction of the clear sky irradiance, in order to normalize the errors with respect to the time of day and year. The standard deviation of these errors is then determined as a function of the time since the forecast was made, as the errors increase at time steps further in the future. Example days with forecasts made at 6 AM, displaying the range of one, three, and five standard deviations around the forecasted generation are shown in Figure 3.9.
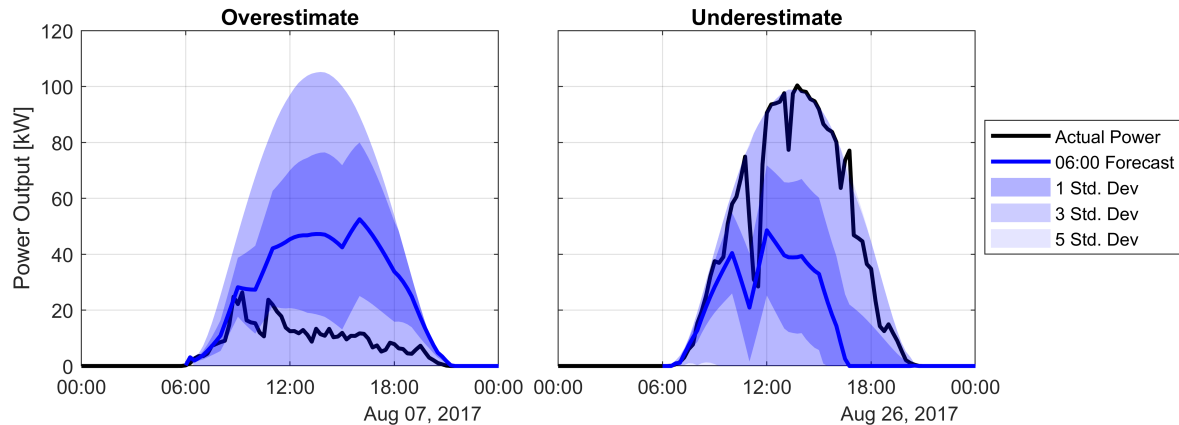
Figure 3.9: Comparison of different standard deviations of forecasting error in solar power production

The range of uncertainty for power generation is limited to being between zero and the clear sky generation. The standard deviation grows wider over the course of the day, because forecasting uncertainty is greater for time steps further in the future. In addition, the standard deviation is dependant on the clear sky forecast. At times when very little solar generation is possible, the forecasting error must be smaller. As can be observed, almost all possible days are within three standard deviations of the forecasted generation, even on days with very large forecasting error. Using these simulated solar generation forecasts, with a quantified range of forecasting errors, it is then possible to develop a smart charging strategy which is able to minimize the peak electricity demand under uncertainty.

3.2. Electric Vehicle Behavior

In order to realistically simulate electric vehicle charging, it is necessary to accurately model the parking and charging behavior of the EVs. The possible methods and techniques for modeling EV behavior are described in Section 2.2.1. For this report, vehicle modeling will be done using a Monte Carlo simulation, with randomly generated vehicle behavior generated based on real-world data, as a Direct Use of Observed Activity-Travel Schedules (DUOATS) model. In every instance, an effort has been made to ensure that the generated behavior of the vehicles is realistic. This is necessary because overly simplified EV behavioral models can lead to a simulation that does not capture the reality of the requirements for EV charging.

In a DUOATS model, it is important to consider that the behavior of electric vehicles may be fundamentally different than that of conventional vehicles. For this reason, data from EVs should be used whenever possible. In this model, two different parking locations were considered. The first location is an airport long-term parking facility, and the second location is a workplace parking lot. For airport long-term parking, no adequate EV-only dataset could be found. Instead, vehicle behavior is based on data from Boston-Logan International Airport [141]. It is assumed that the long-term parking behavior at Logan would be similar to other major airports, including those in the Netherlands. For the input data in this model, data from only Economy Parking was used, as this parking garage is primarily for long term travelers, with 87% of vehicles remaining parked for more than 24 hours.

For workplace parking, vehicle behavior was modeled on data from the EV project, a project run by the United States Department of Energy from 2009 to 2013 which contains data for 8,228 electric vehicles with hundreds of thousands of trips and charging events [142]. This data was broken down into four categories: private residential, private nonresidential, public, and DC fast charging. For this model, only private non-residential is considered, which is the type of parking that might be available at an office parking lot. It is assumed that commuting patterns for office workers in the United States would be relatively similar to those in the Netherlands. For both airport and workplace parking, weekdays and weekends are treated separately.

For each vehicle, four pieces of data were considered: the arrival time, the departure time, the state of charge when the vehicle begins charging, and the battery capacity.

3.2.1. Arrival and Departure Times

The arrival and departure times are generated using a Monte Carlo simulation, based on arrival and departure rates which are based on historical parking data. Rates were calculated separately for an airport and for a workplace. Historical data is frequently used when modeling EV parking behavior [65, 143]. For simplicity, some authors assume that vehicle arrival and departure rates are given by simple Gaussian functions, for example assuming that vehicles arrive with a peak time of 18:00 and a standard deviation of five hours [108]. Another model assumes that the arrival and departure rates are Gaussian functions with a standard deviation of one hour and peaks at 9:00 and 17:00 respectively [104]. This technique ignores the reality that vehicles will arrive and depart throughout the day, likely with multiple peaks. The arrival and departure rates which are used in this model are shown in Figure 3.10. The arrival, departure, and net occupancy rates are in terms of the percentage of total parking spaces per hour.
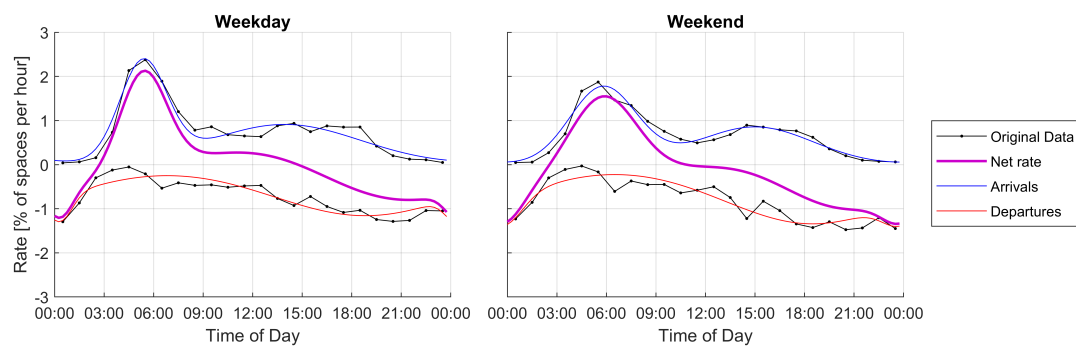
(a) Long-term airport parking
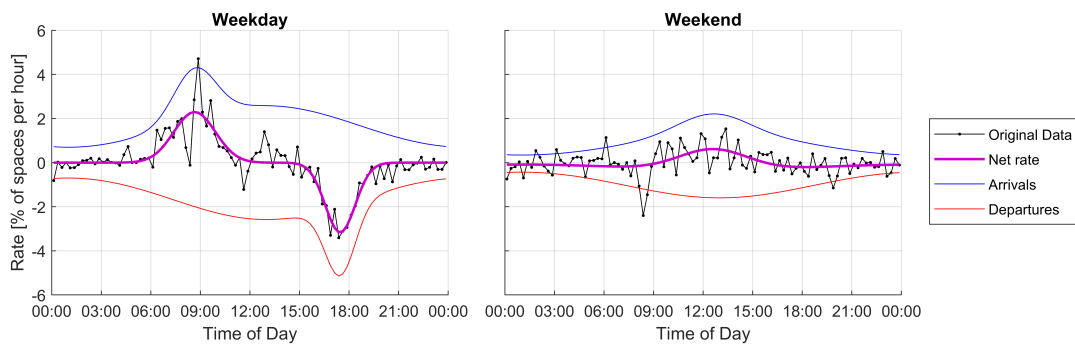
(b) Workplace parking

Figure 3.10: Arrival, departure, and net occupancy rates for EVs

In airport long-term parking, arrival and departure rates are based on one month of data from Boston Logan International airport, which measures the number of vehicles arriving and departing every hour [141]. The arrivals and departures were separated by whether it was a weekday or weekend, and used to generate a Gaussian mixture model, approximating arrivals and departures each as the sum of two Gaussian functions. The arrival and departure rates for long-term airport parking are shown in Figure 3.10a. For workplace parking behavior, data was used from the EV Project, which gave the total fraction of charging stations which were occupied every 15 minutes [142]. By calculating the change in median occupancy at each time step, it is possible to calculate the net rate of arrivals minus departures. For example, if the number of vehicles increases from 11% to 12% over a fifteen minute interval, the change in the net occupancy rate is 1% per fifteen minutes, or 4% per hour. Although the net rate is known, at each time step there are vehicles both arriving and departing, and it is necessary to consider the rates separately. EV project data also includes the total number of vehicle arrivals. Given that the arrival rate integrated over a day will be equal to the total arrivals, it is possible to approximate the arrival and departure rate independently as the sum of two Gaussian functions, as

shown in Figure 3.10b, again considering weekends and weekdays separately.

Once the arrival and departure rates are known, the arrival rates are scaled to control how full the parking lot is. Through trial and error, it was determined that in a parking lot of 40 spaces, the peak rate should be 10 vehicles per hour in a workplace and 1 vehicle per hour in an airport. At these rates, the parking lot is full at the busiest times, but with space consistently available at off-peak hours. The number of vehicles arriving at a given time step can be generated using a Poisson distribution [109]. In this model, time steps are separated at 15 minute intervals, and the arrival time for each new vehicle is chosen at random assuming a uniform distribution of arrival times between the current time step and the next. If there are not sufficient open spaces, then the vehicles fill up the parking lot and the remaining vehicles will go park elsewhere.

In addition to the arrival time, it is also necessary to know the departure time for the vehicles. In some models in the literature, the departure times are chosen randomly from a normal distribution [95, 104, 118]. Less commonly, models can consider the time between a vehicles arrival and departure, assuming that the parking duration is normally distributed [144]. In reality, the probability of departure should be based both on the time of day and on the parking duration, a consideration often ignored in previous literature. The departure rates as a function of the time of day are shown in Figure 3.10, and the distribution of parking durations are shown in Figure 3.11.
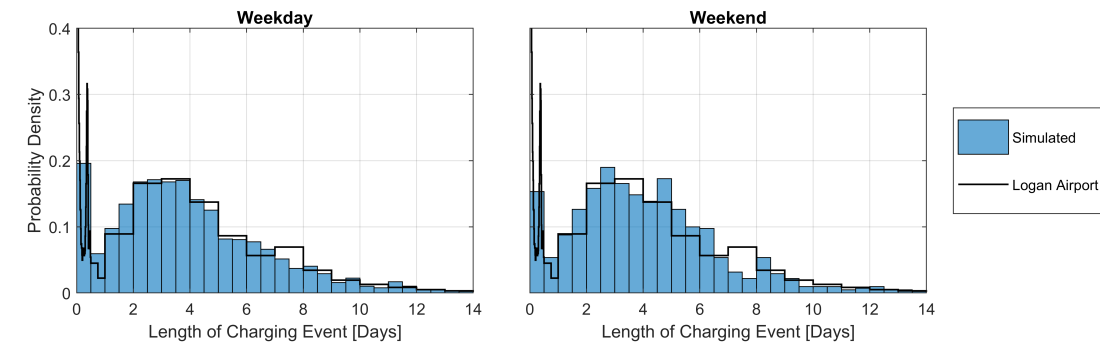
(a) Parking duration at long-term airport parking
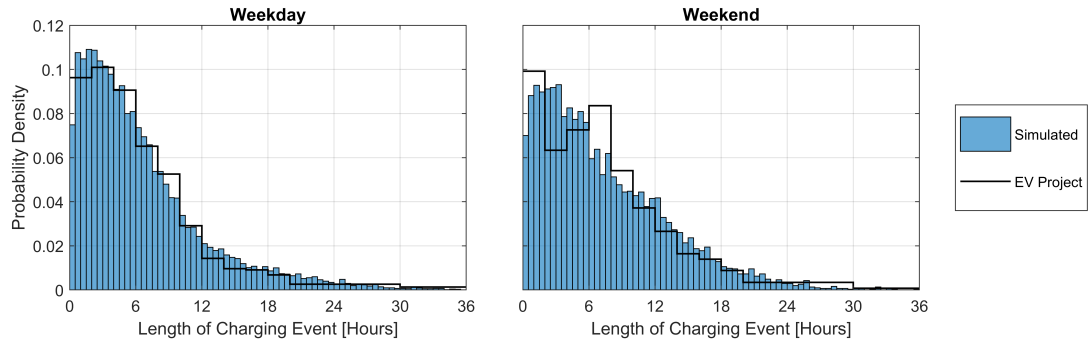
(b) Parking durations at work

Figure 3.11: Parking durations for EVs

At every time step it is randomly determined whether each vehicle will depart or not, with the probability of departure at a given time $p_d(t)$ is based on the departure rate $r_d(t)$ and the average number of vehicles present at that time $N(t)$. However, this probability must also consider the time since the vehicle parked. This model introduces a novel technique to incorporates the parking duration, with the use of a scaling factor $g(t - t_a)$ which is a function of the time since the arrival time t_a. The overall probability is then given by:

$$p_d(t) = \frac{r_d(t)}{N(t)} \cdot g(t - t_a) \tag{3.2.1}$$

For example, if there is a time of day when 20 vehicles are typically present, a departure rate of 2 vehicles per hour would correspond to a departure probability of 10% per hour for each vehicle, multiplied by the dimensionless scaling factor which differs for each vehicle. The value of this function was adjusted through trial and

error such that the distribution of parking durations was comparable for the simulated and measured data. The scaling function is given by:

$$g(t - t_a) = \begin{cases} \min(0.7 + 0.1(t - t_a), 1.3) & \text{Work Weekday} \\ \min(0.8 + 0.15(t - t_a), 2.5) & \text{Work Weekend} \\ \min(0.014(t - t_a), 1.4) + 3 & \text{Airport, } t - t_a < 3 \\ \min(0.014(t - t_a), 1.4) & \text{Airport, } t - t_a \geq 3 \end{cases} \tag{3.2.2}$$

A constant value of $g(t - t_a) = 1$ would imply that the departure probability is independent of the time since arrival. In reality, $g(t - t_a)$ begins at a value below one, as the vehicle is less likely to depart right after it arrives. The value then increases linearly until it reaches a certain maximum value. This value is greater than one, because vehicles which have been parked for a long time are more likely to depart soon. At the airport, there is a significantly increased likelihood of departure in the first three hours after arrival, representing the vehicles which are picking up or dropping off people at the airport. Once a vehicle has been parked for more than three hours, it is likely that the vehicle will remain parked long term.

Vehicle arrivals and departures were generated for a full year. At each time step, it is randomly determined whether each vehicle will depart or not, based on its individual departure probability. The departure time for each vehicle is chosen at random assuming a uniform distribution of departure times between the current time step and the next. A vehicle cannot depart in the same time step during which it arrives, and once a vehicle departs no new vehicle can park in that space until the subsequent time step. A typical week of occupancy for both the airport and the workplace parking lot is shown in Figure 3.12.
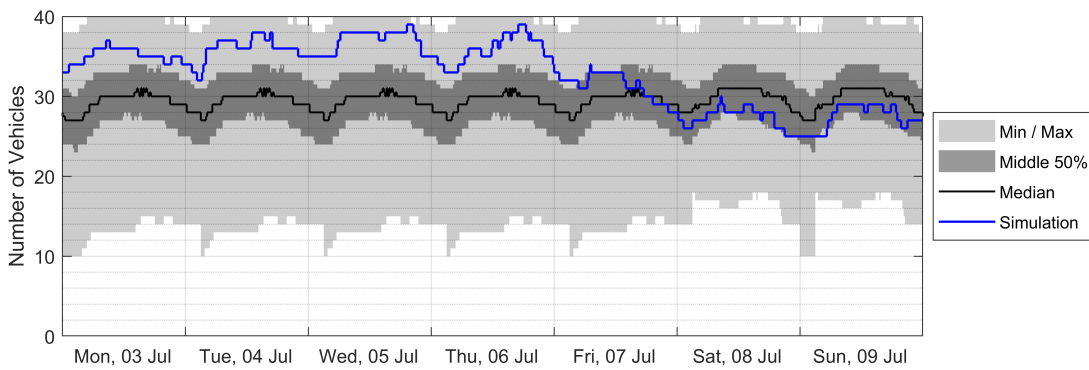
(a) Airport long-term parking
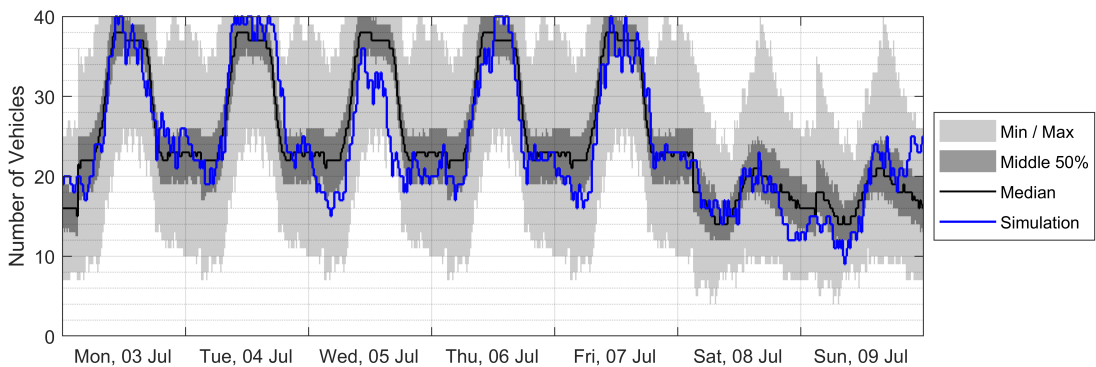
(b) Workplace parking

Figure 3.12: Typical week of simulated parking data

Note that in airport parking, there is little variation over the course of a single day, with the occupancy varying over a longer timescale. In addition, weekend and weekday parking are relatively comparable. At a

workplace parking facility, there are clear patterns of arrivals and departures during weekdays, with weekends having lower arrival rates.

3.2.2. Battery Capacity

In order to model the capacity of EV batteries, a constant battery size is often assumed [94, 145]. For the sake of accuracy, this model uses the distribution of electric vehicles currently registered in the Netherlands. The quantities of electric vehicles, as of January 31 2019, are shown in Table 3.3 [146, 147]. The information for the vehicle registrations is taken from the Netherlands Enterprise Agency, or RVO (*Rijksdienst voor Ondernemend*) [146]. Although battery capacities for the vehicles are publicly available from the manufacturers, vehicle batteries are often prevented by software from fully charging or discharging to prevent battery degradation. The fraction of the battery which can be used is known as the usable capacity, which is the capacity considered in this report. The usable capacity is not publicly available, but can be determined through hardware tests, which have been done for many models. The results of these tests are compiled through the EV Database, a resource cited by the RVO in their reports [147].

Table 3.3: Data for EVs registered in the Netherlands, January 31 2019 [146, 147]

Type	Brand	Model	Number	Battery [kWh]	Usable [kWh]
PHEV	Mitsubishi	Outlander	24,167	12	9
	Volvo	V60	14,082	11.2	8
	Volkswagen	Golf	10,928	8.7	7
	Volkswagen	Passat	8,060	9.9	8
	Audi	A3	6,430	8.8	7
	Other PHEV		33,992		
	Total PHEV		**97,659**		
BEV	Tesla	Model S	12,873	75 / 100	72.5 / 94
	Nissan	Leaf	5,786	40	38
	Tesla	Model X	4,629	75 / 100	72.5 / 94
	Volkswagen	Golf	4,174	35.8	32
	Renault	Zoe	3,847	41	37
	BMW	i3	3,552	22 / 33	18.8 / 27.2
	Jaguar	I-Pace	3,505	90	84.7
	Hyundai	Ioniq	2,579	30.5	28
	Opel	Ampera	1,193	60	58
	Hyundai	Kona	1,087	67.1	64
	Other BEV		5,243		
	Total BEV		**47,381**		

Vehicles are generated randomly based on their frequency as given in Table 3.3. It is assumed that all types of vehicle are equally likely to charge; that is, the fraction of charging events which involve a BEV is equal to the fraction of EVs which are a BEV. Because the RVO data does not include all EVs, but only the most popular models, it is assumed that PHEVs where the model is not known have a battery size distribution which is the same as other PHEVs, with the same being true for BEVs. For PHEVs, this is likely given the homogeneity of battery sizes. For BEVs, almost 90% of registered vehicles are represented by this list, so the vehicles not listed should not significantly change the distribution. The Teslas, as well as the BMW i3, have multiple possible battery sizes which are available to consumers. It is assumed that for these vehicles that half of all vehicles have contain one of the available battery sizes, and half have the other.

It is worth noting that the landscape of EVs is changing rapidly in the Netherlands. For example, the Tesla Model 3 does not even appear on the list of EV registrations, because it was not present in the Netherlands until February 2019. It is now one of the best selling EVs in the country, and is already in eighth place on the list of most common BEVs [16]. Furthermore, PHEVs currently make up the majority of all electric vehicles in the Netherlands, but the number of PHEVs has been slowly declining since December 2016, while the number of BEVs has been growing exponentially, as seen in Fig. 2.4. As BEVs with larger batteries become increasingly affordable and the fraction of PHEVs decreases, charging requirements may change significantly.

3.2.3. Initial State of Charge

The battery state of charge (SOC) is defined as the energy which is stored in a battery as a percentage of the the usable capacity. The initial SOC, at the time when the vehicle begins charging, was simulated as being randomly drawn from a truncated normal distribution, with the parameters based on historical data from EV studies. The distributions of the initial SOC are shown in Figure 3.13.
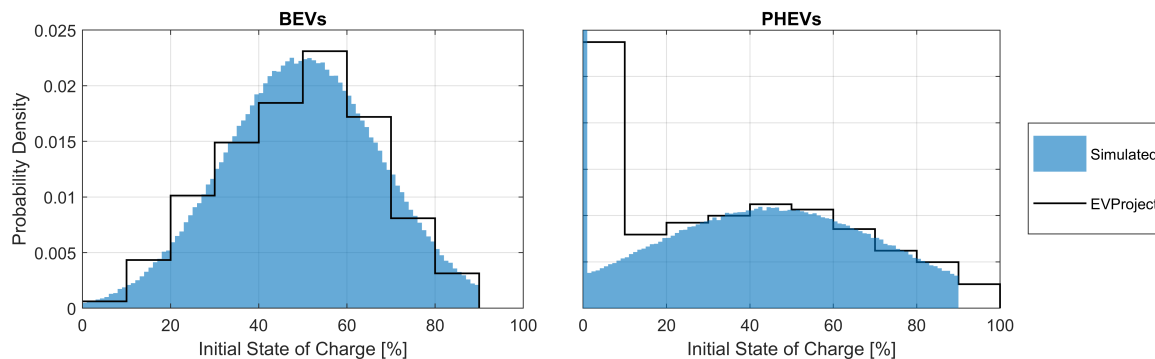
Figure 3.13: Probability densities for battery SOC when charging begins

There are other methods which can be used to model the initial SOC value when the vehicle is plugged in. Some models make the simple yet unrealistic assumption that all vehicles begin charging with their battery completely empty [65, 94]. Other models assume that vehicles start the day with a completely charged battery, and then estimate the energy which is used by the vehicle as it drives to its destination, based on the real-world driving data and the vehicle energy efficiency [110, 148]. This technique is flawed. Firstly, not all EV owners fully charge their vehicle each evening. One study determined that EV drivers only charged their vehicles on average about 0.6 times per day [92]. Furthermore, the decision by the EV owner to begin charging is often dependant on the battery state of charge itself. In a study of 135 EV drivers, 55% stated that they charged their vehicle "whenever I get a chance," but 54% stated that they recharged when the SOC fell below a certain level [149]. Because the decision to begin charging is dependant on the SOC, the distribution of the SOC will not depend only on the driving distance.

The psychological dynamics which determine charging behavior can be described by a User Battery Interaction Style (UBIS), which varies greatly between individuals [150]. High interaction users begin charging based on their specific requirements, such as the distance they plan to drive and the current battery SOC, resulting in their initial SOC tending to be distributed around a clear peak value. Low interaction users, on the other hand, will begin charging based on other factors, such as location or time of day, resulting in their initial SOC being more uniformly distributed. EV drivers are likely to have a higher interaction UBIS when there is a greater density of refueling options [150] or when they have been driving their EV for a longer period of time [149].

Because of the combination of both high- and low-interaction EV drivers, values for the initial SOC tend to approximately follow a truncated Gaussian distribution, as seen in Figure 3.13. The use of a truncated Gaussian is common in the literature, although the characteristics of the distribution are often assumed without a basis in real-world data. One publication used a mean of 50% and a standard deviation of 30% [145], with another choosing a mean of 50% and a standard deviation of 10% [109]. It is preferable to use a realistic distribution of the initial SOC based on historical data.

In this model, the coefficients for the distribution were calculated by fitting the distribution to data from the EV Project [142]. This data closely resembles the results of the study examining 79 BEVs in Germany, suggesting that the initial SOC is comparable across different regions [150]. The distribution for BEVs has a mean of 50% and a standard deviation of 18%, with PHEVs having a slightly lower mean of 45% and a larger standard deviation of 30%. Both distributions are truncated between SOC values of 0% and 90%. PHEVs have a wider distribution because they have a smaller battery, and because they have a conventional fuel tank and internal combustion engine, so drivers do not need to concern themselves with running out of battery power. Because of the ability to drive with an empty battery, many PHEVs will begin charging when the battery is completely discharged, which is not true of BEVs. According to EV Project data, less than 1% of BEVs began charging at an SOC below 10%, but with PHEVs, 20%–40% began charging at this SOC level, depending on the region [142]. This model therefore assumes that 30% of all PHEVs begin charging with an SOC of 0% of the

usable capacity.

3.3. Electric Vehicle Charging

Electric vehicle chargers, also known as Electric Vehicle Supply Equipment (EVSE), are an important component in a smart parking lot. Chargers are available in a number of power ratings and configurations, from a host of manufacturers. In the PowerParking system, the charging stations will be provided by Alfen. This model will consider the case of both unidirectional and bidirectional charging. With bidirectional charging, or Vehicle to Grid (V2G), energy can be discharged from the EV batteries. For simplicity, in a scenario considering V2G it is assumed that all vehicles are capable of and willing to allow bidirectional charging.

3.3.1. Charging Rate

The charging equipment is intended to represent typical slow charging for a commercial parking lot. Electric Vehicle charging stations can be categorized as level 1, 2, or 3 [20]. Level 1 charging uses 120 V AC household outlets, which are the standard in some parts of the world including North America. In Europe, where 230 V AC is the standard, level 1 charging need not be considered. Level 2 charging uses 230 V single phase or 400 V three phase AC power, and these chargers are the primary equipment used for both public and private charging in Europe. For this reason, it is assumed that the chargers in this simulation are single-phase level 2 chargers. Most Level 2 chargers use a dedicated 40 A circuit, with a maximum 32 A usable This corresponds to a power of 7.4 kW. All AC slow chargers ate therefore assumed to have a power of 7.4 kW, with all vehicles able to charge at that power level simultaneously.

Although almost all Level 2 charging involves AC power, it is possible for slow charging to use DC power as well. In a microgrid where power is generated by solar panels, for example, using DC charging could avoid unnecessary conversion of DC power (from the solar panels) to AC power (for the grid) and back to DC (for the EV battery). Because DC power could lead to decreased power losses, this model will also consider DC slow charging. In order to keep AC and DC slow charging as comparable as possible in the simulation results, it is assumed that the DC slow chargers will also have a maximum power of 7.4 kW.

Level 3 charging, or DC fast charging, offers the possibility to charge EVs in less time but will not be considered in this model. Coordinated smart charging is not possible with DC fast charging because the driver typically expects their vehicle to be charged as quickly as possible, providing very little room for flexibility. According to EV project data, 47% of all fast charging events lasted less than 20 minutes, with 97% of events lasting less than 45 minutes [142]. In addition, the parking lots in this model are not ideal locations for DC fast charging stations. The parking lots at the airport and the workplace are both intended for drivers who will be parked for an extended period of time, meaning that there is no clear business case for installing a fast charging station at either parking lot. Although there are some drivers who are parked for shorter durations who might use fast charging at these locations, a fast charger could be better placed in a location where many drivers will frequently need fast charging, such as at highway rest areas and shopping centers. If an airport is installing fast charging stations, they would be better placed at the short term parking for pick-ups and drop-offs. Because there is little relevance to smart charging, and because there is no compelling business case, DC fast charging is not considered in this model.

3.3.2. Charging and Discharging Efficiency

When charging a battery, some of the energy is lost. The increase in the battery SOC is given by the charging efficiency, ir η_{chg}. Similarly, energy is lost when discharging a battery, meaning that the decrease in battery SOC is greater than the energy which is ultimately delivered. This is determined by the discharging efficiency, or η_{dis}. We can also consider the energy which is lost over a complete charge-discharge cycle, known as the round-trip efficiency or η_{batt}. These efficiencies can be defined as [151]:

$$\eta_{chg} = \frac{\Delta E_{batt}}{\Delta E_{in}} \tag{3.3.1}$$

$$\eta_{dis} = \frac{\Delta E_{out}}{\Delta E_{batt}} \tag{3.3.2}$$

$$\eta_{batt} = \frac{\Delta E_{out}}{\Delta E_{in}} \tag{3.3.3}$$

$$= \eta_{chg} \cdot \eta_{dis} \tag{3.3.4}$$

Where ΔE_{batt} is the increase in the stored energy in the battery, ΔE_{in} is the total energy supplied to the battery, and ΔE_{out} is the net energy discharged from the battery. The charging, discharging, and round-trip efficiencies in this model are summarized in Table 3.4.

Table 3.4: Charging and discharging efficiencies

Type	Charging [%]	Discharging [%]	Round trip [%]
EVs, AC	88.35	75.05	66.31
EVs, DC	90.25	90.25	81.45
Fixed battery	95.00	95.00	90.25

When considering the losses during charging and discharging, three types of losses will be considered: losses in the EVSE; losses in the power electronic components in the EV, which convert the AC power from the EVSE to the DC power required by the battery (or vice versa during discharging); and losses in the battery itself. Losses in the EVSE are primarily resistive losses, and are designed to be relatively low. One study found that EVSE losses are dependant on the current, and range from 0.1%–0.32% during charging and 1.39%–1.42% during discharging [152]. These losses are dependant on the current and the SOC of the EV battery.

Power losses are also considered in the power electronics within the EV itself. Energy which is supplied from the EVSE in AC must be converted to DC power in order to charge the EV battery. During discharging, the power electronics must convert DC power from the battery to AC. These losses are again dependant on the current and battery SOC, but for a charger with a voltage of 240 V and a current of 30 A, power electronics losses were 5.73%–7.82% during charging and 19.50%–20.85% during discharging. When considering the losses in the EVSE as well, losses before the power reaches the battery are therefore 5.8%–8.1% during charging and 20.6%–22.0% during discharging. For the purposes of this simulation, the losses are assumed to be 7% and 21% respectively during AC charging and discharging, excluding losses in the battery. Excluding battery losses, the round trip efficiency for an AC charger is therefore 73.5%. Losses in the battery itself reduce that efficiency further.

During DC slow charging, the onboard rectifier in the EV is not needed, which should reduce the efficiency losses. Unfortunately, there is little reliable data about the efficiency of bidirectional slow DC charging, with many papers conflating slow charging with AC charging. Industrial DC-DC converters for EV fast charging can have efficiencies of greater than 98% [153]. Because the slow charging unit will be smaller, with a lower voltage and power output, it is assumed that losses will be higher. In addition, if the vehicles are charged from the grid, energy from AC power must be converted to DC. The overall losses, including rectification, are therefore assumed to be 5%. During V2G, EVs connected to DC EVSE do not need to convert power from DC to AC eliminating losses from the vehicle's internal inverter. It is therefore assumed that losses during discharging are also 5%.

Finally, losses in the battery itself should be considered. These losses are due to internal resistance within the battery, and chemical side reactions which occur during charging and discharging. The efficiency is heavily dependant on the charging or discharging rate, with a higher rate leading to a lower efficiency. The charging and discharging rate are typically measured in terms of the C-rate, which is the ratio of the battery power to the battery capacity. For example, a battery being charged with 10 kW of power and a capacity of 20 kWh would have a C-rate of 10/20 = 0.5. Battery efficiencies are dependant on both the C-rate and the battery state of charge, with the efficiency decreasing at a higher SOC [154]. For this reason, vehicle charging rates are often reduced at higher SOC values.

In this model, the charging rate is already quite low, and therefore does not need to be slowed down at a higher battery SOC. The smallest battery considered in this report are PHEVs with a capacity of 8.7 kWh. At a charging rate of 7.4 kW, this corresponds to a maximum C-rate of 0.85. When considering a larger vehicle, such as a Tesla with a 100 kWh battery pack, the C-rate is only 0.07. At these low charging rates, the effect of varying SOC levels is not considered to be significant. At a current of 30 A, round trip losses in the battery were found to only range from 2.50%–3.26% based on the SOC [152]. Even at a higher current of 70 A, round trip losses only ranged from 5.27%–7.87% depending on SOC, suggesting that charging efficiency is primarily dependant on current and not SOC for slow-charging vehicle batteries. These efficiencies are also in line with other literature values, which found that at a rate of 1 C, round trip losses are roughly 6%–8% [151, 154]. Another study found that in a slightly more conservative value of 9% round-trip losses [155]. Note that these losses are under ideal conditions, with efficiencies decreasing in adverse temperatures and older batteries. For this reason, the charging and discharging efficiency in the battery itself are both assumed to be 95%,

corresponding to round trip losses of 9.75%. The battery efficiency is multiplied by the efficiency of the power electronics to obtain the overall efficiencies, as shown in Table 3.4.

3.4. Fixed Battery Storage

In addition to the electric vehicles, there is also the fixed storage battery which can be used to store energy for later use. This battery is connected to the DC microgrid, allowing it to directly charge from the solar panels without power being converted to AC first. The battery can discharge in order to charge the EVs, through an inverter if necessary.

3.4.1. Battery Capacity and Power

Fixed storage batteries with a range of capacities were investigated as part of this simulation. Larger batteries offer more flexibility, but increase the cost of the system. As will be demonstrated in Section 5.1, the optimal battery capacity was determined to be 50 kWh in a parking lot without bidirectional charging. In a parking lot with V2G, it was determined that additional energy storage in the form of a fixed battery offers no advantages, and so the battery was not included in those simulations.

In order to prevent degradation, the battery is restricted to using a portion of its total capacity. In literature, the recommended maximum depth of discharge for for lithium-ion batteries in stationary storage applications is 80% of total capacity [152]. The SOC of the battery is therefore assumed to be maintained between 20% and 100% of its total capacity. This means that the 50 kWh battery had a usable capacity of 40 kWh. In order to avoid battery degradation, the battery was limited to a C-rate below 1 during both charging and discharging. For the 50 kWh battery, the maximum power to or from the battery was therefore 50 kW.

3.4.2. Charging and Discharging Efficiency

As with electric vehicles, the fixed storage battery will have losses in both the power electronics and the battery itself. Unlike EVs, however, the power electronics which supply power to the fixed storage battery can be much larger and more efficient. The efficiency of the power electronic equipment is therefore assumed to be 98%, which is the efficiency given for a DC-DC converter for EV fast charging [153]. In addition, the fixed storage battery will be better maintained and monitored, resulting in lower internal battery losses. The battery losses are therefore assumed to be 3% during both charging and discharging, which is comparable to literature values for fixed battery storage [151, 154]. The overall efficiency, during both charging and discharging, was therefore assumed to be 95%. This corresponds to a round trip efficiency of 90.25%. The efficiency for the fixed battery storage, as well as for the EV chargers, is listed in Table 3.4.

3.5. Other Loads and Losses

This section will discuss other electrical loads which will contribute to the total demand in the parking lot being simulated. In addition to loads which consume electricity, electrical losses will also be considered. In this simulation, the only load considered, apart from those already described, is LED lighting. Other loads which are not connected directly to the parking lot, such as nearby buildings, are not included, as these do not contribute to the grid exchange of the parking lot itself. Climate control and ventilation, which may be required in some enclosed parking structures, are not needed in a surface parking lot. Other loads such as cameras or ticket machines are considered to be negligible and are not taken into account.

3.5.1. LED Lighting

The lighting for the smart solar parking lot is generated using Light Emitting Diodes, or LEDs. Although older lighting technologies used AC power, the development of low-cost LEDs has led to the increased adoption of these DC devices, due to their high efficiency and long lifetime [156]. In addition, LEDs use DC power and can therefore be powered directly from the DC microgrid. The lighting in the parking lot must be sufficient to ensure a safe and comfortable atmosphere for the users. According the the Netherlands Standardization Institute, the area around parking places should be lighted to a minimum of 75 lux [157]. One possible plan for the PowerParking project is to have LED lighting could be affixed to the underside of the solar canopies, with each canopy having 180 watts of lighting. The luminous efficiency of LEDs can exceed 100 lumens per watt, meaning that each canopy generates more than 18000 lumens [158]. Because the canopies would cover four parking spaces, an area of roughly 65 m^2, this would correspond to an illuminance of 277 lux, well above the minimum requirement of 75 lux. With 10 solar canopies and 180 W of lighting per canopy, the peak power

requirement for lighting is 1.8 kW in total. Note that a single EV charger uses 7.4 kW of power, making lighting relatively insignificant in terms of total energy consumption.

Furthermore, the LEDs need not be constantly illuminated. Smart lighting system can turn the lights off when the sun is shining. At night, occupancy sensors can be used to reduce the lighting to a lower level when the parking lot is unoccupied. In one typical case, a parking lot required lighting 14.2 hours a day on average. By using occupancy sensors, they were able to operate the lighting at a high-power level for only 8.0 hours per day, with a low power level for the remaining 6.2 hours. This reduced electricity consumption by 37% [156]. In this model, it is assumed that occupancy sensors could similarly reduce the average power needed for lighting by 40%. During times when natural light is insufficient, the total power required is for lighting is therefore reduced from 1.8 kW to 1.08 kW. When natural light provides more than 300 lux of illuminance, it is assumed that the LEDs can be turned off completely. The global efficiency of sunlight is 105 lumens per Watt, which means that the LEDs must be turned on if the Global Horizontal Irradiance (GHI) is below 3 Watts per m^2 [159]. This is true on average 12.1 hours per day, with the nighttime hours obviously being longer during the winter and shorter during the summer.

3.5.2. Electrical Losses

Resistive losses in the cables will take place as power is transmitted between the solar panels, battery, EVSE, and EVs. These losses have already been described in the respective sections for each system component. There are also losses in the system when energy is converted between DC and AC or vice versa. Power converted from DC to AC is done through the centralized inverters as described in section 3.1, with the losses discussed there. Power converted from AC to DC is done through rectifiers connected to DC slow chargers for EVs, discussed in section 3.3, or through a rectifier connected to the fixed storage battery, discussed in section 3.4. Losses for these power electronic devices are discussed in those sections. These losses can compound on each other, especially in cases with a great deal of charging and discharging. The overall efficiencies for a few possible scenarios are shown in Table 3.5.

Table 3.5: Overall efficiencies for different scenarios

Scenario	Efficiency [%]	
	AC charging	DC charging
Vehicle charged directly	88.35	90.25
Battery to vehicle	79.74	81.45
Vehicle to vehicle (V2V)	58.58	73.51

In all of these scenarios, the power originates at either the electricity grid or is generated by solar panels. If the solar panels are powering an AC load, there will be additional inverter losses. Similarly, if the grid is powering a DC load, there will be rectifier losses. These losses are not included in Table 3.5 for the sake of simplicity. Due to the efficiency of those components, those losses are considered to be negligible. Because of the low discharging efficiencies as given in Table 3.4, bidirectional charging results in very high losses, especially with AC charging. For this reason, fixed battery storage may be preferable to V2G unless more efficient bidirectional charging technology is developed.

<div style="text-align: right; font-size: 4em;">4</div>

Charging Strategies

In addition to the physical system, the solar parking lot also requires a control system. This control system is responsible for managing the loads, charging vehicles, and controlling power to and from the battery. The general topology of the system, including the flow of electricity and information, is shown in Figure 4.1.
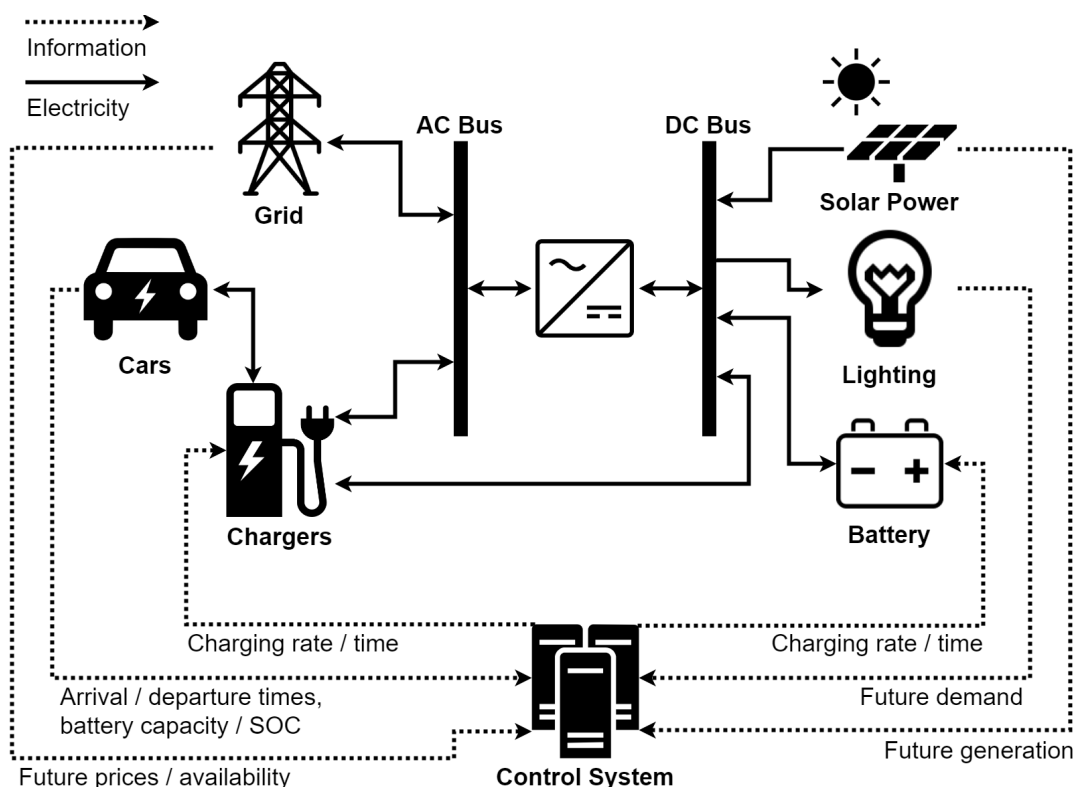
Figure 4.1: Diagram of the smart solar parking, including a control system

There are a number of possible charging strategies for smart solar parking lots. Strategies from the literature have previously been discussed in Section 2.2. In this report, two main strategies will be considered: uncoordinated charging, described in Section 4.1, and coordinated smart charging seeking to minimize the peak electricity demand. Smart charging is first described in Section 4.2 assuming perfect knowledge about future solar power generation and EV behavior. Then, Section 4.3 will describe smart charging strategies which consider solar power uncertainty. Finally, Section 4.4 will describe smart charging strategies which additionally consider unknown EV behavior.

4.1. Uncoordinated Charging

Uncoordinated charging, also referred to as dumb charging, is implemented in this model as a base-case scenario. Vehicles begin charging at the maximum possible rate the moment they are connected, and continue charging until either they are fully charged or they depart. A fixed storage battery is also used, which charges whenever generation for solar power is greater than the current consumption, and discharges whenever the demand from vehicles and other loads is greater than generation. When the battery is unable to charge or discharge further due to the state of charge reaching the allowed limits, energy is bought or sold from the grid. This strategy does not consider any future information about solar generation or electric vehicle demand.

Almost all vehicle charging is currently uncoordinated, with smart charging being the exception rather than the rule. Uncoordinated charging has the advantage of not requiring extra communication networks or charging infrastructure while being simpler for EV drivers. It is therefore the relatively simple and inexpensive to implement. Since the vehicle begins charging at the maximum rate immediately, it will also be the fastest strategy at a given charging power level. Despite the benefits, uncoordinated charging can result in high peaks in the electricity demand. There are uncoordinated charging strategies which seek to reduce these peaks, such as off-peak or delay charging described in Section 2.2, but these strategies can fail to reduce and may even increase the peak demand. Smart charging is therefore considered.

4.2. Smart Charging with Perfect Information

In smart charging, the parking lot operator does not necessarily begin charging vehicles the moment that they are connected. It is possible to delay the start of charging, or to charge at a slower rate. In addition, it is possible for the parking lot operator to make use of fixed battery storage to store electricity when it is available and use it when required. Furthermore, it is possible for some vehicles to engage in Vehicle to Grid (V2G), where the batteries of electric vehicles are discharged to send power to other charging vehicles or other loads. Examples of a vehicles state of charge (SOC) under different charging strategies are shown in Figure 4.2.
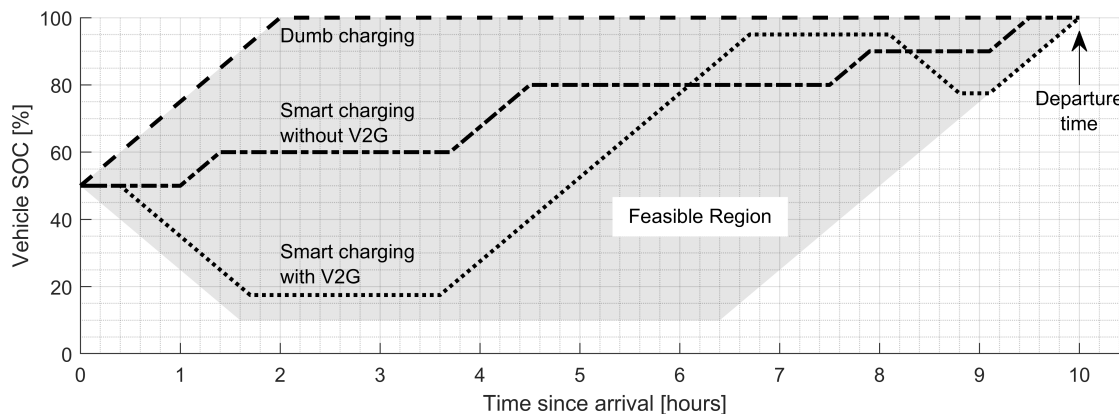
Figure 4.2: Examples of battery state of charge (SOC) over time for different strategies

In this model, it is assumed that EV drivers prefer to have their vehicle as fully charged before they depart, and parking lot operators must therefore charge all the vehicles as much as possible. Within these limitations, the parking lot operator can control the EV charging in order to achieve their own goal. For this analysis, it is assumed that during smart charging the parking lot operator will seek to reduce the peak electricity demand as much as possible, given the reasons described in Section 2.2. Note that this peak shaving behavior may not reduce the overall grid exchange, it will only reschedule the times when electricity is bought and sold. The overall net grid exchange is difficult to change regardless of the strategy, because the total generation is uncontrollable, as is the total energy needed to charge the vehicles. This means that the net grid exchange is relatively unaffected by the charging strategy. Through intelligent control strategies, however, the peak demand can be reduced significantly.

4.2.1. Model Predictive Control

Model Predictive Control (MPC) is a form of control strategy that has become the accepted standard for determining the optimal behavior in complex constrained multivariable problems [160]. In MPC, the control action is determined at each time step by solving an open-loop optimal control problem over a finite horizon. This differentiates MPC from some controllers which use an infinite horizon. Model Predictive Control is capable of handling constraints on inputs, states, and outputs [161], making it suitable for modeling the smart solar EV charging system.

In MPC, an optimization problem is formulated to determine the optimal control sequence for the system. The current state of the system is used as the initial state in this problem. MPC solves the optimization problem at each time step k in the period under consideration:

$$k \in \{1, \dots, N_T\} \tag{4.2.1}$$

where N_T is the number of time steps considered in one full simulation. Rather than considering the full simulation period, The optimization problem is solved for a smaller set of time steps from the current time step to the finite time horizon:

$$t \in \{k, k+1, \dots, k + N_p - 1\} \tag{4.2.2}$$

where t represents a given time step up to the horizon, k is the current time step and N_p is the number of time steps in the horizon. The optimal control sequence is determined at each time step t.

In MPC, only the first control action is implemented to update the system state. The value of k is then incremented by one and the computation is repeated. Because the time horizon recedes with each computation, MPC is also known as receding horizon control [162]. The optimization problem is solved at each time step until the behavior is determined for the full simulation period. MPC differs from conventional control strategies in that the optimization problem is solved online, rather than off-line. This means that the optimal control strategy is not calculated in advance, but is instead determined during operation. MPC is able to handle control problems where off-line computation of a control law may be difficult or impossible. In this system, developing an optimal off-line control strategy is quite difficult, so MPC is used. The total simulation time is 365 days with time steps spaced by 15 minutes. The simulation is finished when the horizon at the end of the time window reaches 365 days, in order to ensure that the size of the time window remains consistent. A time horizon of 24 hours is chosen, meaning that $N_p = 24 \cdot 4 = 96$ and $N_T = 364 \cdot 24 \cdot 4 = 34,944$.

The length of the time horizon in the MPC problem must be chosen carefully. A longer time horizon can lead improved results as the optimization problem considers more information. Increasing the window size, however, will result in increased computation time. The choice of the time horizon in this model is made by simulating the solar parking lot for one year, assuming that perfect information is available. The impact of MPC window size on the grid exchange can be observed in Figure 4.3.
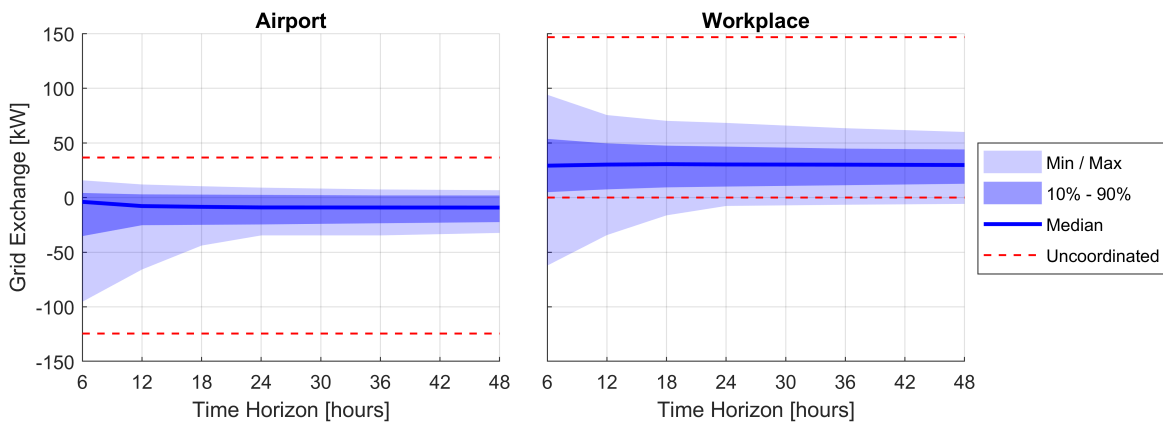

Figure 4.3: Simulated grid exchange vs. MPC time horizon

The figure depicts the minimum and maximum grid exchange, as well as the 10%–90% range and the median. Also depicted are the minimum and maximum grid exchange during uncoordinated charging, for comparison. As can be observed, the peak grid demand, especially in a workplace, is significantly higher

for shorter time horizons. As the horizon gets longer, the maximum demand decreases. Although the optimization problem does not seek to increase the minimum demand, this value also increases with longer time horizons. This is because the controller stores more energy, considering the demand further in the future. The minimum and maximum demand do not change significantly in either parking lot for time horizons longer than 24 hours. The only exception is that workplace peak demand decreases slightly if the time horizon increases from 24 to 48 hours. This longer horizon, however, extended the simulation time from 2.5 hours to 8 hours. Furthermore, forecasting accuracy decreases for longer time horizons, meaning that the benefits of a longer horizon are likely to diminish as uncertainty is introduced into the model. For these reasons, a time horizon of 24 hours was chosen.

Model Predictive Control considers a state-space model of the form:

$$x(k+1) = f(x(k), u(k), v(k)) \tag{4.2.3}$$

$$y(k) = g(x(k), u(k), v(k)) \tag{4.2.4}$$

$$0 \le h(x(k), u(k), v(k)) \tag{4.2.5}$$

where x represents the state variables, u the control variables, v represents auxiliary variables, y represents that output, and h represents constraints on the state, control, and auxiliary variables [160].

We express our optimization problem in the form:

$$\underset{\tilde{u}(t)}{\text{minimize}} \quad J(x(t), \tilde{u}(t)) \qquad \text{such that } 0 \le h(x(k), \tilde{u}(k)) \tag{4.2.6}$$

where J is the objective function and $\tilde{u}(k)$ is the set of all decision variables including the auxiliary variables.

For the sake of computational simplicity, the problem can be formulated such that all equations for the state, output, and constraints are linear. This model can be formulated linearly as a Mixed Integer Linear Programming (MILP) problem, specifically as a Mixed-Logical Dynamical (MLD) system consisting only of continuous and binary variables. This system has the form [163]:

$$x(k+1) = Ax(k) + B_1 u(k) + B_2 \delta(k) + B_3 z(k) \tag{4.2.7}$$

$$y(k) = Cx(k) + D_1 u(k) + D_2 \delta(k) + D_3 z(k) \tag{4.2.8}$$

$$g \le E_1 x(k) + E_2 u(k) + E_3 \delta(k) + E_4 z(k) \tag{4.2.9}$$

The optimization problem was solved using Gurobi, which is able to handle MILP problems quickly and efficiently [164]. The specific formulation of the MLD model will be detailed in the following sections.

4.2.2. Objective Function
We are considering the case of a parking lot operator seeking to reduce the peak demand on the grid. For the optimization problem under consideration then, the objective function is:

$$\text{minimize} \quad \max\big(E_{grid}(k), \dots, E_{grid}(k + N_p - 1)\big) \tag{4.2.10}$$

where $E_{grid}(k)$ is the net energy exchange between the parking lot operator and the electricity grid at time k. In order to simplify the optimization computation, it is desirable to formulate the problem using only linear functions. This is accomplished through the introduction of an auxiliary variable $E_{grid}^{\max}$ which represents the local maximum for the grid exchange over the time horizon under consideration:

$$E_{grid}^{\max} = \max\big(E_{grid}(k), \dots, E_{grid}(k + N_p - 1)\big) \tag{4.2.11}$$

The objective function can be rewritten as:

$$\text{minimize} \quad E_{grid}^{\max} \tag{4.2.12}$$

4.2.3. Decision Variables
In the MPC formulation, the control variables represent the energy transferred to or from each of the batteries. The state variables are then the amount of energy stored in each battery. During each time step within the window considered in MPC, the decision is made to either charge or discharge each electric vehicle, and to either charge or discharge the fixed battery storage. The energy to or from the fixed storage and the electric vehicles is given by $E_i(t)$ where $i \in \{1, \dots, N_b\}, t \in \{k, \dots, k + N_p - 1\}$. Each battery is represented by the index

i, with N_b as the total number of batteries. The electric vehicle charging stations are represented by $i = 1, \ldots, N_b - 1$, and the fixed storage battery is represented by $i = N_b$. Because the simulation considers 40 EV charging stations, $N_b = 41$. The energy used to charge each battery $E_i(t)$ is in units of kWh, and is defined to be positive during charging and negative during discharging. We therefore have the control variables given by:

$$u(t) = E(t) = [E_1(t), \ldots, E_{N_b}(t)]^T \tag{4.2.13}$$

for $t \in t = k, \ldots, k + N_p - 1$. The state variables are defined as:

$$x(k) = S(k) = [S_1(k), \ldots, S_{N_b}(k)] \tag{4.2.14}$$

where $S_i(k)$ is the energy stored in battery i at time k, in units of kWh. The formula for the updated state variable depends on whether the battery is charging or discharging, given by :

$$S_i(k+1) = \begin{cases} S_i(k) + \eta_{chg,i} \cdot E_i(k), & E_i(k) > 0 \\ S_i(k) + \frac{1}{\eta_{dis,i}} E_i(k), & E_i(k) \leq 0 \end{cases} \tag{4.2.15}$$

where $\eta_{chg,i}$ is the efficiency during charging for battery i and $\eta_{dis,i}$ is the efficiency during discharging. The fixed storage battery, AC vehicle chargers, and DC vehicle chargers all have different efficiencies, so the values are dependant on i. Because the charging rate for these batteries is quite low, the efficiency is assumed to be independent of the SOC.

This charging and discharging behavior of the batteries is nonlinear. For computational efficiency, it is desirable to solve the optimization problem using linear programming. The problem is therefore formulated as a Mixed-Logical Dynamical (MLD) system, with the introduction of binary and continuous variables [165]. For each battery at each time step, a binary decision variable $\delta_i(t)$ is introduced, defined by:

$$[\delta_i(t) = 0] \leftrightarrow [E_i(t) > 0] \text{ (EV or battery is charging)} \tag{4.2.16}$$
$$[\delta_i(t) = 1] \leftrightarrow [E_i(t) \leq 0] \text{ (EV or battery is discharging)} \tag{4.2.17}$$

This binary variable can be used to reformulate equation 4.2.15:

$$S_i(k+1) = S_i(k) + \eta_{chg,i} \cdot E_i(k) \cdot (1 - \delta_i(k)) + \frac{1}{\eta_{dis,i}} E_i(k) \cdot \delta_i(k) \tag{4.2.18}$$

Although this formulation is simpler, it is still nonlinear because it contains the product of two decision variables. Another set of continuous decision variables is therefore introduced:

$$z_i(t) = \delta_i(t) \cdot E_i(t) \tag{4.2.19}$$

The state variable is then expressed in terms of a linear combination of the decision variables:

$$S_i(k+1) = S_i(k) + \eta_{chg,i} \cdot E_i(k) + \left(\frac{1}{\eta_{dis,i}} - \eta_{chg,i} \right) z_i(k) \tag{4.2.20}$$

As a final auxiliary variable, we consider the maximum grid exchange within the MPC time window, E_{grid}^{max}, which is needed for a linear objective function. The decision variables are then given by:

$$E_{grid}^{max}, E(t), \delta(t), z(t) \tag{4.2.21}$$

for $t \in \{k, \ldots, k + N_p - 1\}$. We define $E(t) = [E_1(t), \ldots, E_{N_b}(t)]^T$, with the same for $\delta(t)$ and $z(t)$. The number of decision variables in each optimization problem is therefore $3 \cdot N_b \cdot N_p + 1 = 11,809$, with 3,936 of those being binary.

4.2.4. Constraints
In a Mixed Logical Dynamics model, the constraints must be in the form of linear inequalities of the decision, state, and auxiliary variables [165]. Because the MLD formulation in this problem also introduces the auxiliary variable E_{grid}^{max}, we must also consider the constraints on this variable. It is defined as:

$$E_{grid}^{max} = \max(E_{grid}(k), \ldots, E_{grid}(k + N_p - 1)) \tag{4.2.22}$$

$$\text{with } E_{grid}(t) = E_{load}(t) - E_{PV}(t) + \sum_{i=1}^{N_b} E_i(t) \tag{4.2.23}$$

where $E_{load}(t)$ is the energy going to loads such as lighting, and $E_{PV}(t)$ is the energy generated from the PV system. The signs are defined such that positive energy means that the parking lot is buying from the grid, and negative means that they are selling to the grid. Note that because they are uncontrollable, $E_{load}(t)$ and $E_{PV}(t)$ are not considered decision variables. In order to express this as a linear constraint, we establish:

$$E_{grid}^{\max} \geq E_{load}(t) - E_{PV}(t) + \sum_{i=1}^{N_b} E_i(t) \tag{4.2.24}$$

for all $t \in \{k, \dots, k + N_p - 1\}$. Although this equation only defines the lower bound, the objective function increases with higher values of $E_{grid}^{\max}$. Therefore, the objective function will be minimized at the true maximum value of grid exchange within the time window. We then consider a limit to the energy which can be sold to the grid:

$$E_{grid}^{\min} \leq E_{load}(t) - E_{PV}(t) + \sum_{i=1}^{N_b} E_i(t) \tag{4.2.25}$$

for all $t \in \{k, \dots, k + N_p - 1\}$. $E_{grid}^{\min}$ is a constant value that represents the minimum possible value of exchange with the grid. Since energy being sold to the grid is defined to be negative, this is equivalent to the maximum allowable energy which can be sold at a given time step, which is limited by physical restrictions of components like the inverters and the transformer. This constraint is needed because the objective function only considers maximum, and not minimum exchange with the grid. Note that a small limit on the power which can be sent to the grid may require curtailment of solar power at certain times. Because curtailment is not considered in this simulation, the limit is set at a level which is attainable at all time steps, including when solar power is generating at its full capacity and there is no possibility to store energy in any batteries. A suitable value for $E_{grid}^{\min}$ is therefore -128 kW, which is 105% of peak generation capacity.

Next, we consider the constraints for the state variables, which represent the energy stored in the batteries of both the electric vehicles and the fixed storage. By using the definition of the state variable in equation 4.2.20, we can establish:

$$S_i^{\min}(t+1) \leq S_i(t) + \eta_{chg,i} E_i(t) + \left(\frac{1}{\eta_{dis,i}} - \eta_{chg,i} \right) z_i(t) \tag{4.2.26}$$

$$S_i^{\max}(t+1) \geq S_i(t) + \eta_{chg,i} E_i(t) + \left(\frac{1}{\eta_{dis,i}} - \eta_{chg,i} \right) z_i(t) \tag{4.2.27}$$

for all $i \in \{i, \dots, N_b\}$ and $t \in \{k, \dots, k + N_p - 1\}$ where $S_i^{\min}$ and $S_i^{\max}$ are the minimum and maximum acceptable levels of energy stored in each battery at a given time. These limits are based on the technical constraints of the vehicle, as well as the desire that the battery in EVs should charged as much as possible in the time the vehicle is parked.

In order to establish the value of $S_i^{\min}$, we consider that the desired energy in a vehicle is high enough that there is sufficient time to fully charge the vehicle to 100% of its usable capacity before departure, with the desired stored energy given by:

$$S_i^{desired}(t) = C_i - P_{EV}^{\max} \cdot \eta_{chg,i} \cdot (t_{dep,i} - t) \tag{4.2.28}$$

where C_i is the usable capacity of the vehicle in space i, $t_{dep,i}$ is the departure time for the vehicle, and $P_i^{\max}$ is the maximum power which can be supplied by the charging equipment. We must also consider that not all vehicles can be charged in the time available, in which case we must consider the maximum achievable energy which can be stored in a battery at a given time, given by:

$$S_i^{achievable}(t) = S_i(t_{arr,i}) + P_{EV}^{\max} \cdot \eta_{chg} \cdot (t - t_{arr,i}) \tag{4.2.29}$$

where $t_{arr,i}$ is the arrival time for the vehicle and $S_i(t_{arr,i})$ is the energy that was stored in the vehicle battery when it arrived. For electric vehicles, the battery should be charged to the desired level if possible, and to the achievable level if not. For the fixed storage, the energy stored should be kept above $SOC_{batt}^{\min} \cdot C_{batt}$ where C_{batt} is the capacity of the battery in kWh and $SOC_{batt}^{\min}$ is the minimum allowable state of charge for the battery, defined to be 20%, because it is assumed that only 80% of the capacity is usable. This means that the minimum stored energy is defined as:

$$S_i^{\min}(t) = \begin{cases} \max(0, \min(S_i^{desired}(t), S_i^{achievable}(t))) & i = 1, \dots, N_b - 1 \\ SOC_{batt}^{\min} \cdot C_{batt} & i = N_b \end{cases} \tag{4.2.30}$$

The maximum energy allowed is more straightforward. For both the electric vehicles and the fixed storage battery, it is simply the total usable capacity, C_i:

$$S_i^{\max}(t) = C_i \qquad i = 1, \ldots, N_b \tag{4.2.31}$$

Finally, we consider the auxiliary MLD variables $\delta(t)$ and $z(t)$. To define $\delta(t)$, we consider a function of the decision variables $f(x)$ defined such that $[f(x) \leq 0] \leftrightarrow [\delta = 1]$. We also consider the auxiliary variable $z = f(x) \cdot \delta$. These are defined given the constraints [163]:

$$\delta \in \{0, 1\} \tag{4.2.32}$$
$$f(x) \leq M(1 - \delta) \tag{4.2.33}$$
$$f(x) \geq \varepsilon + (m - \varepsilon)\delta \tag{4.2.34}$$
$$z \leq M\delta \tag{4.2.35}$$
$$z \geq m\delta \tag{4.2.36}$$
$$z \leq f(x) - m(1 - \delta) \tag{4.2.37}$$
$$z \geq f(x) - M(1 - \delta) \tag{4.2.38}$$

Where M is the maximum allowable value of $f(x)$, and m is the minimum. An overestimate of M (or an underestimate of m) is also acceptable, but for computational purposes a value close to the true maximum or minimum is preferred. The tolerance ε is a small value, typically the machine precision of the solver. In the case of our model, $f(x) = E_i(t)$. The minimum and maximum values given by:

$$M_i = P_i^{\max} \cdot \Delta t \tag{4.2.39}$$
$$m_i = -P_i^{\max} \cdot \Delta t \tag{4.2.40}$$

where Δt is the length of the interval between time steps. By substituting the chosen values of $f(x)$, M, and m for each battery and time step, we can establish the constraints on these auxiliary variables. Combining all the constraints allows for the full definition of the optimization problem.

4.2.5. Complete Optimization Formulation
Combining the previous sections, we can express this optimization problem using MLD as follows:

$$\underset{E_{grid}^{\max}, E, \delta, z}{\text{minimize}} \quad E_{grid}^{\max} \tag{4.2.41}$$

With the decision variables:

$$E_{grid}^{\max}, E_i(t), \delta_i(t), z_i(t) \qquad \text{for } i \in \{1, \ldots, N_b\}, \quad t \in \{k, \ldots, k + N_p - 1\} \tag{4.2.42}$$

Such that:

$$E_{grid}^{\max} \geq E_{load}(t) - E_{PV}(t) + \sum_{i=1}^{N_b} E_i(t) \qquad \forall\, t \tag{4.2.43}$$

$$E_{grid}^{\min} \leq E_{load}(t) - E_{PV}(t) + \sum_{i=1}^{N_b} E_i(t) \qquad \forall\, t \tag{4.2.44}$$

$$S_i^{\min}(t+1) \leq S_i(t) + \eta_{chg,i} E_i(t) + \left(\frac{1}{\eta_{dis,i}} - \eta_{chg,i} \right) z_i(t) \qquad \forall\, i, t \tag{4.2.45}$$

$$S_i^{\max}(t+1) \geq S_i(t) + \eta_{chg,i} E_i(t) + \left(\frac{1}{\eta_{dis,i}} - \eta_{chg,i} \right) z_i(t) \qquad \forall\, i, t \tag{4.2.46}$$

$$\delta_i(t) \in \{0, 1\} \qquad \forall\, i, t \tag{4.2.47}$$
$$E_i(t) \leq M_i \cdot (1 - \delta_i(t)) \qquad \forall\, i, t \tag{4.2.48}$$
$$E_i(t) \geq \varepsilon + (m_i - \varepsilon) \cdot \delta_i(t) \qquad \forall\, i, t \tag{4.2.49}$$
$$z_i(t) \leq M_i \cdot \delta_i(t) \qquad \forall\, i, t \tag{4.2.50}$$
$$z_i(t) \geq m_i \cdot \delta_i(t) \qquad \forall\, i, t \tag{4.2.51}$$
$$z_i(t) \leq E_i(t) + M_i \cdot (1 - \delta_i(t)) \qquad \forall\, i, t \tag{4.2.52}$$
$$z_i(t) \geq E_i(t) + m_i \cdot (1 - \delta_i(t)) \qquad \forall\, i, t \tag{4.2.53}$$

4.3. Smart Charging with Uncertainty in PV Forecasting

In real world, the true value of the solar power generation $E_{PV}(t)$ is not known exactly. Instead, we have only a forecast of the solar energy generation, given by:

$$E_{fcst}(t) = E_{PV}(t) + \omega_{PV}(t) \tag{4.3.1}$$

where $\omega_{PV}(t)$ represents the error in the solar forecasting. This error can result in uncertainty with regard to the objective function. The state variables, however, represent the stored energy in the batteries, which is known accurately. This means that we do not need to consider uncertainty in the state equations, as is sometimes necessary when performing optimization under uncertainty. Given this error in the solar forecasting, the optimization strategy must be reconsidered. We consider two strategies, nominal optimization and robust optimization.

4.3.1. Nominal Optimization

The nominal strategy is the simplest way of handling uncertainty in solar power generation. The there is no uncertainty in the solar forecasting, $\omega_{PV}(t) = 0$, and bases the optimization decision on the forecasted values. The optimization problem is rewritten as follows:

$$\underset{E_{grid}^{\max}, E, \delta, z}{\text{minimize}} \quad E_{grid}^{\max} \tag{4.3.2}$$

With the decision variables:

$$E_{grid}^{\max}, E_i(t), \delta_i(t), z_i(t) \qquad \text{for } i \in \{1, \ldots, N_b\}, \quad t \in \{k, \ldots, k + N_p - 1\} \tag{4.3.3}$$

Such that:

$$E_{grid}^{\max} \geq E_{load}(t) - E_{fcst}(t) + \sum_{i=1}^{N_b} E_i(t) \qquad\qquad \forall\, i,\, t \tag{4.3.4}$$

$$E_{grid}^{\min} \leq E_{load}(t) - E_{fcst}(t) + \sum_{i=1}^{N_b} E_i(t) \qquad\qquad \forall\, i,\, t \tag{4.3.5}$$

$$(4.2.45) - (4.2.53)$$

Note that this formulation is almost identical to the original, with the only difference being that $E_{fcst}(t)$ replaces $E_{PV}(t)$, as they are assumed to be equivalent. This method has the advantage of being easy to solve, and it is one which is likely to be implemented by parking lot operators when anticipating renewable energy production. The problem is that nominal optimization may lead to a higher peak demand if the forecasting errors are large. We would preferably implement a solution which reduces the peak grid exchange regardless of the forecasting error. For that reason, we use robust optimization.

4.3.2. Robust Optimization

In this strategy, we seek to choose charging behavior that will result in the lowest possible grid exchange regardless of the forecasting error. This means that the system should be robust with regard to the forecasting error. A control system is considered to be robust when stability and performance is guaranteed to be maintained for all possible uncertainties in a certain range. Robust optimization can lead to improved performance when compared to nominal optimization, but it does have two possible drawbacks. Firstly, it is more computationally demanding, and secondly it may lead to control actions which are excessively conservative [114].

Robustness can only be considered with respect to a limited range of uncertainty. As part of the modeling process it is necessary to accurately describe the uncertainty in the system. Errors in solar forecasting can be described as a form of bounded input uncertainty. This means that the uncertainty is limited to an unknown disturbance in the input, but the linear coefficients defining the system are known precisely. This is in contrast to other uncertainty sets, where the system states may be affected by uncertainties [114]. The system with an MLD formulation, considering the bounded input uncertainty, can be expressed given:

$$x(k+1) = Ax(k) + B_1 u(k) + B_2 \delta(k) + B_3 z(k) + B_4 w(k) \tag{4.3.6}$$

$$y(k) = Cx(k) + D_1 u(k) + D_2 \delta(k) + D_3 z(k) + D_4 w(k) \tag{4.3.7}$$

$$g \leq E_1 x(k) + E_2 u(k) + E_3 \delta(k) + E_4 z(k) + E_5 w(k) \tag{4.3.8}$$

where $w(k)$ is a vector of uncertainties in the system. To ensure robustness, we use min max optimization, which minimizes the cost function over the decision variables while maximizing it over all possible uncertainty vectors [166]:

$$\underset{\tilde{u}(t)}{\text{minimize}} \quad \underset{w \in \mathcal{W}}{\text{maximize}} \quad J(x(t), \tilde{u}(t), w(t)) \tag{4.3.9}$$

where $\mathcal{W}$ is the bounded uncertainty set. In this case, the uncertainty under consideration is with regards to the solar energy generation, with an error $\omega_{PV}(t) = E_{fcst}(t) - E_{PV}(t)$. The objective function as given in equation 4.2.6 must then be revised:

$$\underset{E_{grid}^{\max}, E_i(t), \delta_i(t), z_i(t)}{\text{minimize}} \quad \underset{\omega \in \Omega_{PV}(t)}{\text{maximize}} \quad E_{grid}^{\max} \tag{4.3.10}$$

where ω is a vector representing a random possible value for the forecasting errors at each time step t, and $\Omega_{PV}(t)$ is the bounded set of all possible forecasting errors.

One approach to solving this problem relies on multi-parametric mixed integer linear programming (mp-MILP) [167]. The inner problem can be solve first explicitly. The outer problem can then be solved using MILP. However, this can be computationally inefficient with a large vector of parameters and a far prediction horizon [168]. Because this problem considers several thousand variables and an MPC horizon of 96 time steps, this solution is practically infeasible. It was found that for this problem, a robust optimal solution could be found efficiently using Monte Carlo optimization.

For Monte Carlo optimization, we consider a finite but large number of possible error vectors:

$$\Omega_{PV}^* = \{\omega_{PV}^{(1)}, \dots, \omega_{PV}^{(N_e)}\} \subseteq \Omega_{PV} \tag{4.3.11}$$

where N_e is the number of error vectors being considered. If N_e is sufficiently large, we can consider Ω_{PV}^* to be a reasonably good approximation of Ω_{Pt}. In this model, a value of 10,000 is chosen for N_e. Although in reality the forecasting error is normally distributed, a bounded distribution is necessary for robust optimization. For this reason, the distribution is artificially truncated such that:

$$-3\sigma_{PV}(t) \leq \omega_{PV}^{(j)}(t) \leq 3\sigma_{PV}(t) \tag{4.3.12}$$

for all $t \in \{k, \dots, k + N_p - 1\}$ and $j \in \{1, \dots, N_e\}$. The upper and lower bounds are determined by $\sigma_{PV,t}$, the standard deviation of the forecasting error at time t. The forecasting error is also truncated so that the forecasted power generation cannot be less than zero or greater than the clear sky generation. The choice of three standard deviations as a limit, rather than a more conservative value of five or seven, is justified based on simulation results. One year of operation was simulated for the solar parking lot, using robust optimization to consider the solar forecasting errors. The number of standard deviations considered for the bounds on the forecasting error during robust optimization does not noticeably impact the peak demand, leading to the conclusion that three standard deviations is sufficiently robust. The results of these simulations are shown in Figure 4.4.

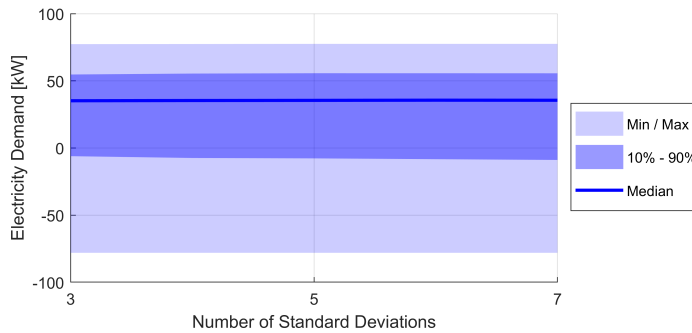Figure 4.4: Electricity demand vs. standard deviations considered during robust optimization

Although the peak demand does not change at more conservative bounds for the forecasting error, the 10th percentile for grid exchange does decease slightly with more standard deviations being considered. With more conservative bounds for the forecasting errors, vehicles are charged earlier in the day, resulting in the

vehicles being fully charged by the middle of the day and solar energy being sent to the grid. This demonstrates how the robust strategy may lower the peak demand at the expense decreasing the self-consumption of renewable energy.

The errors at each time step are therefore drawn randomly from the uniform distribution given by:

$$\omega_{PV}^{(j)}(t) \in \mathcal{U}(-3\sigma_{PV}(t), 3\sigma_{PV}(t)) \tag{4.3.13}$$

We then consider a new auxiliary variable T defined as the maximum value for the objective function under all possible forecasting errors. Because the objective function is not directly dependant on the forecasting uncertainty, T can simply be defined as being equal to the original objective function.

$$T = \max(J(\tilde{u}, x, \omega_{PV}^{(1)}), \dots, J(\tilde{u}, x, \omega_{PV}^{(N_e)})) \tag{4.3.14}$$
$$= E_{grid}^{\max} \tag{4.3.15}$$

We must then consider that the constraints are satisfied for all possible error vectors. The affected constraints are those dependant on the grid exchange, which is given by:

$$E_{grid}(t) = E_{load}(t) - E_{fcst}(t) + \omega_{PV}(t) + \sum_{i=1}^{N_b} E_i(t) \tag{4.3.16}$$

In order for the solution to be robust, the constraints must be satisfied under all forecasting scenarios:

$$E_{grid}^{\max} \geq E_{load}(t) - E_{fcst}(t) + \omega_{PV}^{(1)}(t) + \sum_{i=1}^{N_b} E_i(t) \tag{4.3.17}$$
$$\vdots$$
$$E_{grid}^{\max} \geq E_{load}(t) - E_{fcst}(t) + \omega_{PV}^{(N_e)}(t) + \sum_{i=1}^{N_b} E_i(t)$$

$$E_{grid}^{\min} \leq E_{load}(t) - E_{fcst}(t) + \omega_{PV}^{(1)}(t) + \sum_{i=1}^{N_b} E_i(t) \tag{4.3.18}$$
$$\vdots$$
$$E_{grid}^{\min} \leq E_{load}(t) - E_{fcst}(t) + \omega_{PV}^{(N_e)}(t) + \sum_{i=1}^{N_b} E_i(t)$$

for all $t \in \{k, \dots, k + N_p - 1\}$.

These constraints, however, are redundant when formulating the optimization problem. Consider the minimum and maximum values for the forecasting error at each time step in the MPC window:

$$\omega_{PV}^{\min}(t) = \min\left(\omega_{PV}^{(1)}(t), \dots, \omega_{PV}^{(N_e)}(t)\right) \tag{4.3.19}$$
$$\omega_{PV}^{\max}(t) = \max\left(\omega_{PV}^{(1)}(t), \dots, \omega_{PV}^{(N_e)}(t)\right) \tag{4.3.20}$$

for all $t \in \{k, \dots, k + N_p - 1\}$.

These can be substituted into the constraints containing uncertainty, given by Equations 4.3.17 and 4.3.18, with the general form given in Equation 4.3.8. As proven in [169], the constraints and will hold for all disturbances assuming:

$$g \leq E_1 x(k) + E_2 u(k) + E_3 \delta(k) + E_4 z(k) + E_5 w^{\max}(k) \tag{4.3.21}$$
$$g \leq E_1 x(k) + E_2 u(k) + E_3 \delta(k) + E_4 z(k) + E_5 w^{\min}(k) \tag{4.3.22}$$

meaning that only the minimum and maximum values for the disturbances need be considered, rather than all possible values. This is because a constraint cannot be active at some intermediate value of the disturbance without violating the constraint at an extreme value.

In the case of this model, the matrix E_5 only takes the form of the identity matrix, so it can be determined whether the constraint will be active at the minimum or maximum value of the disturbance. A greater-than constraint will be active only at the maximum value of the disturbance, and a less-than constraint will only be active at the minimum. The constraints in Equations 4.3.17 and 4.3.18 can therefore be simplified, considering only the maximum and minimum values respectively of the solar forecasting uncertainty.

The complete optimization problem is then given by:

$$\underset{T, E_{grid}^{max}, E, \delta, z}{\text{minimize}} \quad T \tag{4.3.23}$$

With the decision variables:

$$T, E_{grid}^{max}, E_i(t), \delta_i(t), z_i(t) \qquad \text{for } i \in \{1, \ldots, N_b\}, \quad t \in \{k, \ldots, k + N_p - 1\} \tag{4.3.24}$$

Such that:

$$T \geq E_{grid}^{max} \tag{4.3.25}$$

$$E_{grid}^{max} \geq E_{load}(t) - E_{fcst}(t) + \omega_{PV}^{max}(t) + \sum_{i=1}^{N_b} E_i(t) \qquad \forall\, i, t \tag{4.3.26}$$

$$E_{grid}^{min} \leq E_{load}(t) - E_{fcst}(t) + \omega_{PV}^{min}(t) + \sum_{i=1}^{N_b} E_i(t) \qquad \forall\, i, t \tag{4.3.27}$$

$$(4.2.45) - (4.2.53)$$

4.4. Smart Charging with Uncertainty in EV Behavior

Another assumption made in the optimization formulation is that the arrival time, departure time, initial state of charge, and battery capacity is known for all vehicles. In reality, this is known only for the vehicles which have already arrived and begun charging. These vehicles are assumed to transmit battery state of charge data to the charger, and the EV driver will tell the system when plugging in when they will be departing. This information, however, is not known before arrival.

Some information may be known before arrival, but with a high degree of uncertainty. For example, some airport parking lots allow the driver to reserve a space in advance, meaning that arrival time $t_{arr,i}$ and possibly even departure time $t_{dep,i}$ could be known for some vehicles before the EV arrives. The capacity C_i and initial state of charge $SOC_i(t_{arr,i})$, however, will not be known until arrival. Furthermore, not all vehicles will reserve a space in this way, meaning that the at least some of the arrivals will be unplanned.

This uncertainty can introduce error into these variables, which affects the optimization formulation. These values determine the minimum and maximum allowable stored energy, $S_i^{min}(t)$ and $S_i^{max}(t)$, through equations 4.2.30 and 4.2.31. These limits are in turn included in constraints 4.2.45 and 4.2.46. Rather than considering all these uncertainties individually, their effect can be included into the uncertainty of the minimum and maximum stored energy:

$$S_i^{min}(t+1) = S_i^{min}(t) + \omega_{S_i^{min}}(t) \tag{4.4.1}$$

$$S_i^{max}(t) = S_i^{min}(t) + \omega_{S_i^{max}}(t) \tag{4.4.2}$$

where $\omega_{S_i^{min}}(t)$ represents the uncertainty in the change in the value of $S_i^{min}(t)$, and $\omega_{S_i^{max}}(t)$ represents the uncertainty in the difference between $S_i^{min}(t)$ and $S_i^{max}(t)$. The bounds of these uncertainties are determined by the uncertainties regarding arrival time, departure time, capacity, and initial SOC. Note that these uncertainties again do not appear directly in the objective function, and do not introduce uncertainty into the values of the state variables, only into the state constraints.

It is then necessary to consider both the uncertainty of solar power generation, and uncertainty of EV charging demand. Solar uncertainty will be dealt with using robust optimization, as described in Section 4.3. EV demand uncertainty will be handled with three different techniques: optimization without EV forecasting, optimization with average EV demand forecasting, and optimization which is robust over a range of possible EV demands.

4.4.1. Optimization Without EV Forecasting

This is the simplest way of handling uncertainty regarding EV charging. In this strategy, the optimal behavior is calculated only for the vehicles present, during the times in which they are present. Spaces not yet occupied, or spaces after a vehicle has departed, are assumed to be empty. This means that for the spaces i which are not known to be occupied at time t:

$$S_i^{min}(t) = S_i^{max}(t) = 0 \tag{4.4.3}$$

The optimization problem is then formulated identically to the formulation in the Section 4.3.2, with solar forecasting uncertainty handled robustly.

This strategy is clearly a poor one, as it ignores the inevitable demand from vehicles which have not yet arrived. A better strategy would consider the inevitable demand from vehicles which will begin charging in the future.

4.4.2. Optimization With Average EV Demand Forecasting
In this strategy, solar forecasting is again handled robustly. Regarding charging demand uncertainty, it is assumed that EVs may be present in any future time slots. For vehicles which have not arrived yet, it is assumed that vehicles will have an energy demand that is average for vehicles in the parking lot. This means that the minimum and maximum stored energy are given by:

$$S_i^{\min}(t) = \overline{S_i^{\min}}(t) \tag{4.4.4}$$

$$S_i^{\max}(t) = \overline{S_i^{\max}}(t) \tag{4.4.5}$$

where $\overline{S_i^{\min}}(t)$ and $\overline{S_i^{\max}}(t)$ represent the average values for these variables. These values are substituted into constraints 4.2.45 and 4.2.46. We can then solve the optimization problem again using robust optimization to consider the PV forecasting error, and the average approach to consider demand from future charging vehicles. Using the formulation for robust optimization from the Section 4.3.2, the optimization problem here is given by:

$$\underset{T,E_{grid}^{\max},E,\delta,z}{\text{minimize}} \quad T \tag{4.4.6}$$

With the decision variables:

$$E_{grid}^{\max}, E_i(t), \delta_i(t), z_i(t) \qquad \text{for } i \in \{1,\dots,N_b\}, \quad t \in \{k,\dots,k+N_p-1\} \tag{4.4.7}$$

Such that:

$$\overline{S_i^{\min}}(t+1) \leq S_i(t) + \eta_{chg,i} E_i(t) + \left(\frac{1}{\eta_{dis,i}} - \eta_{chg,i}\right) z_i(t) \qquad \forall\, i, t \tag{4.4.8}$$

$$\overline{S_i^{\max}}(t+1) \geq S_i(t) + \eta_{chg,i} E_i(t) + \left(\frac{1}{\eta_{dis,i}} - \eta_{chg,i}\right) z_i(t) \qquad \forall\, i, t \tag{4.4.9}$$

$$(4.2.47) - (4.2.53)$$

$$(4.3.25) - (4.3.27)$$

4.4.3. Optimization with Robust Consideration of EV Demand
In this strategy, a charging strategy is found which is robust with regard to uncertainty of EV energy demands in addition to solar forecasting uncertainty. It is necessary to consider the uncertainty for the minimum and maximum amount of energy which is allowed to be stored in a vehicle battery.

$$S_i^{\min}(t+1) = S_i^{\min}(t) + \omega_{S_i^{\min}}(t) \tag{4.4.10}$$

$$S_i^{\max}(t) = S_i^{\min}(t) + \omega_{S_i^{\max}}(t) \tag{4.4.11}$$

First, note that $S_i^{\min}(t)$ is non-strictly increasing, because as the vehicle grows closer to its departure time and the required stored energy can never decrease. This means that $\omega_{S_i^{\min}}(t) \geq 0$. In addition, the increase in the required stored energy can never be greater than the maximum possible energy which is able to be charged to a battery during a single time step. This means that:

$$0 \leq \omega_{S_i^{\min}}(t) \leq \eta_{chg,i} \cdot P_i^{\max} \Delta t \tag{4.4.12}$$

where Δt is the length of each time step. Although this serves as a suitable upper bound for $\omega_{S_i^{\min}}(t)$, it was determined that in airport charging the demand for energy is much lower than at a workplace. In order for robust optimization to avoid overly-conservative behavior, it is necessary that the uncertainty is bounded with realistic values. The upper bound for $\omega_{S_i^{\min}}(t)$ was therefore taken to be $\omega_{S_i^{\min}}(t) \leq \eta_{chg,i} \cdot P_i^{\max}$ only for workplace parking, and 10% of that value in airport parking.

We then note that the maximum allowable stored energy is determined by the battery capacity and initial stored energy, and is by definition greater then the minimum required stored energy, meaning $S_i^{\max}(t) - S_i^{\min}(t) = \omega_{S_i^{\max}}(t) \geq 0$. This uncertainty reaches its maximum value when $S_i^{\min} = 0$ and $S_i^{\max}$ is as large as possible. This cannot be greater than the usable capacity of any of the EV batteries, which is a Tesla with 94 kWh. This means that:

$$0 \leq \omega_{S_i^{\max}}(t) \leq 94 \tag{4.4.13}$$

As with the PV uncertainty, we perform a robust Monte Carlo simulation with a set of many possible uncertain values:

$$\Omega_{S^{\min}}^*(t) = \{\omega_{S^{\min}}^{(1)}(t), \ldots, \omega_{S^{\min}}^{(N_e)}(t)\} \tag{4.4.14}$$

$$\Omega_{S^{\max}}^*(t) = \{\omega_{S^{\max}}^{(1)}(t), \ldots, \omega_{S^{\max}}^{(N_e)}(t)\} \tag{4.4.15}$$

where N_e is the number of uncertainty vectors under consideration. The values for these uncertainties are selected from a uniform distribution of their possible values:

$$\omega_{S_i^{\min}}^{(j)} \in \mathcal{U}(0, \eta_{chg,i} \cdot P_i^{\max} \cdot \Delta t) \tag{4.4.16}$$

$$\omega_{S_i^{\min}}^{(j)} \in \mathcal{U}(0, 94) \tag{4.4.17}$$

for all i, j, and t. We can then substitute these values into the constraints for the optimization problem:

$$S_i^{\min}(t) + \omega_{S_i^{\min}}^{(1)}(t) \leq S_i(t) + \eta_{chg,i}E_i(t) + \left(\frac{1}{\eta_{dis,i}} - \eta_{chg,i}\right)z_i(t) \tag{4.4.18}$$

$$\vdots$$

$$S_i^{\min}(t) + \omega_{S_i^{\min}}^{(N_e)}(t) \leq S_i(t) + \eta_{chg,i}E_i(t) + \left(\frac{1}{\eta_{dis,i}} - \eta_{chg,i}\right)z_i(t)$$

$$S_i^{\min}(t) + \omega_{S_i^{\min}}^{(1)}(t) + \omega_{S_i^{\max}}^{(1)}(t) \geq S_i(t) + \eta_{chg,i}E_i(t) + \left(\frac{1}{\eta_{dis,i}} - \eta_{chg,i}\right)z_i(t) \tag{4.4.19}$$

$$\vdots$$

$$S_i^{\min}(t) + \omega_{S_i^{\min}}^{(N_e)}(t) + \omega_{S_i^{\max}}^{(N_e)}(t) \geq S_i(t) + \eta_{chg,i}E_i(t) + \left(\frac{1}{\eta_{dis,i}} - \eta_{chg,i}\right)z_i(t)$$

for all $i \in \{1, \ldots, N_b - 1\}$, $t \in \{k, \ldots, k + N_p - 1\}$. As with the PV uncertainty, we can consider the minimum and maximum uncertainties:

$$\omega_i^{\max}(t) = \max\left(\omega_{S_i^{\min}}^{(1)}(t), \ldots, \omega_{S_i^{\min}}^{(N_e)}(t)\right) \tag{4.4.20}$$

$$\omega_i^{\min}(t) = \min\left(\omega_{S_i^{\min}}^{(1)}(t) + \omega_{S_i^{\max}}^{(1)}(t), \ldots, \omega_{S_i^{\min}}^{(N_e)}(t) + \omega_{S_i^{\max}}^{(N_e)}(t)\right) \tag{4.4.21}$$

Again, we can then substitute these extreme values into the constraints without any change to the optimization problem. This is because the less-than constraints will only be active at the upper bound for the left-hand side of the inequality, and the greater-than constraints will only be active at the lower bound:

$$S_i^{\min}(t) + \omega_i^{\max}(t) \leq S_i(t) + \eta_{chg,i}E_i(t) + \left(\frac{1}{\eta_{dis,i}} - \eta_{chg,i}\right)z_i(t) \tag{4.4.22}$$

$$S_i^{\min}(t) + \omega_i^{\min}(t) \geq S_i(t) + \eta_{chg,i}E_i(t) + \left(\frac{1}{\eta_{dis,i}} - \eta_{chg,i}\right)z_i(t) \tag{4.4.23}$$

These constraints are problematic, because they risk making the problem infeasible if $\omega_i^{\max}(t) > \omega_i^{\min}(t)$, which is highly likely. In robust optimization, when constraints on the state variables can potentially lead to infeasibility, there are two options. The first is to simply remove constraints for some portion of the prediction horizon until the problem is again feasible. This, however, can lead to large constraint violations in the closed-loop, without providing any option to control the size of the violations. The preferred solution is to use a soft constrained technique, where the constraints on these state variables are relaxed, and the violation is penalized as part of the cost function. This allows for the problem to remain feasible, while providing the ability to tune the performance based on the penalty function [170]. Using soft constraints for

state variables in robust MPC optimization is typically preferred over other solutions because it allows for the control strategy to consider the presence of errors and noise, whereas using hard state constraints may lead to overly-conservative behavior [114].

In this problem, the state constraints are maintained as hard constraints for vehicles which are present at time k, as their minimum and maximum stored energy are known with certainty. The remainder are expressed as soft constraints:

$$S_i^{\min}(t) + \omega_i^{\max}(t) \leq S_i(t) + \eta_{chg,i} E_i(t) + \left(\frac{1}{\eta_{dis,i}} - \eta_{chg,i} \right) z_i(t) + \epsilon_i^1(t) \tag{4.4.24}$$

$$S_i^{\min}(t) + \omega_i^{\min}(t) \geq S_i(t) + \eta_{chg,i} E_i(t) + \left(\frac{1}{\eta_{dis,i}} - \eta_{chg,i} \right) z_i(t) - \epsilon_i^2(t) \tag{4.4.25}$$

for all $i \in \{1, \dots, N_b - 1\}$, $t \in \{k, \dots, k + N_p - 1\}$. The slack variables $\epsilon_i^1(t) \geq 0$ and $\epsilon_i^2(t) \geq 0$ correspond respectively to the constraints for the minimum and maximum stored energy, and are added to the optimization problem as an auxiliary decision variables. Because there is no uncertainty regarding the fixed storage battery, we do not consider the case of $i = N_b$.

The slack variables are then included in the cost function in order to tune the performance. If there is no penalty for constraint violation, the problem is equivalent to the optimization problem without EV forecasting. If the penalty is large, there will be a greater incentive to follow constraints as tightly as possible. The penalty function of the slack variable must be positive definite [170]. In order to use MILP in this problem, the penalty function must be linear. For simplicity, the function is taken to be constant. More advanced cost functions could also be functions of time; for example, it might be advantageous to have the penalty for constraint violation decrease for time steps which are further in the future. The cost function is given by:

$$J(x(t), \tilde{u}(t), \epsilon(t)) = T + \frac{1}{(N_b - 1) \cdot N_p} \sum_{i=1}^{N_b - 1} \sum_{t=k}^{k+N_p - 1} c_1 \epsilon_i^1(t) + c_2 \epsilon_i^2(t) \tag{4.4.26}$$

where c_1 and c_2 are constants. It is empirically determined that the peak demand was minimized for penalties of $c_1 = 1, c_2 = 1$, although increasing the penalty above these values did not significantly affect the peak demand. The complete optimization formulation is then given by:

$$\underset{T, E_{grid}^{\max}, E, \delta, z, \epsilon}{\text{minimize}} \quad T + \frac{1}{(N_b - 1) \cdot N_p} \sum_{i=1}^{N_b - 1} \sum_{t=k}^{k+N_p - 1} c_1 \epsilon_i^1(t) + c_2 \epsilon_i^2(t) \tag{4.4.27}$$

With the decision variables:

$$T, E_{grid}^{\max}, E_i(t), \delta_i(t), z_i(t), \epsilon_i^1(t), \epsilon_i^2(t) \qquad \text{for } i \in \{1, \dots, N_b\}, \quad t \in \{k, \dots, k + N_p - 1\} \tag{4.4.28}$$

Such that:

$$\epsilon_i^1(t), \epsilon_i^2(t) \geq 0 \qquad\qquad\qquad \forall\, i, t \tag{4.4.29}$$

$$S_i^{\min}(t) + \omega_i^{\max}(t) \leq S_i(t) + \eta_{chg,i} E_i(t) + \left(\frac{1}{\eta_{dis,i}} - \eta_{chg,i} \right) z_i(t) + \epsilon_i^1(t) \qquad \forall\, i, t \tag{4.4.30}$$

$$S_i^{\min}(t) + \omega_i^{\min}(t) \geq S_i(t) + \eta_{chg,i} E_i(t) + \left(\frac{1}{\eta_{dis,i}} - \eta_{chg,i} \right) z_i(t) - \epsilon_i^2(t) \qquad \forall\, i, t \tag{4.4.31}$$

$$(4.2.47) - (4.2.53)$$

$$(4.3.25) - (4.3.27)$$

5

Results and Discussion

Using the model developed in Chapter 3 and the charging strategies discussed in Chapter 4, smart charging in solar parking lots was simulated. In this chapter, the results of these simulations will be presented and analyzed. First, Section 5.1 will discuss the performance of the system with varying system parameters. Then, Section 5.2 will examine the impact of forecasting uncertainty on the system performance. Conclusions based on these results will be given in Chapter 6.

5.1. Effect of Different System Parameters

Many of the system design parameters are based on results from real-world data or literature. However, some aspects of the system design must be determined experimentally. In order to determine these system parameters, various simulations were run examining the performance of smart charging with different parameters. Based on these simulations, the preferred system design was determined. The system parameters which are discussed in this section are: the capacity of the fixed battery storage; the use of AC vs DC chargers; and the battery capacity of the EVs which charge in the parking lot.

When simulating the solar parking lot, the energy at each time step is determined. Plots of this energy of time are useful in understanding the behavior of the system under various conditions and strategies. As a baseline, one week of charging using uncoordinated charging is shown in Figure 5.1
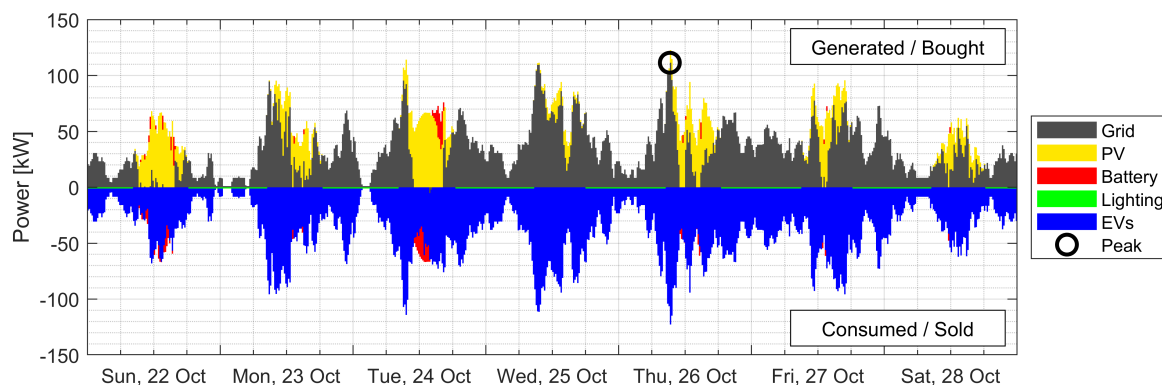
Figure 5.1: Power flows at a workplace with uncoordinated charging

The energy at each time step is shown as stacked areas. By convention, energy entering the system from generation or the grid is positive, and energy leaving the system through consumption or sale is negative. At each time step, the total energy generated and bought must equal the total consumed and sold, making the graph symmetric about the x axis. Different colors correspond to different types of energy. Grid electricity is shown in grey, with energy being positive when it is bought and negative when it is sold. Solar power generation, always positive, is in yellow. Fixed battery storage is shown in red, and is positive when the battery is

being discharged and negative when it is charged. The LED lighting is shown in green and is always negative, although the contribution from lighting to the total load is negligible. EV charging is shown in blue, with the total power being discharged from EVs being positive and the total power being charged to EVs being negative. The losses during charging and discharging the fixed battery and EVs are included in those categories. In addition, the peak demand over the course of the week is indicated through a black circle. The graph then allows for the observation of the different contributions from various sources and loads by comparing the relative heights of the stacked areas.

There are a few observations that can be made based on Figure 5.1 specifically. Firstly, the amount of energy from solar power is not nearly as much as the amount required for charging EVs in a workplace parking lot. Therefore, a significant amount of energy must be purchased from the grid. Secondly, batteries are not very effective at reducing the peak electricity demand. The peak demand during this week is on Thursday morning, when the 111.4 kW is drawn from the grid. This is slightly above the demand on Wednesday morning. On Tuesday, a high level of solar irradiance led to some excess generated solar energy. That energy was stored in the 50 kWh fixed battery, but it was quickly used up on Tuesday afternoon. A larger battery would not have avoided the peaks on Wednesday and Thursday, because the battery was already completely discharged by then. Finally, note that vehicles tend to arrive on weekday mornings, with many plugging in simultaneously. In uncoordinated charging, this leads to large spikes in the power delivered to EVs on weekday mornings. Because there is very little solar energy available at the beginning of the day, these spikes in demand are powered with energy from the electricity grid, leading to high peak demand at those times. In order to avoid these peaks, smart charging is used.

5.1.1. Fixed Storage Capacity

In the parking lot, there is a fixed storage battery system attached to the DC microgrid. This battery can be charged and discharged in order to reduce the peak grid exchange. A larger battery would enable more energy to be stored, enabling greater flexibility and reducing the peak load. However, this comes at a greater expense to the parking lot operator, meaning that the battery should be no larger than necessary. In addition, the optimal capacity for the battery will depend on whether or not there is bidirectional charging. If Vehicle to Grid (V2G) is possible in the parking lot, the discharging vehicles can potentially replace a fixed storage battery. Systems with different fixed battery storage capacities were simulated, assuming that perfect information was available. The relationship between peak grid demand and fixed battery capacity is shown in Figure 5.2. Note that only 80% of the fixed battery capacity is usable.
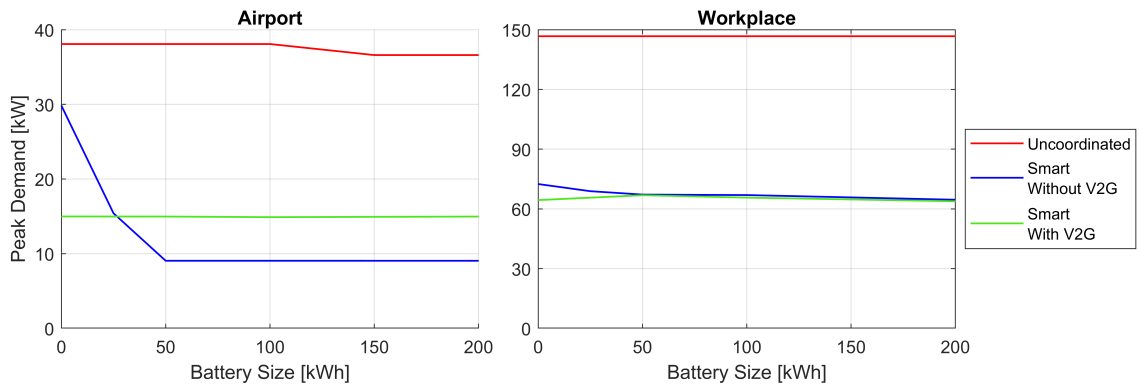
Figure 5.2: Peak grid demand vs. fixed battery storage capacity

As can be observed, smart charging with or without Vehicle to Grid (V2G) can decrease the peak electricity demand compared to uncoordinated charging. These advantages, however, are limited. Somewhat surprisingly, at both an airport and a workplace parking there is no advantage in having a fixed storage battery larger than 50 kWh. This is equivalent to 40 kWh of usable capacity, which is only 1 kWh of usable capacity per parking space.

In order to see how smart charging can reduce the peak demand, Figure 5.3 shows one week of power flows for a workplace parking lot with a 50 kWh battery, where future solar energy production and EV charging demands are known perfectly. In order to reduce the peak electricity demand, charging is redistributed so that the grid exchange is nearly flat over the course of the day. This peak-shaving behavior can reduce the

maximum demand by 52.6% on Wednesday afternoon, from 111.4 kW to only 52.8 kW. Smart charging also lead to valley-filling, where more power is drawn from the grid at times of low demand to charge vehicles. On Tuesday night into Wednesday morning, power was drawn from the grid to fully charge the fixed storage battery, so that the electricity could be used on Wednesday morning to charge the newly arrived vehicles. Most of the peak shaving and valley filling behavior, however is not accomplished using the fixed storage battery. Instead, it is accomplished using the flexibility inherent to the vehicles, by charging them evenly over the course of the day and taking advantage of solar energy when it is available.
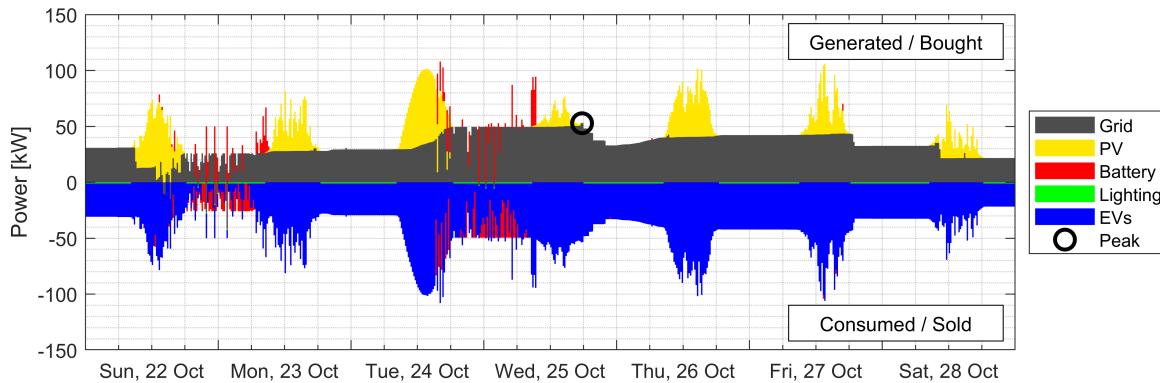

Figure 5.3: Power flows at a workplace with smart charging with perfect information

Figure 5.3 demonstrates why a larger battery is not beneficial in reducing the peak demand. Because of the flexibility inherent to the vehicles, charging can be rescheduled to even out the demand with minimal use of the battery. The opportunity to charge the battery is limited. This is because there is rarely any excess solar energy. Charging the battery from the grid can reduce the peak demand somewhat, but too large of a battery would put excessive strain on the grid when charging. A fixed storage battery cannot generate energy, and since the demand is higher than the generation power must always be drawn from the grid at some point. The battery only enables that power to be drawn as evenly as possible over the course of the day, and for that purpose 50 kWh is sufficient. Drawing power from the grid further in advance and storing it for a longer time is not possible, because fixed battery storage is sufficient only to handle mismatch in supply and demand lasting a few hours. With a couple of days of low solar generation, even a very large battery will quickly run out of energy. Because batteries cannot practically store enough energy for days or weeks, as would be required, 50 kWh is sufficient to handle short term fluctuations.
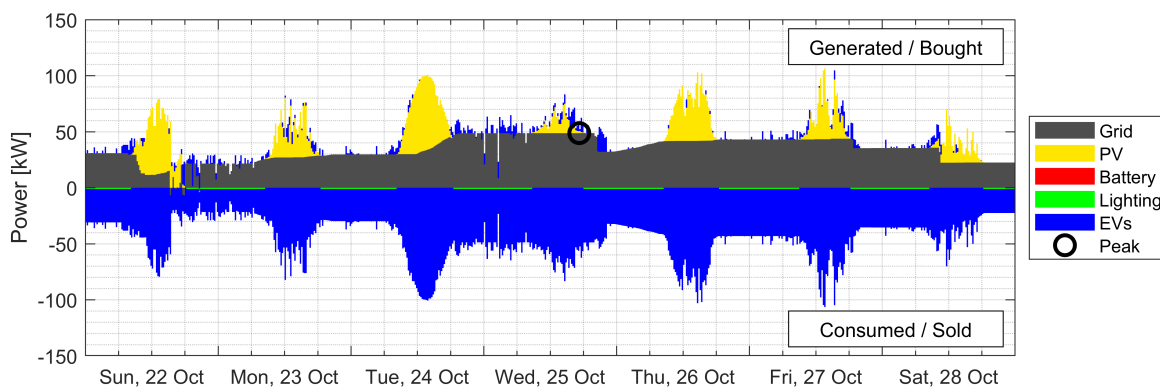

Figure 5.4: Power flows at a workplace with smart charging with perfect information using V2G

For systems with bidirectional charging, no fixed battery storage is needed, as demonstrated by Figure 5.4. This is because the storage in the vehicles themselves is sufficient to enable short-term flexibility. As can

be observed, at a workplace the power which is drawn from vehicles is much lower than the power needed to charge them. The total energy storage required is minimal, and as a result a fixed storage battery is not needed in systems where V2G is in use. For parking lots that have V2G, the peak grid demand can be reduced by 61% in an airport and 56% in the workplace when compared to uncoordinated charging. Although the charging patterns for electric vehicles are somewhat different, the grid demand in Figures 5.3 and 5.4 are quite similar, demonstrating how both fixed storage and V2G are able to reduce the peak demand.

It is interesting to note that, as seen in Figure 5.2 peak demand at a workplace with bidirectional charging is the same as for a parking lot with a fixed battery. For airport parking, however, V2G results in a higher peak demand. This is somewhat surprising, because V2G is often assumed to be a valuable technique in reducing peak electricity demand. The reason for the increased peak is that vehicles parked at an airport use more energy when engaged in V2G, as seen in Table 5.1.

Table 5.1: Energy used for AC electric vehicle charging with perfect information

Charging strategy	Energy demand [kWh / day]	
	Workplace	Airport
Uncoordinated charging	1019	107
Smart charging with fixed battery	1045	107
Smart charging with V2G	1080	176

Energy losses during discharging mean that more energy is needed if V2G is used. At a workplace, almost all vehicles depart within 24 hours, meaning that the controller can anticipate this additional energy demand and V2G is not used unless it is necessary. This means that overall energy demand is only slightly affected and the peak does not increase. At an airport, however, vehicles can remain parked for days or even weeks. Vehicles are therefore discharged to reduce the peak load in the short term. In airport long term parking, an average of 18.7 kWh is discharged from each vehicle during the time it is parked, while at a workplace parking lot that figure is only 0.9 kWh per vehicle. Losses during discharging result in airport smart charging consuming 64% more energy per vehicle, compared to charging without V2G. This increased electricity consumption means that V2G will lead to a greater peak demand when vehicles needs to be recharged, especially in a system where they are parked for longer periods of time.

Even without energy storage in vehicles or a battery, smart charging can still reduce the peak demand with or without a fixed storage battery. With a 50 kWh battery smart charging is able to reduce the peak demand by 54% in a workplace and 76% in an airport when compared to uncoordinated charging. Without a fixed battery the peak demand could not be reduced as substantially, although it can still be decreased by 51% in workplace parking and 22% in airport parking. This means that for a parking lot operator seeking to decrease their construction costs, a fixed storage battery may not be necessary in order to fully realize the benefits of smart charging, especially with workplace charging. For these simulations, however, either V2G or a 50 kWh fixed battery was used as a form of energy storage.

5.1.2. AC or DC Vehicle Charging
Slow charging in vehicles is generally done using AC power, with DC power being reserved for fast charging. Most slow charging, therefore, considers only AC charging equipment. DC slow charging should be able to reduce losses as the efficiency for DC charging is higher than the efficiency of AC charging, especially during V2G, as can be observed in Table 3.4. With V2G using an AC charger, the DC power from the battery must be converted to AC power through an on-board inverter, which can have high losses. When charging is done with DC equipment, these losses can be avoided. In this model, slow DC charging was considered in addition to AC charging. The relationship between peak grid exchange and charging type is shown in Figure 5.5. In all cases, 40 charging stations are considered in total, meaning that 0 DC chargers corresponds to 40 AC chargers and vice versa.

Despite these benefits of DC charging, there is no major difference compared to AC charging with regard to the peak demand. For uncoordinated charging or unidirectional smart charging, the difference in efficiency does not significantly impact the peak demand. The only exception is in airport charging with V2G. As has already been discussed, the longer parking durations at airports result in greater quantities of energy being discharged from vehicle batteries when V2G is considered, compared with workplace charging. This means that the improved discharging efficiency can marginally decrease the peak demand. At an airport, DC
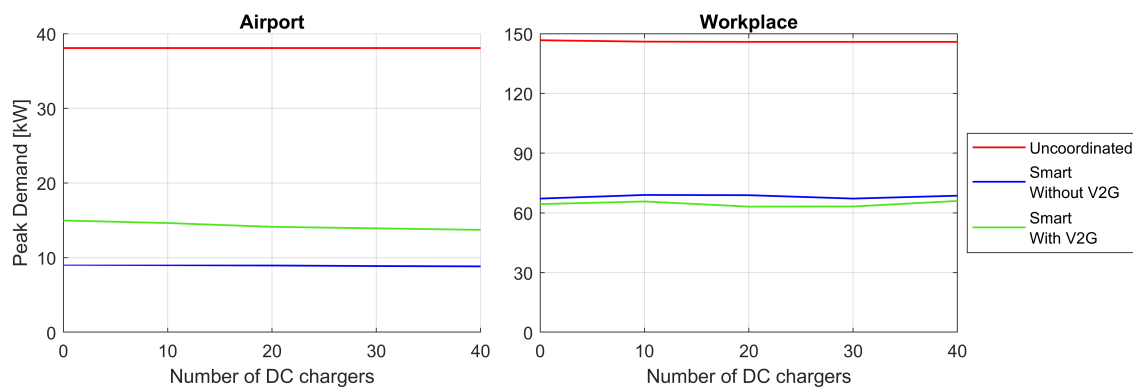
Figure 5.5: Peak demand vs. number of DC chargers

chargers result in a peak demand of 13.73 kW, compared to 14.98 for AC charging, a decrease of 8%. For unidirectional charging, the decrease is only 2.4%, and in workplace parking there is not decrease in peak demand, with or without V2G.

Due to their higher efficiency, DC chargers also reduce the total energy demand, as seen in Table 5.2. These values compared to the energy required for AC charging, as given in Table 5.1. For workplace charging, the improvement in efficiency leads to a marginal decrease in the total energy. Even for V2G, however, the energy use only drops 3.3%. Similarly, airport unidirectional and uncoordinated charging do not use significantly less energy with DC compared to AC chargers. With V2G, however, the difference is substantial. For an airport parking lot with bidirectional AC chargers, EVs require an average of 176 kWh per day. If DC chargers are used, that quantity drops 20% to 140 kWh. DC charging may therefore be valuable in a parking lot which heavily utilizes bidirectional charging, such as airport long term parking. In this model, however, only AC chargers are considered. This is because commercial DC slow charging is more or less non-existent, as AC charging remains the standard around the world for slow EV charging equipment.

Table 5.2: Energy used for DC electric vehicle charging with perfect information

Charging strategy	Energy demand [kWh / day]	
	Workplace	Airport
Uncoordinated charging	1003	104
Smart charging with fixed battery	1028	105
Smart charging with V2G	1044	140

5.1.3. Battery Capacity of EVs

The properties of electric vehicles in the Netherlands are changing rapidly. With the introduction of lower-priced EVs with larger batteries, it is likely that the energy demand of BEVs will also increase. As shown in Figure 2.3, the range for affordable EVs has increased from roughly 125 km in 2013 to an anticipated 300 km in 2020. This increase in battery size, combined with the increasing popularity of EVs, results in a higher energy demand. In 2013, the average public charging station in the Netherlands would consume 5.0 kWh of electricity per day. By 2018, that figure had grown to 9.9 kWh per day, and it is anticipated that the average consumption will increase by a further 50% by 2025–2030 [74].

Even if vehicle batteries remain the same size they are currently, the demand for electricity to charge EVs in the Netherlands will continue to grow. This is because the number of battery electric vehicles (BEVs) is increasing exponentially, while the number of plug-in hybrid electric vehicles (PHEVs) is steadily decreasing, as shown in Figure 2.4. On 31 December 2016, the fraction of EVs which were fully electric was only 11.7%. By 31 January 2019, that number had increased to 32.7%. Because January 2019 was the latest data available when simulations were being run, it is the date used for models in this report. Already, this model is out of date. As of 31 May 2019, the fraction of BEVs has risen to 37.5%, with BEV registrations increasing from 44,984 to 57,947 over just five months as PHEV registrations decreased from 97,702 to 96,662 [16]. If these trends

continue, BEVs will make up more than 50% of all electric vehicles in the Netherlands by the middle of 2020.

These trends could have significant consequences for solar parking lots with EV charging. This report considers primarily a system where only 32.7% of EVs are BEVs. But if that fraction increases, the average energy required in a charging event will increase as well. The relationship between the energy consumed by a vehicle during charging and the proportion of BEVs is shown in Figure 5.6a. Because the vehicles require more energy, charging events will last longer. This means that uncoordinated charging with more BEVs will result in a higher peak demand, as as shown in Figure 5.6b.

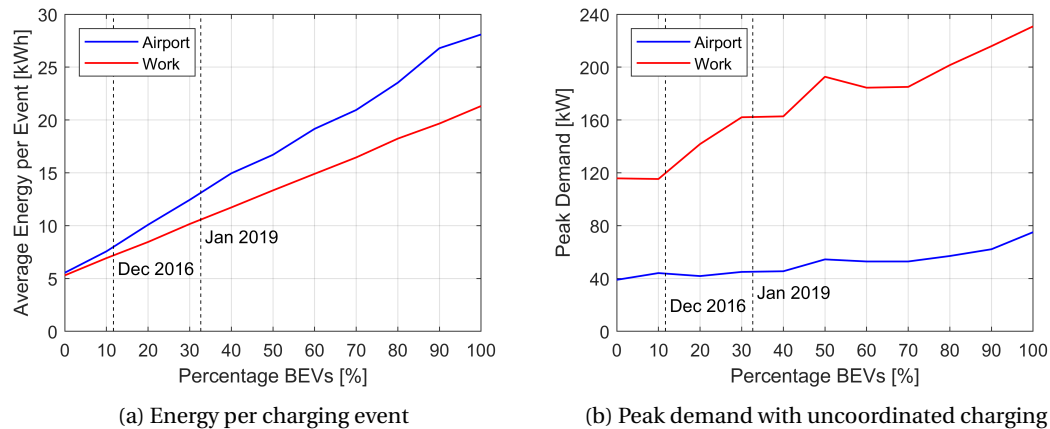(a) Energy per charging event   (b) Peak demand with uncoordinated charging

Figure 5.6: Effect of the percentage of EVs which are fully electric on charging demand

At the current proportion of BEVs, the energy demand is roughly 10.6 kWh per vehicle in a workplace, and 13.1 kWh per vehicle in an airport. If 100% of all EVs were BEVs, the required energy would approximately double to 21.3 kWh at a workplace and 28.1 kWh at an airport. Vehicles charging at an airport require more energy than those at a workplace because workplace charging sessions are shorter, and therefore more likely to be interrupted before the vehicle is able to charge fully. A Tesla car with a usable capacity of 94 kWh would take over 12 hours to charge from an empty battery. Because most vehicles in a workplace parking lot remain parked for less than 12 hours, the energy per event is limited for these parking lots. In airports, where vehicles are parked for longer, almost all vehicles have enough time to charge fully. This means that the energy per event is higher for airports.

As the overall demand for energy increases, so does the peak demand. Considering uncoordinated charging, if all EVs were plug-in hybrids, the peak demand at a workplace would be only 115 kW, but at the current rate of 32.7%, the peak demand is 146 kW. If all EVs were BEVs, peak demand would leap to 231 kW, more than double the peak demand with only PHEVs. A similar trend is observed with airport charging, where the peak demand increases from 39 kW to 75 kW as the fleet switches from all PHEVs to all BEVs. Using smart charging could potentially reduce the peak demand for electricity, but as vehicles continue to inevitably grow, the energy and peak demand will grow as well. Any plan for smart parking lots must take into account this future growth.

5.2. Effect of Uncertainty

In the previous section, simulation results considered only smart charging with perfect information. That is, it was assumed that solar power forecasts were perfectly accurate. It was also assumed that EV arrival times departure times, battery capacities, and battery SOC on arrival would all be known perfectly in advance. These assumptions are commonly made in smart charging models, but they are clearly flawed. In reality, solar power forecasts are frequently mistaken. Information about EVs such as the battery capacity, state of charge, arrival time, and departure time is often not known until after the vehicle arrives. In Chapter 4, charging strategies were developed which allow for the consideration of these uncertainties in smart charging. The peak energy demand under different control strategies will be presented here. First, uncertainty and error in PV forecasting will be discussed. Then, the impact of unknown EV arrivals will be determined.

5.2.1. Solar Power Forecasting Uncertainty

Since solar generation is not known perfectly in advance, strategies were developed in Section 4.3 to consider this uncertainty. First a nominal strategy was described, where the forecasted values are used in determining the charging actions without considering forecasting errors. A robust strategy was also detailed, which determines the optimal strategy for reducing the peak demand over a range of possible forecasting errors. The robust strategy is more effective at reducing the peak demand over the course of the year, as demonstrated in Figure 5.7. The peak demand is compared to the root mean squared error (RMSE) in Figure 5.7a and to the mean bias error (MBE) in Figure 5.7b.
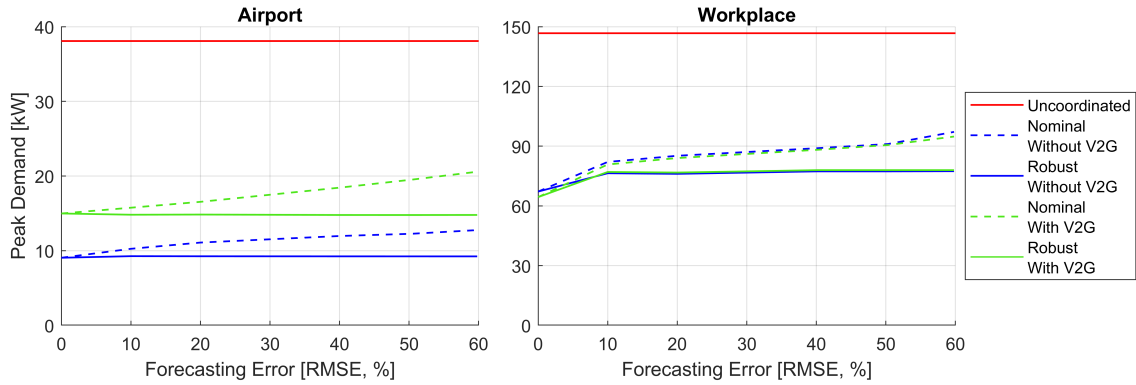
(a) Peak demand vs. root mean square error (RMSE)
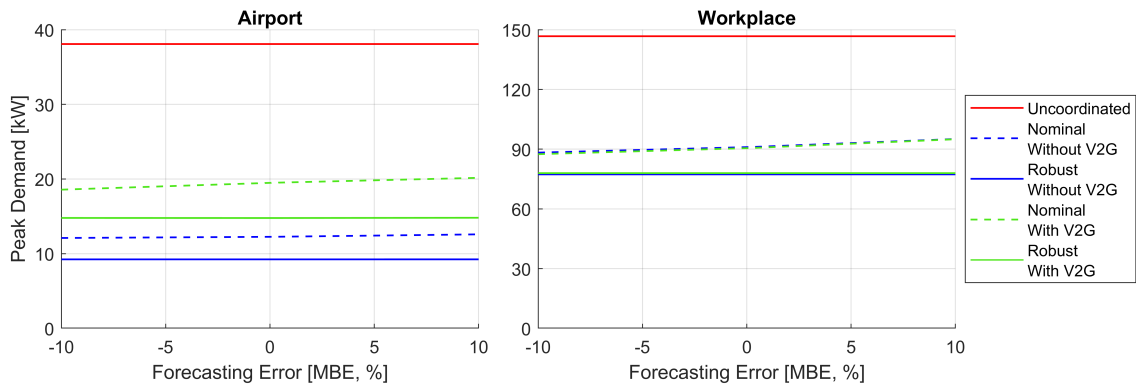
(b) Peak demand vs. mean bias error (MBE)

Figure 5.7: Peak demand vs. forecasting errors for solar power generation

The RMSE is analogous to the standard deviation of the forecasting error, meaning that a larger RMSE corresponds to forecasting errors which are more widely distributed. In this simulation, the typical value for the RMSE is taken to be 50%. When using nominal smart charging, an increasing RMSE results in a larger peak demand. This is because a larger RMSE will mean larger over-and underestimations of the forecast for the upcoming day, resulting in higher peak demand under the planned control strategy. Robust optimization avoids this problem, by selecting an optimization strategy which has the best performance under a wide range of forecasting errors. Robust optimization therefore leads to a lower peak demand than nominal optimization for systems both with and without V2G. Interestingly, the peak demand when using the robust strategy is not very sensitive to the magnitude of the RMSE. This is because as the RMSE grows larger, the range of forecasting errors considered by the controller grows as well.

The MBE is analogous to the mean of the forecasting error, meaning that a positive MBE corresponds to chronic overestimation of future solar generation, and a negative MBE corresponds to consistently underestimating future generation. In this simulation, the typical value for the MBE is taken to be 0%. As with the RMSE, robust optimization is relatively insensitive to the MBE, because over-and underestimation in solar forecasts are already considered by the optimization controller. The nominal optimization is somewhat dependant on the MBE, with a larger MBE leading to a greater peak demand, and a more negative MBE leading to a lower demand. If the MBE is positive, the solar forecast will be on average overestimate the true genera-

tion, leading to vehicle charging being delayed, with the plan to charge when solar energy is available. When the forecast is wrong and insufficient solar power is generated, more energy will need to be drawn from the grid. Similarly, a negative MBE will cause the controller to behave more conservatively, resulting in a lower peak electricity demand, as overestimating future solar production is less likely in this scenario.

The performance of nominal and robust strategies can also be compared by examining the power flows over a typical week. Power flows for one week using the nominal strategy are shown in Figure 5.8.
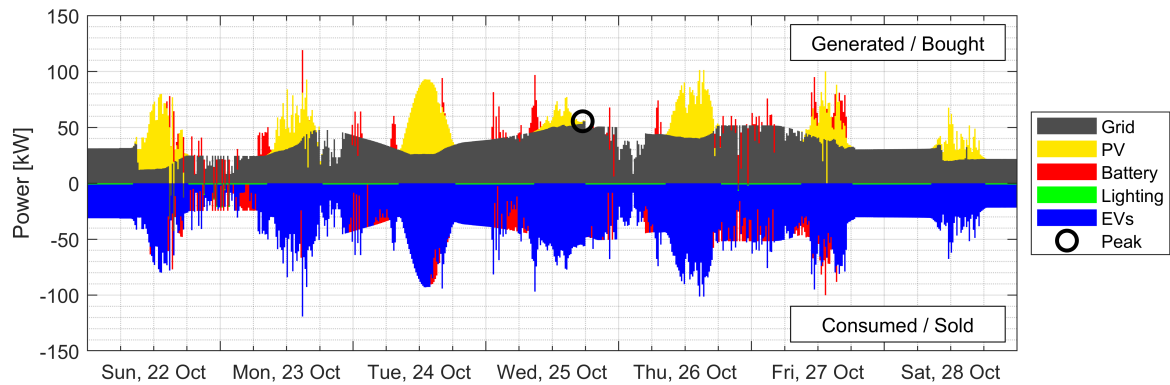

Figure 5.8: Power flows for workplace smart charging with nominal solar forecasting

In order to compensate for the forecasting errors, energy is charged to and discharged from the fixed battery storage. As the forecast becomes more accurate over the course of the day, the changing behavior can be observed. On Tuesday, solar energy was quite high, but the forecast underestimated the production. As a result, more energy from the grid was used Monday evening and Tuesday morning to charge vehicles and the fixed battery storage. As the day went on, the forecast improved and the system updated itself, ultimately reducing the energy that needed to be bought from the grid. This is why a downward slope is visible for the grid energy on Tuesday morning. Wednesday suffered from the opposite problem, with the forecasted energy being higher than the actual production, As a result, more energy needed to be bought from the grid as the control system updated over the course of the day. This led to the peak demand for the week increasing slightly from the ideal scenario, with 55.5 kW being drawn from the grid on Wednesday afternoon.
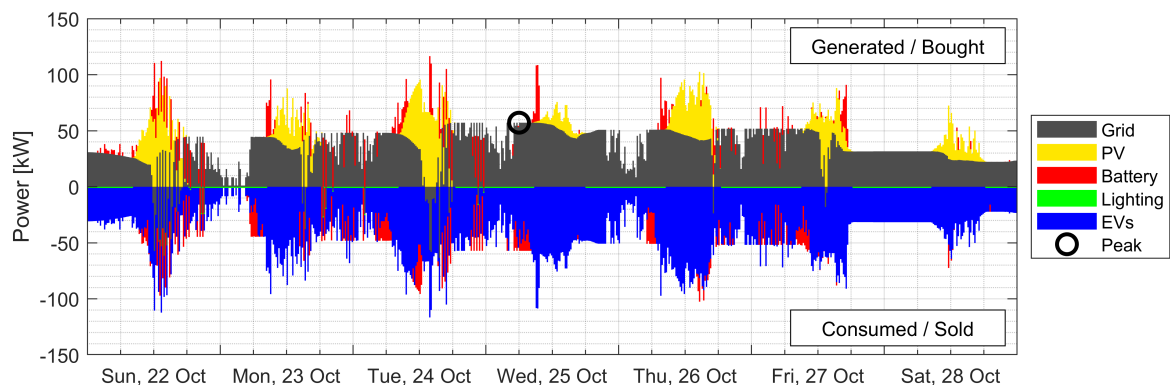
Figure 5.9: Power flows for workplace smart charging with robust solar forecasting

In order to consider forecasting uncertainty, robust optimization was used, as shown in Figure 5.9. With robust optimization, vehicles charging is scheduled considering the possibility that forecasted solar power may be not end up being generated. As with nominal optimization, forecasts improve over the course of the day, leading to more variable grid exchange when compared with ideal smart charging. With robust optimization, however, more vehicle charging is done in the morning, in order to avoid higher demand later in the day

in the event that there is little solar energy. Robust optimization is often excessively conservative, leading to more charging in the morning than is necessary. As a result, the peak demand during robust optimization occurred on Wednesday morning, with a maximum load of 57.2 kW. As the day went on, some solar energy was used to charge vehicles, and the demand on the grid reduced. This pattern is even starker on Tuesday, where energy was also drawn from the grid to charge the fixed battery and vehicles, in anticipation that the forecasted generation would be an overestimate. In reality, solar generation on Tuesday was underestimated. On Tuesday afternoon, there was more solar power than there was demand from vehicles. Because the fixed battery was already full, some energy had to be sold to the grid.

Because of this overly-conservative behavior, when considering solar forecasting uncertainty robust optimization leads to a higher peak demand than nominal optimization on most days of the year, despite the fact that the annual peak is still lower for the robust strategy. Robust optimization considers the worst-case scenario for forecasting errors, which can lead to the robust optimization to rely less on solar power generation when it is available. As a result, nominal optimization results in a lower peak demand most days of the year, as seen in Figure 5.10. In this figure, the maximum electricity demand is shown for each day of the year at the airport parking lot, considering nominal optimization, robust optimization, and optimization with perfect information.
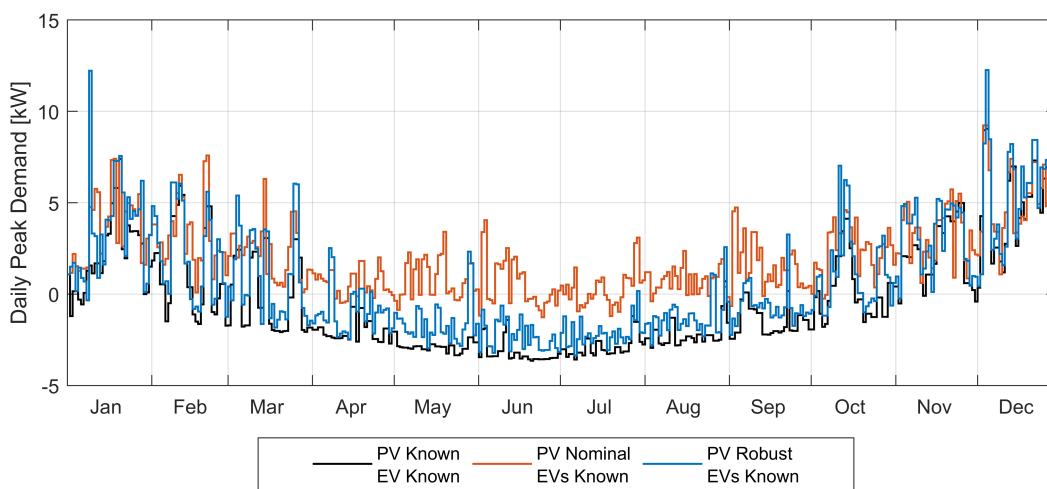
Figure 5.10: Daily peak demand at an airport considering PV uncertainty

Most of the time, especially during the summer, the nominal optimization results in a lower daily peak. This is because at times when solar energy is available, nominal optimization relies on the forecast when charging the vehicles. If the forecast is wrong, however, and overestimates the solar energy which will be available, robust optimization can result in a lower daily peak demand. Because the winter days with little solar energy, are the days with the highest peak demand, robust optimization performs better when looking at the year as a whole. On more than 80% of all days, however, the nominal optimization has a lower peak demand for electricity. This overly conservative behavior, where robust optimization does not rely on solar electricity, can also lead to more solar energy being sent to the grid, as seen in Table 5.3.

Table 5.3: Net energy exchange with different strategies

	Airport [kWh]			Workplace [kWh]		
	To grid	From grid	Net	To grid	From grid	Net
Uncoordinated	101,730	14,319	-87,411	14,258	258,422	244,164
PV Known, EVs Known	91,319	5,797	-85,522	8,748	262,534	253,786
PV Nominal, EVs Known	93,050	6,282	-86,768	8,914	262,540	253,626
PV Robust, EVs Known	95,668	8,413	-87,255	31,138	287,882	256,743

In airport charging, the energy required to charge EVs is less than the energy generated by solar energy.

This means that the net grid exchange is negative. During uncoordinated charging, vehicles are charged without considering the availability of solar energy, so a large amount of energy needs to be purchased from the grid. Smart charging reduces that problem, delaying charging until solar energy is available. Using robust optimization, the controller relies less on future solar energy, because the forecast may be mistaken. This means that more energy must be purchased from the grid. Robust optimization therefore results in 34% more energy being purchased compared to nominal optimization. Despite robust optimization purchasing 2,131 kWh more from the grid, in total 487 kWh more are sent to the grid. This is because energy which is sent to the grid results in fewer efficiency losses compared to being stored in a battery. In workplace charging, a similar effect is observed. Robust optimization purchases 9.7% more energy from the grid compared to nominal optimization. Again, the net energy used is roughly the same, meaning that more energy must be sent back to the electricity grid. In total, the solar panels produce 133,625 kWh over the course of a year. Using nominal optimization, only 6.5% of that energy is sent to the grid with workplace charging. With uncoordinated charging, 10.7% of solar energy is sent to the grid. Using robust optimization, that figure is 23.3%. Although robust optimization does reduce the peak demand, it comes at the cost of a higher average electricity demand and a lower level of self-consumption.
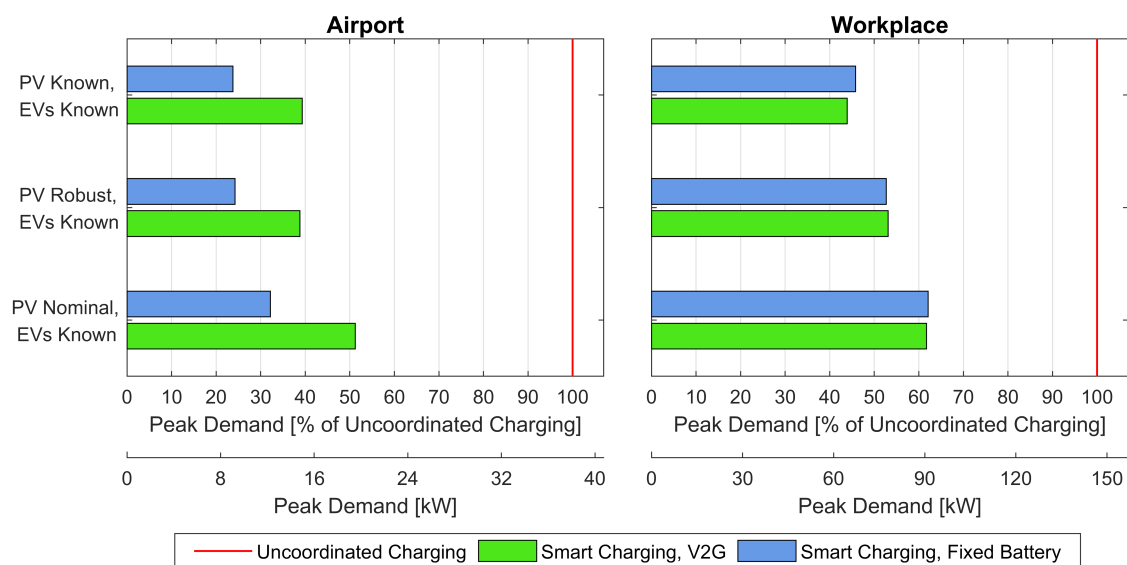

Figure 5.11: Peak demand for different control strategies considering PV uncertainty

The conclusions from this section are summarized in Figure 5.11. Using robust optimization results in a peak demand which is lower than that of nominal optimization, although it is still higher than ideal charging using perfect information. Despite the uncertainty of solar generation, robust and nominal optimization still have a much lower peak demand compared to uncoordinated charging. In addition, note that at airport parking, bidirectional charging results in a higher peak electricity demand, whereas at the workplace these numbers are roughly equal. This is because airport charging results in more energy being discharged from a vehicle compared to workplace charging. Because of the higher energy demand due to losses during discharging at an airport parking lot with V2G, the peak demand in these systems is higher than at an airport parking lot with only fixed battery storage.

5.2.2. Electric Vehicle Behavior Uncertainty

The charging demand of EVs is not known before they arrive. The vehicles' arrival time, departure time, battery capacity, and initial state of charge will all be unknown before the vehicle begins charging. Without this information, smart charging cannot as effectively plan the vehicle charging for the coming day. Section 4.4 considers three strategies to handle this uncertainty. The no-forecast strategy determines the optimal behavior for the vehicles already present, without considering the possibility of future arrivals. The average strategy considers future arrivals by assuming an average energy demand for vehicles which have not yet arrived. Both the no-forecast and average strategies are nominal, meaning that they consider only one possible scenario, rather than a many scenarios for the EV energy demand. The robust strategy considers a range of possible

future arrivals, seeking to minimize the peak demand robustly over all possible future sets of vehicles. For all of these strategies, a robust approach is also used to consider the errors in the solar power forecasting.
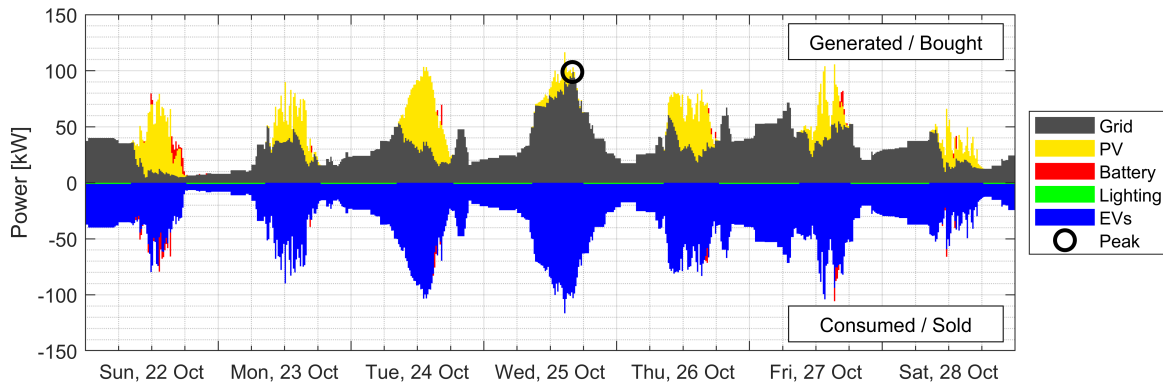

Figure 5.12: Power flows for workplace smart charging with no forecasted EV demand

The simplest way of handling this uncertainty is with no EV forecasting. The resulting power flows for a typical week are shown in Figure 5.12. Because the charging strategy does not plan for future arrivals, vehicles are not charged nearly as quickly overnight or in the mornings. This charging is delayed to reduce the peak demand at these times. This creates a problem when a large number of vehicles arrives during the day, and there is not much solar energy to charge those vehicles. On Wednesday, a large number of vehicles begin charging, and the resulting demand resulted in a peak load of 98.9 kW. This peak is much higher than smart charging with perfect information, and only slightly lower than the peak during uncoordinated charging as shown in Figure 5.1. Although the no-forecast strategy is relatively simple to implement, it is quite ineffective at reducing peak power demand. To solve this problem, the average strategy can be implemented, as seen in Figure 5.13.
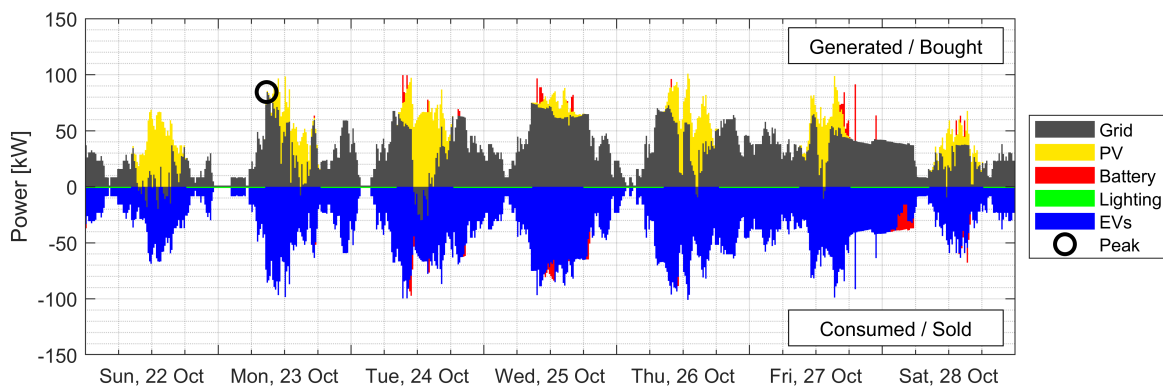
Figure 5.13: Power flows for workplace smart charging with average forecasted EV demand

In the average strategy, the forecast for future EV charging demand is based on the average demand of vehicles. This allows the control strategy to plan for future arrivals, charging vehicles in such a way that the peak demand will be minimized when new vehicles begin charging. As can be observed, more EVs are charged in Wednesday morning in Figure 5.13 compared with Figure 5.12. Because the future arrivals were anticipated, the peak demand on Wednesday was reduced from 98.9 kW to 73.4 kW. This strategy is not without its downsides however. If the actual EV charging demand is below average, the nominal strategy may lead to excessive charging in the morning, in anticipation of a nonexistent demand. On Tuesday, this results in energy being drawn from the grid in order to charge vehicles in the morning, leading to excess solar energy being sold to the grid in the afternoon. On Monday, with a below average demand for EV charging, vehicles are still charged

primarily in the morning. As a result, the peak demand occurs on Monday morning, drawing 84.5 kW from the grid. Although the peak was higher when no forecasting was considered, this is still a substantially larger demand than the scenario with perfect forecasting.
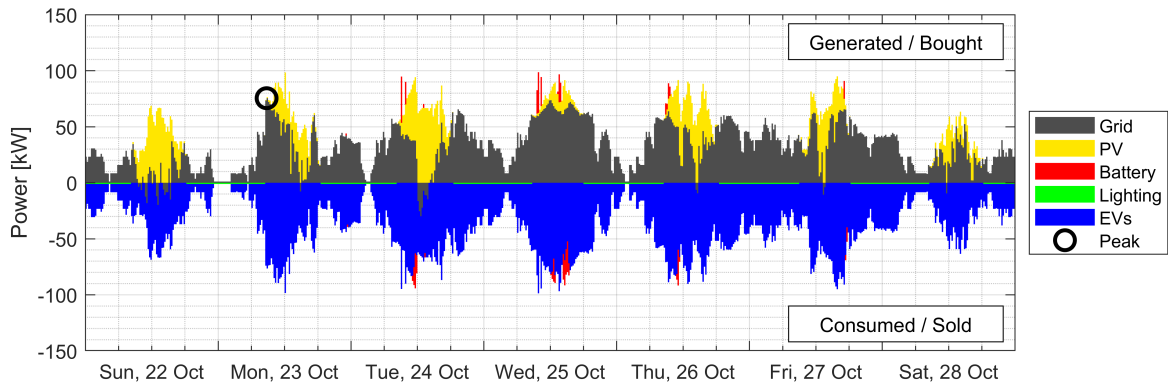

Figure 5.14: Power flows for workplace smart charging with robust EV demand forecasting

Through the use of robust charging strategies, this peak can be further reduced, as seen in Figure 5.14. Robust optimization considers a range of possible EV charging requirements, and implements a charging strategy which results in the lowest peak load regardless of the energy demand. In the robust consideration of EV uncertainty, the controller is able to schedule vehicle charging so as to avoid the largest peak demands of both the no forecasting and the nominal optimization. On Wednesday, vehicles are charged more evenly over the day, resulting in a peak demand of 73.7 kW, compared to 98.9 kW for optimization without forecasting. On Monday, more charging is delayed until the afternoon, resulting in a peak of 75.5 kW, compared to 84.5 kW for the average strategy. As a result, robust optimization leads to the lowest peak demand.
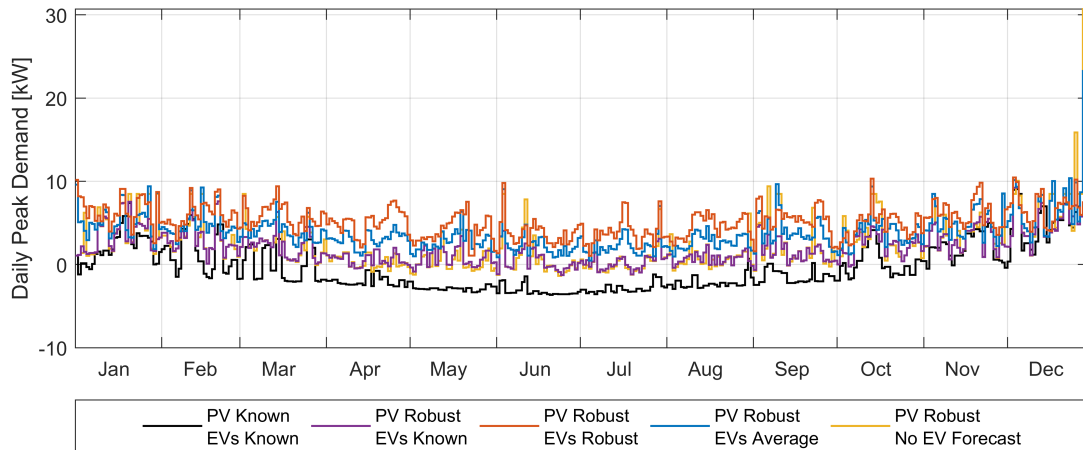
Figure 5.15: Daily peak demand at an airport considering EV demand uncertainty

When handling uncertainty with EV behavior, robust optimization often leads to a higher peak demand, as seen in Figure 5.15. This figure depicts the maximum demand on the grid each day of the year, for the different optimization strategies. As can be observed, perfect information leads to the lowest peak demand, as would be expected. On many days, in particular during the summer, the peak demand is less than zero, meaning that electricity is never bought from the grid. When PV generation is uncertain, even if the EV demand is known, there are far fewer days when no electricity is bought from the grid. Still, the annual peak demand is relatively low as long as EV demand is known. When this demand is uncertain, the annual peak can increase significantly.

With airport charging, future vehicle arrivals are infrequent enough that the no-forecast strategy results in a relatively low peak demand on most days. On days like December 28th, however, the no-forecast strategy leads to the largest peak load. A high demand for energy to charge vehicles on that day leads to a sharp spike in the demand, as seen in Figure 5.15. The strategy with average forecasted demand anticipated this load to an extent, charging the fixed battery, but this was not sufficient to minimize the peak demand. Only the robust strategy was able to maintain a low peak demand over the course of the year. These peaks can lead to serious problems for infrastructure such as transformers. Robust optimization is an effective strategy for reducing these high peaks in the demand for power. As discussed in Section 2.2, transformer lifetimes can be significantly shorted by even short events where the load on the transformer is well above the rated capacity. This suggests that the robust behavior, where the peak load on most days is higher but the overall maximum demand is minimized, will result in a longer transformer lifetime than other strategies with a lower peak on most days but a few events with very high loading for short intervals.

Robust optimization can lead to more conservative behavior, as it did when considering uncertain solar forecasting. The robust strategy can again lead to more energy being sold to and bought from the grid, as seen in Table 5.3. At an airport parking lot, the long charging periods for the vehicles leads to a lot of excess energy being sold to the grid. With perfect information, relatively little energy then needs to be bought from the grid, with a total of only 5,797 kWh over the course of a year. With EV behavior being known and robust optimization for solar forecasting, that total increases to 8,413 kWh, because vehicles are charged earlier and more aggressively under the concern that there may not be sufficient solar power in the future. If future vehicles are unknown, this conservative behavior is intensified. More energy is drawn from the grid to preemptively charge the parked vehicles and the fixed battery, so that the peak demand will be lower regardless of how many vehicles arrive and need to be charged. As a result, the energy bought from the grid increases to 19,255 kWh. Although it is able to minimize the annual peak electricity demand, the robust charging strategy will still lead to lower self-consumption of solar power and more energy in total being drawn from the grid.
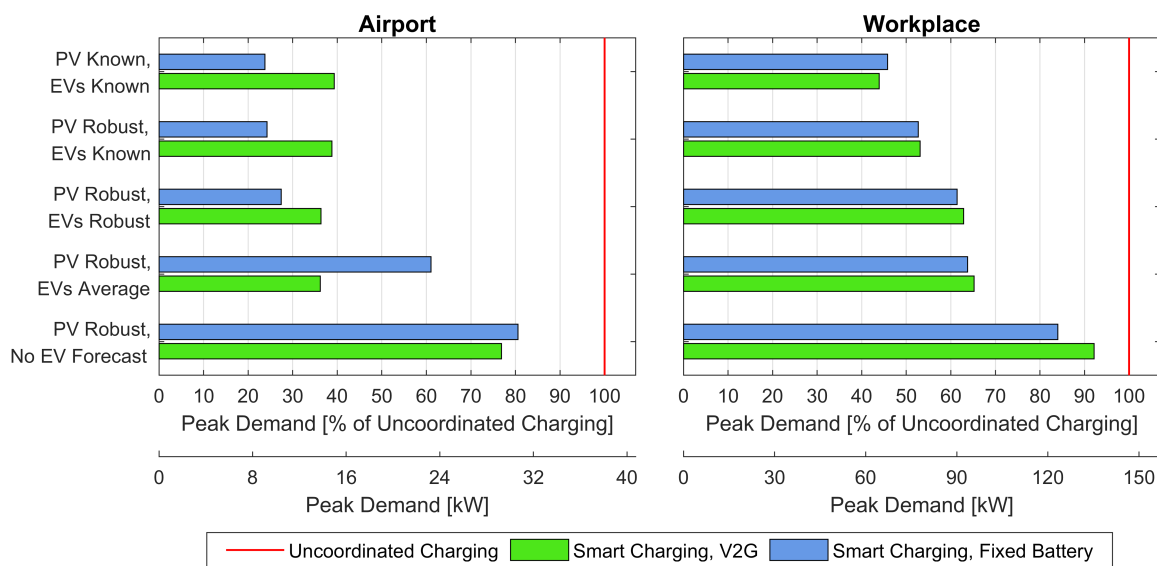
Figure 5.16: Peak demand for different control strategies considering EV demand uncertainty

The peak demand with various optimization strategies is shown in Figure 5.16. In a long-term parking lot at an airport, smart charging can reduce the peak demand by 76.2% if fixed battery storage is used. If the solar generation is uncertain the peak demand will increase, but a robust strategy will still allow for the peak demand to be reduced by 75.7%. When EV demand uncertainty is considered with a robust strategy, the peak demand can still be reduced by 72.6%. Considering uncertainty with robust strategies is therefore nearly as effective at reducing the peak demand as smart charging using perfect information. The use of robust strategies is crucial in achieving this goal. If the no-forecast strategy is used instead to account for EV uncertainty, the peak demand will only be reduced by 19.4%. Although robust strategies can lead to an increased peak demand on most days, and a lower self consumption, robust optimization is still the most effective way to minimize the peak demand.

Although the potential for peak shaving is greatest at an airport, the peak demand can also be effectively reduced in a workplace parking lot. With perfect information, smart charging using fixed battery storage can reduce the annual peak demand by 54.2%. Introducing solar forecasting uncertainty leads to a peak reduction of 47.3%, and including unknown EV charging demand as well results in a peak demand reduction of only 38.6%. Although smart charging is not able to reduce the peak demand at a workplace as much as at an airport, even under uncertainty it is still an effective tool for peak shaving at both types of parking lot. Again, robust strategies are critical in ensuring that the peak demand is reduced. Using the no-forecast strategy results in a peak demand of only 16.0% when compared with uncoordinated charging.

The societal benefits of peak shaving have already been discussed, but this reduction in peak demand can also provides financial benefits to the parking lot operator. The grid connection for a single EV charging station in the Netherlands is estimated to cost €750 up front and an additional €190 each year. The peak demand can be reduced by 72.6% at an airport and 38.6% at a workplace. If the grid connection costs could be reduced proportionately, smart charging at an airport could result in a total savings over the first ten years of operation of €1924 per charging station. Although workplace smart charging is not able to reduce the peak demand as much, the savings for each charging station could still total €1023 over the first ten years. Smart charging to facilitate peak shaving could therefore offer significant savings to parking lot operators, although a more comprehensive study of all the costs and benefits is still required.

Bidirectional charging, or V2G, is often discussed in the context of smart charging and peak shaving. In workplace parking, V2G is able to reduce the peak demand about as much as a fixed battery storage system. Vehicles at a workplace are parked for relatively short periods of time, meaning that energy is discharged from the vehicles relatively rarely and the power needed to recharge the vehicles does not significantly increase the peak demand. At an airport, however, V2G results in substantial higher peak demands than fixed battery storage when using robust charging strategies. This is because vehicles are parked for a longer time, allowing for more energy to be drawn from their batteries in order to charge other vehicles. When the vehicles need to be recharged, the increased load results in a higher peak demand. If the system is increasingly uncertain, the peak demand in V2G strategies surprisingly decreases. For example, with perfect information and V2G, the peak demand at an airport parking lot is 60.7% lower than it would be using uncoordinated charging. If solar forecasting is uncertain and EV demand is unknown, robust strategies lead to a decrease in peak load of 63.7%. This is because scenarios with less certainty result in less energy being drawn from vehicles batteries, saving the stored energy in case it is needed later. By decreasing the amount of energy drawn from the vehicle batteries, the peak demand is therefore reduced. When using average forecast or no-forecast approaches to handle unknown EV charging demand, V2G can reduce the peak demand more than battery storage. As previously discussed, these strategies do not ensure that the fixed battery storage will be sufficiently charged when it is needed, whereas V2G always allows vehicles to provide power at times of high demand. Despite this possible advantage, the peak demand can still be reduced most effectively through the use of fixed battery storage and robust charging strategies.

Through either fixed battery storage or V2G, energy storage of some form is critical in minimizing the peak demand as much as possible when compared with uncoordinated charging. This is especially true when uncertainty is considered. At a workplace with perfect information, the peak demand will be 67.2 kW with a battery, but 72.5 kW without one. When solar forecasting and future EVs are accounted for using robust optimization, the peak demand will increase to 90.1 kW with a fixed storage battery, but 116.2 kW if there is no battery. During smart charging at a workplace, battery storage offers only a minor advantage when vehicle behavior and solar power is known in advance, but is much more valuable when these inputs are uncertain. Airport charging suffers from the same problem. The peak demand with perfect information is 9.1 kW with a battery, increasing to 29.8 kW without ones. When uncertainty is considered, the peak demand increases to only 10.4 kW if a battery is used, but to 30.7 kW if there is no battery or V2G. This means that, when accounting for uncertainty, the peak demand can only be reduced by 20.8% at a workplace and 19.4% at an airport if no form of energy storage is available. Smart charging is capable of reducing the peak demand at a solar parking lot, but robust strategies and energy storage are important in enabling peak shaving to operate at its full potential.

<div style="text-align: right; font-size: 4em;">6</div>

Conclusions and Recommendations

In this report, smart charging has been investigated as a means to reduce peak electricity demand when charging electric vehicles (EVs) using solar energy. The goal was to build a realistic computer model of a solar parking lot, in order to answer the following research question:

How can smart electric vehicle charging be used to minimize the peak electricity demand at a workplace or airport solar parking lot, considering uncertainty in solar power forecasting and electric vehicle charging demand?

The findings in this report have served to answer this question. In this chapter, some key conclusions will be discussed in Section 6.1. Of course, there is still a great deal of research left to be done on this topic. Section 6.2 will discuss questions which must be answered by future researchers.

6.1. Conclusions

In this section, a number of key conclusions from this report will be highlighted and summarized. Many of these conclusions are demonstrated in Figure 6.1.

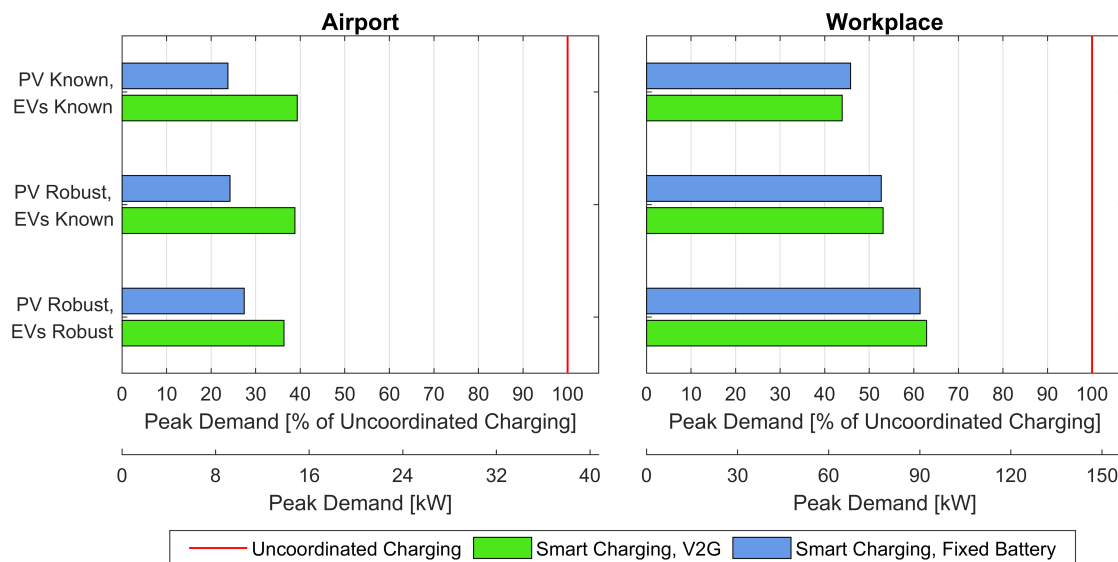Figure 6.1: Peak demand, with future PV power and EV charging demand either known or handled robustly

The peak electricity demand for the system is given, considering smart charging with either bidirectional charging with Vehicle-to-Grid (V2G) or unidirectional charging with fixed battery storage. The peak demand with with uncoordinated charging is also given. Furthermore, the effect of uncertainty is demonstrated. If

the future PV generation or EV charging demand is unknown, a robust charging strategy is used to minimize the peak demand. In this section, these results will be discussed.

6.1.1. Smart charging can reduce peak electricity demand

Uncoordinated charging of EVs can lead to very high peak electricity demand at parking lots, even when solar canopies are used to generate electricity. At a workplace parking lot, uncoordinated charging can result in a peak electricity demand of 3.7 kW per parking space. At an airport parking lot, because vehicles remain parked for longer, the peak demand is lower, but still amounts to 1.2 kW per space. Using smart charging can reduce these peaks, redistributing the energy needed to charge EVs so that less power is used at times of peak demand, and more power is used when demand is low. These smart charging practices are known as peak-shaving and valley-filling. With perfect information about future solar generation and EV charging demand, using fixed battery storage, smart charging can reduce the peak electricity demand by 54.2% at a workplace parking lot and 76.2% at an airport. This corresponds to the "PV Known, EVs Known" category in Figure 6.1. This reduction in the peak demand offers a number of benefits for parking lot operators, electricity grid operators, and society as a whole. High peaks in demand can require inefficient or polluting fossil fuel plants to ramp up production, and even threaten the stability of the electricity grid. These peaks can also lead to under-voltages, current harmonics, and overloading of components like power lines and transformers. This can lead to the lifetime of this equipment being shortened. Coordinated smart charging is an effective way avoid these issues by achieving peak shaving in solar parking lots.

6.1.2. PV forecasting errors lead to higher peak loads

Smart charging relies on knowledge of the future in order to schedule vehicle charging. If solar energy will be generated later in the day, EV charging can be delayed in order to take advantage of that energy. This relies on accurate knowledge of future solar energy generation. Although many models assume that this information is known in advance, in reality solar forecasting is subject to errors and uncertainty. This uncertainty will result in an increase in the peak demand, but through the use of robust charging strategies, this increase can be minimized. When considering solar generation forecasting errors, peak demand can still be reduced below the level of uncoordinated charging by 75.7% at an airport, and 47.3% at a workplace. This corresponds to the "PV Robust, EVs Known" category in Figure 6.1, demonstrating that with robust strategies, the peak demand increases by only 2% at an airport and 15% at a workplace compared to a scenario with perfect information. The alternative to robust optimization is nominal optimization, which assumes that the forecasted solar generation is accurate. Nominal optimization can increase peak demand by 36% at a workplace and 35% at an airport compared to optimization with perfect information, although the peak is still far lower than it would be with uncoordinated charging. Although robust optimization has results in a lower peak demand, it also leads to higher demand much of the time, with more energy being drawn from the grid. Compared to nominal optimization, robust optimization draws 9.7% more energy from the grid at a workplace, and 34% at an airport. These peak shaving strategies are therefore at odds with the goal of increasing the self-consumption of renewable energy.

6.1.3. Uncertainty about EV charging demand further increases peak loads

Smart charging strategies rely on a knowledge of the vehicles which need to be charged. Almost all models assume that it is known well in advance what time the vehicles will arrive, when they will depart, and what their battery capacity and initial state of charge will be. In reality, this information is often unknown before the vehicle arrives at the parking lot. As a result, optimal charging strategies cannot be planned in advance, and the peak demand is higher than it would be in a system with perfect information. Even considering uncertainty in the EV energy demand, the peak load using robust smart charging strategies is still lower than it would be using uncoordinated charging, by 72.6% at an airport and 38.6% at a workplace. This corresponds to the "PV Robust, EVs Robust" category in Figure 6.1, and represents an increase in the peak demand of 15% at an airport and 34% at a workplace. Although this uncertainty leads to a higher peak demand, robust smart charging is still highly effective at peak shaving. Robust strategies are again needed to consider EV demand uncertainty. One alternative approach relies on scheduling the charging behavior for only vehicles which have already arrived, without forecasting any additional demand. Although this strategy is simple, it does not reduce the peak demand as much as the robust strategy, leading to reductions of only 19.4% at an airport and 16.0% at a workplace. Although smart charging can reduce the peak demand, some strategies described in the literature at not effective at achieving this goal. In designing smart solar parking lots, care must therefore be taken to ensure that the charging strategy is robust with respect to forecasting uncertainties.

6.1.4. Energy storage is important in reducing peak demand

In order to implement smart charging with the goal of peak shaving, it is important that excess energy can be stored for later use. Energy can be stored in either a fixed battery storage installation, or the battery of an electric vehicle which is able to discharge through Vehicle-to-Grid (V2G) technologies. At workplace parking, because the charging demand is so high, charging can often be scheduled so that peak demand is reduced and a battery is not necessary. When future information is known perfectly, the peak demand can be reduced by 54% if battery storage is used and 56% if V2G is employed. Without any form of energy storage, the peak demand can still be reduced by 51%. When uncertainty is considered, energy storage becomes more critical. If future solar generation and EV demands are unknown, the peak demand at a workplace can be reduced by 38.6% with a battery and 37.1% with V2G. If there is no form of energy storage at all, the peak can only be reduced by 20.8%. When uncertainty is considered, energy storage becomes even more crucial when trying to reduce peak demand.

At an airport parking lot, where the energy demand is already lower, reducing the peak demand is more difficult, making energy storage even more critical. With perfect information, peak demand can be reduced at an airport by 76.2% with battery storage and 60.7% with V2G, but only by 21.7% with no form of energy storage at all. When considering uncertainty, the peak demand can still be reduced by 72.6/% using battery storage and 63.7% using V2G, but only 19.4% with no energy storage. Energy storage, either in the form of a fixed storage battery or V2G, is therefore crucial in reducing the peak demand, especially when uncertainty is being considered.

It was determined that at both workplace and airport parking lots there is no benefit to fixed battery storage with a capacity larger than 50 kWh (1 kWh of usable capacity per parking space). This is because the battery is only capable of handling short term fluctuations. After several days with low solar output, the battery will run out of stored energy regardless of its capacity, meaning that a bigger battery cannot further reduce peak demand. It was also determined that there was no benefit to combining both V2G and battery storage, as they serve practically the same purpose. Adding fixed battery storage to a system with V2G does not reduce the peak demand.

6.1.5. Fixed battery storage can reduce peak demand more that vehicle-to-grid

Vehicle-to-grid (V2G) is a technology in which EVs are able to charge bidirectionally. In addition to drawing power from the charging equipment to charge the battery, vehicles are also able to discharge their batteries, sending power to the grid or to charging equipment for other vehicles. Although V2G is a possible form of energy storage, the round-trip efficiency is lower than a fixed battery due to losses in the power electronic equipment. In addition, EVs which are discharged must later be recharged before their departure, resulting in a higher energy demand when V2G is used. This means that the more bidirectional charging is used in a system, the higher the peak demand will be. In workplace charging, where vehicles are not parked very long, V2G does not result in a peak demand which is much different from the peak demand when using fixed battery storage, as shown in Figure 6.1. When perfect information is known in advance, V2G can actually lead to a slightly lower peak demand, but once uncertainty is introduced battery storage allows for a lower peak demand than V2G at a workplace. At an airport, where vehicles are parked for a longer duration, V2G can substantially increase the peak demand, as vehicles are more deeply discharged in order to provide power for other vehicles. As a result, fixed battery storage results in a lower peak demand when compared to V2G, especially at an airport. V2G already faces concerns over issues like increased battery degradation for vehicles which regularly engage in bidirectional charging. Due to the greater risk and lower effectiveness of V2G with regards to peak shaving, battery storage is recommended in smart solar parking lots.

6.1.6. Grid independence is not possible in the system which was modeled

One possible goal for a solar parking lot could be complete independence from the electricity grid. This self sustaining microgrid would be able to generate all the electricity it needs from solar power. Such a system could have a number of advantages, including lower costs as the expense of a grid connection could be avoided entirely. In the system modeled for this report, such grid independence is not possible, even for airport long-term parking which uses substantially less energy than a workplace parking lot. Even with perfect information, and a battery of up to 1000 kWh, there are always some times when drawing power from the grid is necessary. Because there will always be prolonged periods of time with very little solar energy, this problem cannot be solved by simply increasing the solar power or size of the battery. More significant changes to the system are required in order to achieve total grid independence. Some possible approaches are discussed in Section 6.2.

6.2. Questions for Future Work

This research has provided insight into the subject of smart solar parking lots, and how their peak electricity demand can be minimized under uncertain conditions. Despite these findings, a number of questions still remain which were unable to be properly addressed by this report.

6.2.1. What will this system cost?

In this report, the costs of the solar parking lot were not calculated. Future work could expand on this report in order to determine the financial viability of smart charging in solar parking lots. A detailed cost analysis would consider the optimal system topology, including the capacity of fixed battery storage, the availability of bidirectional vehicle chargers, and the sizing of the PV system. Such an analysis would also need to consider the cost benefits of smart charging, including the need to purchase less electricity and the potential to sell peak-shaving as an auxiliary service to grid operators. Smart charging could also lower the cost for the electricity grid connection, which is a significant fraction of the price for a new vehicle charging station. We estimate that over the first ten years of operation, smart charging could lead to a savings of €1924 at an airport and €1023 at a workplace for each charging station. Given the tremendous potential for savings, a full economic analysis may find that smart charging pays for itself.

Ultimately, such an analysis depends on the findings of this report. In order to determine the desired capacity for the fixed battery storage, or whether it is worth it to include battery storage at all, it is first necessary to determine how the battery capacity affects the performance of smart charging. In order to find the savings achieved by reducing the grid connection, it is first essential to calculate the true potential for smart charging to reduce the peak demand considering all the possible uncertainties. A meaningful financial analysis, therefore, depends of an understanding of the system behavior when solar forecasting and EV behavior is uncertain. Now that the performance of smart charging under uncertainty has been realistically modeled and quantified, an accurate economic analysis can be conducted.

6.2.2. How can the model be improved?

As the British statistician George Box once famously remarked, "All models are wrong, but some are useful." [171]. Naturally, no model will be sufficient to completely describe a complex system with perfect accuracy and this model is no exception. Whenever possible, however, the assumptions which were made are clarified and justified. This model was constructed with the goal of considering many details, including the uncertainty in solar generation and EV behavior, details which have often been omitted in previous research. Still, further models could possibly improve on the accuracy of this one by utilizing better input data and improving on assumptions which were made. One possible improvement could be the use of better EV behavioral data. The EV project data which was used considered only American EV drivers in the period of 2009–2013. It may be that drivers in another time or place would behave differently, and newer data on charging behavior could lead to more accurate results. In addition, charging behavior in airport long-term parking was based on conventional vehicles, as no suitable dataset could be found for EVs. If airport EV charging data was used, the results could be improved. These changes, however, are unlikely to radically alter the conclusions of this report.

It could also be interesting to consider other system topologies. For example, the only loads considered other than EV charging was the lighting for the parking lot. Larger loads, such as a nearby office building or DC fast charging stations, might lead to different strategies and conclusions. At an airport, the charging load from the parking lot could be combined with the demand from the airport buildings, with the goal of reducing the overall peak demand at the airport behind the meter. In this case, other charging strategies might be preferred, and the effectiveness of smart charging for peak shaving might be different.

6.2.3. How well would other charging strategies work?

In this report, different strategies were considered in order to minimize the peak demand. As a base scenario, uncoordinated charging was considered. For smart charging, model predictive control (MPC) was implemented, considering both nominal and robust techniques for handling the uncertainty in the model. Of course, there are more optimization techniques which could be considered, which are discussed in section 2.2. Delay or off-peak charging could be used to reduce peak demand without coordinated charging behavior, although previous research has found that these strategies can be ineffective or even counterproductive. Real-time charging can allow for coordinated charging without the need for forecasting, although it is unclear how well this strategy would perform under real-world conditions. Other optimization techniques could also

be used when considering forecasting errors, such as stochastic programming. Furthermore, other objective functions could be considered beyond the reduction of peak demand. For example, the the system controller could seek to maximize self-consumption of renewable energy or minimize the cost of purchasing electricity. Smart charging with these goals has also typically ignored forecasting uncertainty in the past.

6.2.4. What will the requirements be for a solar parking lot in the future?

Many of the details of this model are based on current technologies, which might lead to systems looking different in the future. For example, the efficiency of EV chargers or solar panels might improve. This improvement, however, is likely to be small and will probably not affect the conclusions significantly. In addition, uncertainty may change in the future, as solar power forecasts improve. Uncertainty regarding EV behavior may decrease if vehicles reserve parking spaces online in advance, as is common at many airports. Even with reservations, however, some vehicles will always park without advance planning, resulting in some uncertainty.

The electricity demand due to electric vehicles has been quickly increasing in recent years, and it is likely to continue to do so. Battery technology has been dropping in price, leading to larger and larger batteries in EVs. In addition, changing financial incentives in the Netherlands have resulted in the number of Battery Electric Vehicles (BEVs) with larger batteries dramatically increasing in number, while plug-in hybrid electric vehicles (PHEVs) with smaller batteries have seen registrations slowly decrease. As BEVs become more popular, and PHEVs become less common, the energy per charging event will increase. This means that parking lot operators in the future will need to prepare for the increasing electricity demand from the new generation of EVs.

6.2.5. Is a fully grid independent solar parking lot possible?

Currently, the solar parking lot which was modeled cannot be completely grid-independent, even at an airport. This is because there will always be some demand for charging EVs at a time when solar energy is not available and there is not enough stored energy. One way to avoid this problem is to curtail vehicle charging. If vehicle charging was limited to the power which is available from energy storage and solar panels, the system could be energy-independent. This might be problematic for drivers whose vehicles are not charged, although most vehicles would probably be charged in the time before departing. Curtailment would probably most severely affect vehicles which are only parked for a short time, whereas vehicles parked for several days would probably be able to charge completely before departure.

In theory, the airport parking lot should be able to charge all the vehicles without curtailment, relying only on locally generated solar energy. On average, the solar canopies in this system generated a total of 3341 kWh per parking space over the course of the year. The energy demand for charging EVs, however, was only 941 kWh per space per year. Even as the energy demand per EV increases, there should still be more than enough solar energy to charge all the vehicles in the parking lot. The greatest barrier is storage. Most of the solar energy is generated during the summer months, and an independent microgrid would need to store that energy until the winter. Batteries are insufficient for seasonal storage, meaning a different technology would need to be used.

Hydrogen storage could enable a solar parking lot to operate without a connection to the electricity grid. Electrolyzers could be used to generate hydrogen from excess solar energy during the summer months. This energy could then be used to run fuel cells during the winter, allowing for the solar parking lot to use 100% renewable energy year-round. Because the energy generated in this system is substantially greater than the energy consumed, this system should be possible even considering the efficiency losses in hydrogen generation, storage, and consumption. Further research is needed to evaluate the feasibility of such a system, but there is theoretical potential for a hydrogen-powered grid-independent solar microgrid for charging EVs at an airport long-term parking lot.

Bibliography

[1] Rolf Heynen, Peter Groot, Henriette Vrisekoop, Daan Witkop, Julia Koster, and Kevin Kolenbrander. Dutch Solar Trend Report 2019. Technical report, Dutch New Energy Research, The Netherlands, 2019. URL https://www.solarsolutions.nl/en/solar-trendrapport/#download.

[2] Ministry of Economic Affairs. *Energy Agenda: Towards a low-carbon energy supply*. Ministry of Economic Affairs, The Hague, March 2017. URL https://www.government.nl/binaries/government/documents/reports/2017/03/01/energy-agenda-towards-a-low-carbon-energy-supply/Energy+agenda.pdf.

[3] Harold Anuta, Pablo Ralon, and Michael Taylor. Renewable Power Generation Costs in 2018. Technical Report ISBN 978-92-9260-126-3, International Renewable Energy Agency (IRENA), Abu Dhabi, May 2019. URL https://www.irena.org/publications/2019/May/Renewable-power-generation-costs-in-2018.

[4] Netherlands Enterprise Agency. SDE+ Spring 2019: Instructions on how to apply for a subsidy for the production of renewable energy. Technical Report RVO-205-1801/BR-DUZA, Ministry of Economic Affairs and Climate Policy, Zwolle, April 2019. URL https://english.rvo.nl/sites/default/files/2019/04/Brochure%20SDE%20Spring%202019.pdf.

[5] Christoph Kost, Shivenes Shammugam, Verena Jülch, Huyen-Tran Nguyen, and Thomas Schlegl. Levelized Cost of Electricity - Renewable Energy Technologies. Technical report, Fraunhofer Institute for Solar Energy Systems ISE, Freiburg, Germany, March 2018. URL https://www.ise.fraunhofer.de/content/dam/ise/en/documents/publications/studies/EN2018_Fraunhofer-ISE_LCOE_Renewable_Energy_Technologies.pdf.

[6] Eric Wiebes. Verbreding van de SDE+ naar de SDE ++, April 2019. URL https://www.rijksoverheid.nl/documenten/kamerstukken/2019/04/26/kamerbrief-over-verbreding-van-de-sde-naar-de-sde.

[7] J.P.M Sijm, Pieter Gockel, Marit van Hout, Özge Özdemir, Joost van Stralen, Koen Smekens, Adriaan ven der Welle, Jeroen de Joode, Werner ven Westerling, and Michiel Musterd. Demand and supply of flexibility in the power system of The Netherlands, 2015-2050. Summary report of the FLEXNET project. ECN publication ECN-E-17-053, ECN Policy Studies, Petten, the Netherlands, November 2017. URL http://www.ecn.nl/publications/ECN-E--17-053.

[8] J.G.J. Olivier, K.M. Schure, and J.A.H.W. Peters. Trends in global CO2 and total greenhouse gas emissions - 2017 Report. Technical Report 2674, PBL Netherlands Environmental Assessment Agency, The Hague, December 2017. URL https://www.pbl.nl/sites/default/files/cms/publicaties/pbl-2017-trends-in-global-co2-and-total-greenhouse-gas-emissons-2017-report_2674.pdf.

[9] Dave Turk. Global EV Outlook 2018. Technical report, International Energy Agency (IEA), 2018. URL https://webstore.iea.org/download/direct/1045?filename=global_ev_outlook_2018.pdf.

[10] Linda Ager-Wick Ellingsen, Bhawna Singh, and Anders Hammer Strømman. The size and range effect: lifecycle greenhouse gas emissions of electric vehicles. *Environmental Research Letters*, 11(5):054010, 2016. ISSN 1748-9326. doi: 10.1088/1748-9326/11/5/054010. URL http://stacks.iop.org/1748-9326/11/i=5/a=054010.

[11] Bert Klerk and Formule E-Team. Maak Elektrisch Rijden Groot. Technical report, Nederland Elektrisch, Den Haag, June 2016.

[12] Jan Ros and Jeroen Peters. Implications of innovative options for transport on the level of the energy system. Technical Report 1152, PBL Netherlands Environmental Assessment Agency, The Hague / Bilthoven, December 2013. URL http://www.pbl.nl/sites/default/files/cms/publicaties/pbl-2013-implications-of-innovative-options-for-transport-on-the-level-of-the-energy-system-1152.pdf.

[13] Bas Stoffelsen. Electric transport in the Netherlands. Technical report, Netherlands Enterprise Agency, Utrecht, the Netherlands, April 2018. URL https://www.rvo.nl/sites/default/files/2018/04/Highlights%20EV%202017%20English.pdf.

[14] People's Party for Freedom and Democracy (VVD), Christian Democratic Alliance (CDA), Democrats '66 (D66), and Christian Union (CU). Confidence in the Future: 2017–2021 Coalition Agreement, October 2017. URL https://www.government.nl/documents/publications/2017/10/10/coalition-agreement-confidence-in-the-future.

[15] VDL. VDL Bus & Coach - Europe's largest electric bus fleet in operation, March 2018. URL http://www.vdlbuscoach.com/News/News-Library/2018/Europa-s-grootste-elektrische-busvloot-in-operatie.aspx.

[16] Netherlands Enterprise Agency. May 2019: Statistics Electric Vehicles and Charging in The Netherlands, May 2019. URL https://www.rvo.nl/sites/default/files/2019/06/Statistics%20Electric%20Vehicles%20and%20Charging%20in%20The%20Netherlands%20up%20to%20and%20including%20May%202019.pdf.

[17] PricewaterhouseCoopers. Smart Charging of electric vehicles: Institutional bottlenecks and possible solutions. Technical report, PricewaterhouseCoopers, October 2017. URL https://www.elaad.nl/uploads/files/201710-_PwC_Smart_Charging_rapport_Final_STC_ENG.pdf.

[18] Tesla Team. Introducing V3 Supercharging, March 2019. URL https://www.tesla.com/blog/introducing-v3-supercharging.

[19] Wieland Brúch. Research project "FastCharge": ultra-fast charging technology ready for the electrically powered vehicles of the future., December 2018. URL https://www.press.bmwgroup.com/global/article/detail/T0288583EN/research-project-\T1\textquotedblleftfastcharge\T1\textquotedblright:-ultra-fast-charging-technology-ready-for-the-electrically-powered-vehicles-of-the-future?language=en.

[20] Hussain Shareef, Md. Mainul Islam, and Azah Mohamed. A review of the stage-of-the-art charging technologies, placement methodologies, and impacts of electric vehicles. *Renewable and Sustainable Energy Reviews*, 64:403–420, October 2016. ISSN 1364-0321. doi: 10.1016/j.rser.2016.06.033. URL http://www.sciencedirect.com/science/article/pii/S1364032116302568.

[21] Salman Habib, Muhammad Kamran, and Umar Rashid. Impact analysis of vehicle-to-grid technology and charging strategies of electric vehicles on distribution networks – A review. *Journal of Power Sources*, 277:205–214, March 2015. ISSN 0378-7753. doi: 10.1016/j.jpowsour.2014.12.020. URL http://www.sciencedirect.com/science/article/pii/S0378775314020370.

[22] Willett Kempton and Jasna Tomić. Vehicle-to-grid power fundamentals: Calculating capacity and net revenue. *Journal of Power Sources*, 144(1):268–279, June 2005. ISSN 03787753. doi: 10.1016/j.jpowsour.2004.12.025. URL http://linkinghub.elsevier.com/retrieve/pii/S0378775305000352.

[23] E. Sortomme and M. A. El-Sharkawi. Optimal Charging Strategies for Unidirectional Vehicle-to-Grid. *IEEE Transactions on Smart Grid*, 2(1):131–138, March 2011. ISSN 1949-3053. doi: 10.1109/TSG.2010.2090910.

[24] Kwo Young, Caisheng Wang, Le Yi Wang, and Kai Strunz. Electric Vehicle Battery Technologies. In Rodrigo Garcia-Valle and João A. Peças Lopes, editors, *Electric Vehicle Integration into Modern Power Networks*, Power Electronics and Power Systems, pages 15–56. Springer New York, New York, NY, 2013. ISBN 9781461401346. doi: 10.1007/978-1-4614-0134-6_2. URL https://doi.org/10.1007/978-1-4614-0134-6_2.

[25] Christophe Guille and George Gross. A conceptual framework for the vehicle-to-grid (V2g) implementation. *Energy Policy*, 37(11):4379–4390, November 2009. ISSN 0301-4215. doi: 10.1016/j.enpol.2009.05.053. URL http://www.sciencedirect.com/science/article/pii/S0301421509003978.

[26] Justin D. K. Bishop, Colin J. Axon, David Bonilla, Martino Tran, David Banister, and Malcolm D. McCulloch. Evaluating the impact of V2g services on the degradation of batteries in PHEV and EV. *Applied Energy*, 111:206–218, November 2013. ISSN 0306-2619. doi: 10.1016/j.apenergy.2013.04.094. URL http://www.sciencedirect.com/science/article/pii/S0306261913004121.

[27] Michael MacLeod and Chris Cox. V2g Market Study: Answering the Preliminary Questions for V2g: What, where and how much? Technical report, Cenex, July 2018. URL https://www.seev4-city.eu/wp-content/uploads/2018/08/V2G-Market-Study-2018.pdf.

[28] Honda. Honda installs new bi-directional charging technology at European R&D centre, December 2017. URL https://hondanews.eu/eu/en/corporate/media/pressreleases/124178/honda-installs-new-bi-directional-charging-technology-at-european-randd-centre.

[29] Electrive. BMW i3 soon capable of bi-directional charging (video) - electrive.com, August 2018. URL https://www.electrive.com/2018/08/22/bmw-i3-soon-capable-of-bi-directional-charging-video/.

[30] Volkswagen. Charging infrastructure | Volkswagen Newsroom, September 2018. URL https://www.volkswagen-newsroom.com/en/id-workshop-electric-for-all-4193/charging-infrastructure-4198.

[31] Mitsubishi. News Release | Mitsubishi Motors Corporation, October 2017. URL https://www.mitsubishi-motors.com/en/newsrelease/2017/detail1082.html.

[32] Hitachi. Hitachi, Mitsubishi Motors and ENGIE explore using electric car batteries as renewable energy storage for office buildings | Hitachi in Europe, March 2018. URL http://www.hitachi.eu/en/press/hitachi-mitsubishi-motors-and-engie-explore-using-electric-car-batteries-renewable-energy.

[33] PSA Groupe. GridMotion Project: reducing electric vehicle usage cost thanks to smart charging process | Media Groupe PSA, May 2017. URL https://media.groupe-psa.com/en/gridmotion-project-reducing-electric-vehicle-usage-cost-thanks-smart-charging-process.

[34] GreenCarGuide. Peugeot iOn/Citroen C-Zero - GreenCarGuide.co.uk, 2018. URL https://www.greencarguide.co.uk/green-car-guides/mitsubishi-i-mievpeugeot-ioncitroen-c-zero/.

[35] Fred Lambert. Tesla could 'revisit' vehicle-to-grid technology, says Elon Musk - Electrek, July 2018. URL https://electrek.co/2018/07/05/tesla-vehicle-to-grid-technology-v2g-elon-musk/.

[36] Emrah Biyik, Mustafa Araz, Arif Hepbasli, Mehdi Shahrestani, Runming Yao, Li Shao, Emmanuel Essah, Armando C. Oliveira, Teodosio del Caño, Elena Rico, Juan Luis Lechón, Luisa Andrade, Adélio Mendes, and Yusuf Baver Atlı. A key review of building integrated photovoltaic (BIPV) systems. *Engineering Science and Technology, an International Journal*, 20(3):833–858, June 2017. ISSN 2215-0986. doi: 10.1016/j.jestch.2017.01.009. URL http://www.sciencedirect.com/science/article/pii/S2215098616309326.

[37] Pedro Nunes, Raquel Figueiredo, and Miguel C. Brito. The use of parking lots to solar-charge electric vehicles. *Renewable and Sustainable Energy Reviews*, 66:679–693, December 2016. ISSN 1364-0321. doi: 10.1016/j.rser.2016.08.015. URL http://www.sciencedirect.com/science/article/pii/S1364032116304294.

[38] Dunbar P. Birnie. Solar-to-vehicle (S2v) systems for powering commuters of the future. *Journal of Power Sources*, 186(2):539–542, January 2009. ISSN 0378-7753. doi: 10.1016/j.jpowsour.2008.09.118. URL http://www.sciencedirect.com/science/article/pii/S0378775308018946.

[39] Jeroen van der Wal, Pouya Zarbanoui, and Sjors Broersen. Solar panels could provide half of Dutch electricity demand | State of the State report. Technical report, Deloitte Netherlands, The Netherlands, March 2018. URL https://www2.deloitte.com/nl/nl/pages/data-analytics/articles/solar-panels.html.

[40] moovel Lab. What the Street!?, June 2017. URL https://lab.moovel.com/blog/about-what-the-street.

[41] Amélie Y. Davis, Bryan C. Pijanowski, Kimberly D. Robinson, and Paul B. Kidwell. Estimating parking lot footprints in the Upper Great Lakes Region of the USA. *Landscape and Urban Planning*, 96 (2):68–77, May 2010. ISSN 0169-2046. doi: 10.1016/j.landurbplan.2010.02.004. URL http://www.sciencedirect.com/science/article/pii/S0169204610000356.

[42] Mikhail Chester, Andrew Fraser, Juan Matute, Carolyn Flower, and Ram Pendyala. Parking Infrastructure: A Constraint on or Opportunity for Urban Redevelopment? A Study of Los Angeles County Parking Supply and Growth. *Journal of the American Planning Association*, 81(4):268–286, October 2015. ISSN 0194-4363. doi: 10.1080/01944363.2015.1092879. URL https://doi.org/10.1080/01944363.2015.1092879.

[43] Christopher Jackson and Gaynor Hartnell. Solar car parks: a guide for owners and developers. Technical report, BRE National Solar Center, Par, UK, 2016. URL https://www.r-e-a.net/upload/rea-bre_solar-carpark-guide-v2_bre114153_lowres.pdf.

[44] Smets, A.H.M., Jäger, K., Isabella, O., Swaaij, van R.A.C.M.M., Zeman, M., and Plasma & Materials Processing. *Solar energy : the physics and engineering of photovoltaic conversion technologies and systems*. UIT, 2016. URL https://research.tue.nl/nl/publications/solar-energy--the-physics-and-engineering-of-photovoltaic-conversion-technologies-and-systems(d116cb6a-0b85-47df-8854-ee1d3a3f030c).html.

[45] A. Shekhar, V. K. Kumaravel, S. Klerks, S. de Wit, P. Venugopal, N. Narayan, P. Bauer, O. Isabella, and M. Zeman. Harvesting Roadway Solar Energy—Performance of the Installed Infrastructure Integrated PV Bike Path. *IEEE Journal of Photovoltaics*, 8(4):1066–1073, July 2018. ISSN 2156-3381. doi: 10.1109/JPHOTOV.2018.2820998.

[46] KACO New Energy. Up and running: giant solar carport in Turkey, March 2019. URL https://kaco-newenergy.com/news-and-events/notice-detail/giant-solar-carport-in-turkey/.

[47] Todd Brady. Now That's One Big Carport!, February 2016. URL https://blogs.intel.com/csr/2016/02/now-thats-one-big-carport/.

[48] Fastned. Fastned opens first fast charging station in Germany, June 2018. URL http://fastned.nl/en/blog/post/fastned-opent-eerste-snellaadstation-in-duitsland.

[49] Maryland Energy Administration. Maryland Energy Administration Announces Awardees for 2018 Solar Canopy EV Charging Program, December 2017. URL http://news.maryland.gov/mea/2017/12/19/maryland-energy-administration-announces-awardees-for-2018-solar-canopy-ev-charging-program/.

[50] Raquel Figueiredo, Pedro Nunes, and Miguel C. Brito. The feasibility of solar parking lots for electric vehicles. *Energy*, 140:1182–1197, December 2017. ISSN 0360-5442. doi: 10.1016/j.energy.2017.09.024. URL http://www.sciencedirect.com/science/article/pii/S0360544217315438.

[51] P. Tulpule, V. Marano, S. Yurkovich, and G. Rizzoni. Energy economic analysis of PV based charging station at workplace parking garage. In *IEEE 2011 EnergyTech*, pages 1–6, May 2011. doi: 10.1109/EnergyTech.2011.5948504.

[52] PowerParking. Public Summary: 'Kansen voor West II' Application. Technical report, PowerParking, October 2016.

[53] Juriaan van Tilburg, Maurice van Duijnhoven, Hans Schneider, Frans Provoost, Dennis Meerburg, Edwin Abbink, Tim Zijderveld, and Ad van Wijk. DC elektriciteitsnet op Amsterdam-Lelystad Airport/Airport Garden City, February 2015.

[54] Rishabh Ghotge. The PowerParking Project: Initial investigations, technology survey and proposal for the Green Village pilot, December 2017.

[55] Projectplan: Kansen voor West II aanvraag, tweede indiening, October 2016.

[56] Oscar van Vliet, Anne Sjoerd Brouwer, Takeshi Kuramochi, Machteld van den Broek, and André Faaij. Energy use, cost and CO2 emissions of electric cars. *Journal of Power Sources*, 196(4):2298–2310, February 2011. ISSN 0378-7753. doi: 10.1016/j.jpowsour.2010.09.119. URL `http://www.sciencedirect.com/science/article/pii/S037877531001726X`.

[57] P. S. Moses, M. A. S. Masoum, and S. Hajforoosh. Overloading of distribution transformers in smart grid due to uncoordinated charging of plug-In electric vehicles. In *2012 IEEE PES Innovative Smart Grid Technologies (ISGT)*, pages 1–6, January 2012. doi: 10.1109/ISGT.2012.6175689.

[58] G. R. Chandra Mouli, P. Bauer, and M. Zeman. System design for a solar powered electric vehicle charging station for workplaces. *Applied Energy*, 168:434–443, April 2016. ISSN 0306-2619. doi: 10.1016/j.apenergy.2016.01.110. URL `http://www.sciencedirect.com/science/article/pii/S0306261916300988`.

[59] Moslem Uddin, Mohd Fakhizan Romlie, Mohd Faris Abdullah, Syahirah Abd Halim, Ab Halim Abu Bakar, and Tan Chia Kwang. A review on peak load shaving strategies. *Renewable and Sustainable Energy Reviews*, 82:3323–3332, February 2018. ISSN 1364-0321. doi: 10.1016/j.rser.2017.10.056. URL `http://www.sciencedirect.com/science/article/pii/S13640321173142 72`.

[60] Eduard Cubi, Ganesh Doluweera, and Joule Bergerson. Incorporation of electricity GHG emissions intensity variability into building environmental assessment. *Applied Energy*, 159:62–69, December 2015. ISSN 0306-2619. doi: 10.1016/j.apenergy.2015.08.091. URL `http://www.sciencedirect.com/science/article/pii/S0306261915010272`.

[61] Imran Khan, Michael W. Jack, and Janet Stephenson. Analysis of greenhouse gas emissions in electricity systems using time-varying carbon intensity. *Journal of Cleaner Production*, 184:1091–1101, May 2018. ISSN 0959-6526. doi: 10.1016/j.jclepro.2018.02.309. URL `http://www.sciencedirect.com/science/article/pii/S0959652618306474`.

[62] Rita Garcia and Fausto Freire. Marginal Life-Cycle Greenhouse Gas Emissions of Electricity Generation in Portugal and Implications for Electric Vehicles. *Resources*, 5(4):41, December 2016. doi: 10.3390/resources5040041. URL `https://www.mdpi.com/2079-9276/5/4/41`.

[63] Joshua S. Graff Zivin, Matthew J. Kotchen, and Erin T. Mansur. Spatial and temporal heterogeneity of marginal emissions: Implications for electric cars and other electricity-shifting policies. *Journal of Economic Behavior & Organization*, 107:248–268, November 2014. ISSN 0167-2681. doi: 10.1016/j.jebo.2014.03.010. URL `http://www.sciencedirect.com/science/article/pii/S0167268114000808`.

[64] A. Dubey and S. Santoso. Electric Vehicle Charging on Residential Distribution Systems: Impacts and Mitigations. *IEEE Access*, 3:1871–1893, 2015. ISSN 2169-3536. doi: 10.1109/ACCESS.2015.2476996.

[65] E. Akhavan-Rezai, M. F. Shaaban, E. F. El-Saadany, and A. Zidan. Uncoordinated charging impacts of electric vehicles on electric distribution grids: Normal and fast charging comparison. In *2012 IEEE Power and Energy Society General Meeting*, pages 1–7, July 2012. doi: 10.1109/PESGM.2012.6345583.

[66] J. C. Gomez and M. M. Morcos. Impact of EV battery chargers on the power quality of distribution systems. *IEEE Transactions on Power Delivery*, 18(3):975–981, July 2003. ISSN 0885-8977. doi: 10.1109/TPWRD.2003.813873.

[67] International Electrotechnical Commission (IEC). IEC TS 61000-3-4:1998 Electromagnetic compatibility (EMC) - Part 3-4: Limits - Limitation of emission of harmonic currents in low-voltage power supply systems for equipment with rated current greater than 16 A. *Technical Specification*, TC 77/SC 77A - EMC - Low frequency phenomena(33.100.10 - Emission):29, October 1998. URL `https://webstore.iec.ch/publication/4151`.

[68] S. Shao, M. Pipattanasomporn, and S. Rahman. Challenges of PHEV penetration to the residential distribution network. In *2009 IEEE Power Energy Society General Meeting*, pages 1–8, July 2009. doi: 10.1109/PES.2009.5275806.

[69] C. Farmer, P. Hines, J. Dowds, and S. Blumsack. Modeling the Impact of Increasing PHEV Loads on the Distribution Infrastructure. In *2010 43rd Hawaii International Conference on System Sciences*, pages 1–10, January 2010. doi: 10.1109/HICSS.2010.277.

[70] IEEE. IEEE Guide for Loading Mineral-Oil-Immersed Transformers and Step-Voltage Regulators. *IEEE Std C57.91-2011 (Revision of IEEE Std C57.91-1995)*, pages 1–123, March 2012. ISSN 978-0-7381-7195-1. doi: 10.1109/IEEESTD.2012.6166928. URL https://ieeexplore.ieee.org/document/6166928.

[71] Marit van Hout, Paul Koutstaal, Ozge Ozdemir, and Ad Seebregts. Quantifying flexibility markets. Technical Report ECN-E–14-039, ECN, December 2014. URL https://www.tennet.eu/fileadmin/user_upload/Company/Publications/Technical_Publications/Dutch/TP_2014_TenneT_ECN_Quantifying_flexibility_markets.pdf.

[72] PricewaterhouseCoopers. Fiscale barrières voor Smart Charging. Technical report, ELaadNL, January 2017. URL https://www.deingenieur.nl/uploads/media/588f833d68ee6/Fiscale_barrieres_voor_Smart_Charging_PWC_voor_ElaadNL.pdf.

[73] Margaret Smith and Johnathan Castellano. Costs Associated With Non-Residential Electric Vehicle Supply Equipment: Factors to consider in the implementation of electric vehicle charging stations. Technical Report DOE/EE-1289, U.S. Department of Energy Vehicle Technologies Office, Washington, DC United States 20585, November 2015. URL https://trid.trb.org/view/1377403.

[74] R. F. P. Blok. Verslag Benchmark Publiek Laden 2018 - Sneller naar een volwassen markt. Technical report, NKL Nederland, Emmen, NL, December 2018. URL https://www.nklnederland.nl/uploads/files/Verslag_Benchmark_Publiek_Laden_2018_-_Sneller_naar_een_volwassen_markt_FINAL.pdf.

[75] J. Bauman, M. B. Stevens, S. Hacikyan, L. Tremblay, E. Mallia, and C. J. Mendes. Residential Smart-Charging Pilot Program in Toronto: Results of a Utility Controlled Charging Pilot. *World Electric Vehicle Journal*, 8(2):531–542, June 2016. doi: 10.3390/wevj8020531. URL https://www.mdpi.com/2032-6653/8/2/531.

[76] Nissan. MEDIA ADVISORY: GOVERNMENT'S ANNOUNCEMENT ON NISSAN LED VEHICLE-TO-GRID IUK WINNING PROJECT, February 2018. URL https://uk.nissannews.com/en-GB/releases/release-426218103#.

[77] Nissan. Nissan, Enel and Nuvve operate world's first fully commercial vehicle-to-grid hub in Denmark, August 2016. URL https://europe.nissannews.com/en-GB/releases/release-149186.

[78] Enel. ENEL ENERGIA, NISSAN ITALIA AND IIT JOIN FORCES FOR THE DEVELOPMENT OF ELECTRIC MOBILITY - enel.com, May 2017. URL https://www.enel.com/media/press/d/2017/05/enel-energia-nissan-italia-and-iit-join-forces-for-the-development-of-electric-mobility.

[79] Nissan. Nissan LEAF helps to power company's North American facilities with new charging technology - Nissan Online Newsroom, November 2018. URL https://nissannews.com/en-US/nissan/usa/releases/nissan-leaf-helps-to-power-company-s-north-american-facilities-with-new-charging-technology.

[80] N. B. Arias, S. Hashemi, P. B. Andersen, C. Træholt, and R. Romero. V2g enabled EVs providing frequency containment reserves: Field results. In *2018 IEEE International Conference on Industrial Technology (ICIT)*, pages 1814–1819, February 2018. doi: 10.1109/ICIT.2018.8352459.

[81] Seev4-City. Operational Pilots, Interreg VB North Sea Region Programme, December 2018. URL https://northsearegion.eu/seev4-city/operational-pilots/.

[82] Jedlix. The Nr. 1 Smart Charging App, 2019. URL https://jedlix.com/en/.

[83] Mart van der Kam and Wilfried van Sark. Smart charging of electric vehicles with photovoltaic power and vehicle-to-grid technology in a microgrid; a case study. *Applied Energy*, 152:20–30, August 2015. ISSN 0306-2619. doi: 10.1016/j.apenergy.2015.04.092. URL http://www.sciencedirect.com/science/article/pii/S0306261915005553.

[84] Wilfried van Sark. Smart Solar Charging: the role of photovoltaics in the sharing economy, September 2017. URL http://smartsolarcharging.eu/wp-content/uploads/sites/274/2017/10/vanSark-SSC-EUPVSEC33.pdf.

[85] Franziska Schmalfuß, Claudia Mair, Susen Döbelt, Bettina Kämpfe, Ramona Wüstemann, Josef F. Krems, and Andreas Keinath. User responses to a smart charging system in Germany: Battery electric vehicle driver motivation, attitudes and acceptance. *Energy Research & Social Science*, 9:60–71, September 2015. ISSN 2214-6296. doi: 10.1016/j.erss.2015.08.019. URL http://www.sciencedirect.com/science/article/pii/S2214629615300426.

[86] Christian Will and Alexander Schuller. Understanding user acceptance factors of electric vehicle smart charging. *Transportation Research Part C: Emerging Technologies*, 71:198–214, October 2016. ISSN 0968-090X. doi: 10.1016/j.trc.2016.07.006. URL http://www.sciencedirect.com/science/article/pii/S0968090X16301127.

[87] European Parliament and Council. Directive (EU) 2019/944 on common rules for the internal market for electricity and amending Directive 2012/27/EU. *Official Journal of the European Union*, L 158/125, June 2019. URL https://eur-lex.europa.eu/eli/dir/2019/944/oj.

[88] C. Latinopoulos, A. Sivakumar, and J. W. Polak. Response of electric vehicle drivers to dynamic pricing of parking and charging services: Risky choice in early reservations. *Transportation Research Part C: Emerging Technologies*, 80:175–189, July 2017. ISSN 0968-090X. doi: 10.1016/j.trc.2017.04.008. URL http://www.sciencedirect.com/science/article/pii/S0968090X17301134.

[89] Nicolò Daina, Aruna Sivakumar, and John W. Polak. Modelling electric vehicles use: a survey on the methods. *Renewable and Sustainable Energy Reviews*, 68:447–460, February 2017. ISSN 1364-0321. doi: 10.1016/j.rser.2016.10.005. URL http://www.sciencedirect.com/science/article/pii/S1364032116306566.

[90] J. S. Vardakas, N. Zorba, and C. V. Verikoukis. A Survey on Demand Response Programs in Smart Grids: Pricing Methods and Optimization Algorithms. *IEEE Communications Surveys Tutorials*, 17(1):152–178, 2015. ISSN 1553-877X. doi: 10.1109/COMST.2014.2341586.

[91] John Brady and Margaret O'Mahony. Modelling charging profiles of electric vehicles based on real-world electric vehicle charging data. *Sustainable Cities and Society*, 26:203–216, October 2016. ISSN 2210-6707. doi: 10.1016/j.scs.2016.06.014. URL http://www.sciencedirect.com/science/article/pii/S221067071630124X.

[92] A. P. Robinson, P. T. Blythe, M. C. Bell, Y. Hübner, and G. A. Hill. Analysis of electric vehicle driver recharging demand profiles and subsequent impacts on the carbon content of electric vehicle trips. *Energy Policy*, 61:337–348, October 2013. ISSN 0301-4215. doi: 10.1016/j.enpol.2013.05.074. URL http://www.sciencedirect.com/science/article/pii/S0301421513004266.

[93] Chioke B. Harris and Michael E. Webber. An empirically-validated methodology to simulate electricity demand for electric vehicle charging. *Applied Energy*, 126:172–181, August 2014. ISSN 0306-2619. doi: 10.1016/j.apenergy.2014.03.078. URL http://www.sciencedirect.com/science/article/pii/S0306261914003183.

[94] K. Clement-Nyns, E. Haesen, and J. Driesen. The Impact of Charging Plug-In Hybrid Electric Vehicles on a Residential Distribution Grid. *IEEE Transactions on Power Systems*, 25(1):371–380, February 2010. ISSN 0885-8950. doi: 10.1109/TPWRS.2009.2036481.

[95] Filipe Soares, Joao Abel Lopes, Pedro Almeida, C Moreira, and L Seca. A stochastic model to simulate electric vehicles motion and quantify the energy required from the grid. In *17th Power Systems Computation Conference*, Stockholm, Sweden, August 2011.

[96] L. Knapen, B. Kochan, T. Bellemans, D. Janssens, and G. Wets. Activity based models for countrywide electric vehicle power demand calculation. In *2011 IEEE First International Workshop on Smart Grid Modeling and Simulation (SGMS)*, pages 13–18, October 2011. doi: 10.1109/SGMS.2011.6089019.

[97] Nicolò Daina, Aruna Sivakumar, and John W. Polak. Electric vehicle charging choices: Modelling and implications for smart charging services. *Transportation Research Part C: Emerging Technologies*, 81:36–56, August 2017. ISSN 0968-090X. doi: 10.1016/j.trc.2017.05.006. URL http://www.sciencedirect.com/science/article/pii/S0968090X17301365.

[98] Mobashwir Khan and Kara M. Kockelman. Predicting the market potential of plug-in electric vehicles using multiday GPS data. *Energy Policy*, 46:225–233, July 2012. ISSN 0301-4215. doi: 10.1016/j.enpol.2012.03.055. URL http://www.sciencedirect.com/science/article/pii/S0301421512002601.

[99] Jarod C. Kelly, Jason S. MacDonald, and Gregory A. Keoleian. Time-dependent plug-in hybrid electric vehicle charging based on national driving patterns and demographics. *Applied Energy*, 94:395–405, June 2012. ISSN 0306-2619. doi: 10.1016/j.apenergy.2012.02.001. URL http://www.sciencedirect.com/science/article/pii/S0306261912000931.

[100] J. A. P. Lopes, F. J. Soares, and P. M. R. Almeida. Integration of Electric Vehicles in the Electric Power System. *Proceedings of the IEEE*, 99(1):168–183, January 2011. ISSN 0018-9219. doi: 10.1109/JPROC.2010.2066250.

[101] T. Zhang, C. Chu, and R. Gadh. A two-tier energy management system for smart electric vehicle charging in UCLA: A Solar-To-Vehicle (S2v) case study. In *2016 IEEE Innovative Smart Grid Technologies - Asia (ISGT-Asia)*, pages 288–293, November 2016. doi: 10.1109/ISGT-Asia.2016.7796400.

[102] E. Sortomme and M. A. El-Sharkawi. Optimal Scheduling of Vehicle-to-Grid Energy and Ancillary Services. *IEEE Transactions on Smart Grid*, 3(1):351–359, March 2012. ISSN 1949-3053. doi: 10.1109/TSG.2011.2164099.

[103] P. Richardson, D. Flynn, and A. Keane. Optimal Charging of Electric Vehicles in Low-Voltage Distribution Systems. *IEEE Transactions on Power Systems*, 27(1):268–279, February 2012. ISSN 0885-8950. doi: 10.1109/TPWRS.2011.2158247.

[104] Nikolaos G. Paterakis and Madeleine Gibescu. A methodology to generate power profiles of electric vehicle parking lots under different operational strategies. *Applied Energy*, 173:111–123, July 2016. ISSN 0306-2619. doi: 10.1016/j.apenergy.2016.04.024. URL http://www.sciencedirect.com/science/article/pii/S0306261916304743.

[105] K. Mets, T. Verschueren, W. Haerick, C. Develder, and F. De Turck. Optimizing smart energy control strategies for plug-in hybrid electric vehicle charging. In *2010 IEEE/IFIP Network Operations and Management Symposium Workshops*, pages 293–299, April 2010. doi: 10.1109/NOMSW.2010.5486561.

[106] Jamil Jannati and Daryoosh Nazarpour. Optimal energy management of the smart parking lot under demand response program in the presence of the electrolyser and fuel cell as hydrogen storage system. *Energy Conversion and Management*, 138:659–669, April 2017. ISSN 0196-8904. doi: 10.1016/j.enconman.2017.02.030. URL http://www.sciencedirect.com/science/article/pii/S019689041730136X.

[107] A. Brooks, E. Lu, D. Reicher, C. Spirakis, and B. Weihl. Demand Dispatch. *IEEE Power and Energy Magazine*, 8(3):20–29, May 2010. ISSN 1540-7977. doi: 10.1109/MPE.2010.936349.

[108] Y. Cao, S. Tang, C. Li, P. Zhang, Y. Tan, Z. Zhang, and J. Li. An Optimized EV Charging Model Considering TOU Price and SOC Curve. *IEEE Transactions on Smart Grid*, 3(1):388–393, March 2012. ISSN 1949-3053. doi: 10.1109/TSG.2011.2159630.

[109] L. Chen, C. Y. Chung, Y. Nie, and R. Yu. Modeling and optimization of electric vehicle charging load in a parking lot. In *2013 IEEE PES Asia-Pacific Power and Energy Engineering Conference (APPEEC)*, pages 1–5, December 2013. doi: 10.1109/APPEEC.2013.6837301.

[110] Sulabh Sachan and Nadia Adnan. Stochastic charging of electric vehicles in smart power distribution grids. *Sustainable Cities and Society*, 40:91–100, July 2018. ISSN 2210-6707. doi: 10.1016/j.scs.2018.03. 031. URL http://www.sciencedirect.com/science/article/pii/S221067071830338X.

[111] S. Deilami, A. S. Masoum, P. S. Moses, and M. A. S. Masoum. Real-Time Coordination of Plug-In Electric Vehicle Charging in Smart Grids to Minimize Power Losses and Improve Voltage Profile. *IEEE Transactions on Smart Grid*, 2(3):456–467, September 2011. ISSN 1949-3053. doi: 10.1109/TSG.2011.2159816.

[112] Abdul Rauf Bhatti, Zainal Salam, Mohd Junaidi Bin Abdul Aziz, Kong Pui Yee, and Ratil H. Ashique. Electric vehicles charging using photovoltaic: Status and technological review. *Renewable and Sustainable Energy Reviews*, 54:34–47, February 2016. ISSN 13640321. doi: 10.1016/j.rser.2015.09.091. URL http://linkinghub.elsevier.com/retrieve/pii/S1364032115010618.

[113] Bunyamin Yagcitekin and Mehmet Uzunoglu. A double-layer smart charging strategy of electric vehicles taking routing and charge scheduling into account. *Applied Energy*, 167:407–419, April 2016. ISSN 0306-2619. doi: 10.1016/j.apenergy.2015.09.040. URL http://www.sciencedirect.com/science/article/pii/S0306261915011101.

[114] Alberto Bemporad and Manfred Morari. Robust model predictive control: A survey. In A. Garulli and A. Tesi, editors, *Robustness in identification and control*, Lecture Notes in Control and Information Sciences, pages 207–226. Springer London, 1999. ISBN 978-1-84628-538-7.

[115] I. Sarantis, F. Alavi, and B. De Schutter. Optimal power scheduling of fuel-cell-car-based microgrids. In *2017 IEEE 56th Annual Conference on Decision and Control (CDC)*, pages 5062–5067, December 2017. doi: 10.1109/CDC.2017.8264409.

[116] T. Ma, A. Mohamed, and O. Mohammed. Optimal charging of plug-in electric vehicles for a car park infrastructure. In *2012 IEEE Industry Applications Society Annual Meeting*, pages 1–8, October 2012. doi: 10.1109/IAS.2012.6374035.

[117] Saber Falahati, Seyed Abbas Taher, and Mohammad Shahidehpour. A new smart charging method for EVs for frequency control of smart grid. *International Journal of Electrical Power & Energy Systems*, 83:458–469, December 2016. ISSN 0142-0615. doi: 10.1016/j.ijepes.2016.04.039. URL http://www.sciencedirect.com/science/article/pii/S0142061516307244.

[118] Samy Faddel, Ali T. Al-Awami, and M. A. Abido. Fuzzy Optimization for the Operation of Electric Vehicle Parking Lots. *Electric Power Systems Research*, 145:166–174, April 2017. ISSN 0378-7796. doi: 10.1016/j.epsr.2017.01.008. URL http://www.sciencedirect.com/science/article/pii/S0378779617300081.

[119] Y. He, B. Venkatesh, and L. Guan. Optimal Scheduling for Charging and Discharging of Electric Vehicles. *IEEE Transactions on Smart Grid*, 3(3):1095–1105, September 2012. ISSN 1949-3053. doi: 10.1109/TSG.2011.2173507.

[120] L. Gan, U. Topcu, and S. H. Low. Optimal decentralized protocol for electric vehicle charging. *IEEE Transactions on Power Systems*, 28(2):940–951, May 2013. ISSN 0885-8950. doi: 10.1109/TPWRS.2012.2210288.

[121] Z. Ma, D. S. Callaway, and I. A. Hiskens. Decentralized Charging Control of Large Populations of Plug-in Electric Vehicles. *IEEE Transactions on Control Systems Technology*, 21(1):67–78, January 2013. ISSN 1063-6536. doi: 10.1109/TCST.2011.2174059.

[122] Canadian Solar (USA) Inc. Standard Solar Panels CS6p-P | CS6k-P | CS6k-M | Canadian Solar, November 2018. URL https://www.canadiansolar.com/solar-panels/standard.html.

[123] G. R. Walker and P. C. Sernia. Cascaded DC-DC converter connection of photovoltaic modules. In *2002 IEEE 33rd Annual IEEE Power Electronics Specialists Conference. Proceedings (Cat. No.02CH37289)*, volume 1, pages 24–29 vol.1, June 2002. doi: 10.1109/PSEC.2002.1023842.

[124] SolarEdge. Application Note: SolarEdge Fxed String Voltage, Concept of Operation, February 2019. URL https://www.solaredge.com/sites/default/files/se_application_fixed_string_voltage.pdf.

[125] Canadian Solar. Three Phase String Inverter 50-66 kW, August 2017. URL `https://s1.solacity.com/docs/CSI/CS_Datasheet_Three-Phase_50-66K_V2.0_E2_NA.pdf`.

[126] Wouter Knap. *Horizon at station Cabauw*. PANGAEA, 2007. doi: 10.1594/PANGAEA.669511. URL `https://doi.org/10.1594/PANGAEA.669511`.

[127] S. Wilcox and W. Marion. Users Manual for TMY3 Data Sets (Revised). Technical Report NREL/TP-581-43156, National Renewable Energy Lab. (NREL), Golden, CO (United States), May 2008. URL `https://www.osti.gov/biblio/928611`.

[128] J. S. Stein, W. F. Holmgren, J. Forbess, and C. W. Hansen. PVLIB: Open source photovoltaic performance modeling functions for Matlab and Python. In *2016 IEEE 43rd Photovoltaic Specialists Conference (PVSC)*, pages 3425–3430. 2016 IEEE 43rd Photovoltaic Specialists Conference (PVSC), June 2016. doi: 10.1109/PVSC.2016.7750303.

[129] Fritz Kasten and Andrew T. Young. Revised optical air mass tables and approximation formula. *Applied Optics*, 28(22):4735–4738, November 1989. ISSN 2155-3165. doi: 10.1364/AO.28.004735. URL `https://www.osapublishing.org/ao/abstract.cfm?uri=ao-28-22-4735`.

[130] Richard Perez, Pierre Ineichen, Robert Seals, Joseph Michalsky, and Ronald Stewart. Modeling daylight availability and irradiance components from direct and global irradiance. *Solar Energy*, 44(5):271–289, January 1990. ISSN 0038-092X. doi: 10.1016/0038-092X(90)90055-H. URL `http://www.sciencedirect.com/science/article/pii/0038092X9090055H`.

[131] P.G. Loutzenhiser, H. Manz, C. Felsmann, P.A. Strachan, T. Frank, and G.M. Maxwell. Empirical validation of models to compute solar irradiance on inclined surfaces for building energy simulation. *Solar Energy*, 81(2):254–267, February 2007. ISSN 0038092X. doi: 10.1016/j.solener.2006.03.009. URL `http://linkinghub.elsevier.com/retrieve/pii/S0038092X06000879`.

[132] H. Li, J. Harvey, and A. Kendall. Field measurement of albedo for different land cover materials and effects on thermal performance. *Building and Environment*, 59:536–546, January 2013. ISSN 0360-1323. doi: 10.1016/j.buildenv.2012.10.014. URL `http://www.sciencedirect.com/science/article/pii/S036013231200279X`.

[133] Jay A. Kratochvil, William Earl Boyson, and David L. King. Photovoltaic array performance model. Technical Report SAND2004-3535, 919131, Sandia National Laboratories, August 2004. URL `http://www.osti.gov/servlets/purl/919131-sca5ep/`.

[134] W. De Soto, S.A. Klein, and W.A. Beckman. Improvement and validation of a model for photovoltaic array performance. *Solar Energy*, 80(1):78–88, January 2006. ISSN 0038092X. doi: 10.1016/j.solener.2005.06.010. URL `http://linkinghub.elsevier.com/retrieve/pii/S0038092X05002410`.

[135] Ali Naci Celik and Nasır Acikgoz. Modelling and experimental verification of the operating current of mono-crystalline photovoltaic modules using four- and five-parameter models. *Applied Energy*, 84(1):1–15, January 2007. ISSN 0306-2619. doi: 10.1016/j.apenergy.2006.04.007. URL `http://www.sciencedirect.com/science/article/pii/S0306261906000511`.

[136] M. G. Villalva, J. R. Gazoli, and E. R. Filho. Comprehensive Approach to Modeling and Simulation of Photovoltaic Arrays. *IEEE Transactions on Power Electronics*, 24(5):1198–1208, May 2009. ISSN 0885-8993. doi: 10.1109/TPEL.2009.2013862.

[137] Mohammad Reza Maghami, Hashim Hizam, Chandima Gomes, Mohd Amran Radzi, Mohammad Ismael Rezadad, and Shahrooz Hajighorbani. Power loss due to soiling on solar panel: A review. *Renewable and Sustainable Energy Reviews*, 59:1307–1316, June 2016. ISSN 1364-0321. doi: 10.1016/j.rser.2016.01.044. URL `http://www.sciencedirect.com/science/article/pii/S1364032116000745`.

[138] Richard Perez, Sergey Kivalov, James Schlemmer, Karl Hemker, David Renné, and Thomas E. Hoff. Validation of short and medium term operational solar radiation forecasts in the US. *Solar Energy*, 84(12):2161–2172, December 2010. ISSN 0038-092X. doi: 10.1016/j.solener.2010.08.014. URL `http://www.sciencedirect.com/science/article/pii/S0038092X10002823`.

[139] Richard Perez, Elke Lorenz, Sophie Pelland, Mark Beauharnois, Glenn Van Knowe, Karl Hemker, Detlev Heinemann, Jan Remund, Stefan C. Müller, Wolfgang Traunmüller, Gerald Steinmauer, David Pozo, Jose A. Ruiz-Arias, Vicente Lara-Fanego, Lourdes Ramirez-Santigosa, Martin Gaston-Romero, and Luis M. Pomares. Comparison of numerical weather prediction solar irradiance forecasts in the US, Canada and Europe. *Solar Energy*, 94:305–326, August 2013. ISSN 0038-092X. doi: 10.1016/j.solener. 2013.05.005. URL http://www.sciencedirect.com/science/article/pii/S0038092X13001886.

[140] Pierre Ineichen and Richard Perez. A new airmass independent formulation for the Linke turbidity coefficient. *Solar Energy*, 73(3):151–157, September 2002. ISSN 0038-092X. doi: 10.1016/S0038-092X(02) 00045-2. URL http://www.sciencedirect.com/science/article/pii/S0038092X02000452.

[141] Stewart Dalzell. Boston-Logan International Airport 2016 Environmental Data Report. Technical Report EOEA #3247, Massachusetts Port Authority, Boston, MA, May 2018. URL http://www.massport.com/media/2817/2016_loganairport_edr_cd_.pdf.

[142] Jim Francfort. EV Project Data & Analytic Results, June 2014. URL https://www.energy.gov/sites/prod/files/2014/07/f18/vss137_francfort_2014_o.pdf.

[143] Elham Azadfar, Victor Sreeram, and David Harries. The investigation of the major factors influencing plug-in electric vehicle driving patterns and charging behaviour. *Renewable and Sustainable Energy Reviews*, 42:1065–1076, February 2015. ISSN 13640321. doi: 10.1016/j.rser.2014.10.058. URL http://linkinghub.elsevier.com/retrieve/pii/S1364032114008831.

[144] T. Ma and O. A. Mohammed. Optimal Charging of Plug-in Electric Vehicles for a Car-Park Infrastructure. *IEEE Transactions on Industry Applications*, 50(4):2323–2330, July 2014. ISSN 0093-9994. doi: 10.1109/TIA.2013.2296620.

[145] Mariz B. Arias and Sungwoo Bae. Electric vehicle charging demand forecasting model based on big data technologies. *Applied Energy*, 183:327–339, December 2016. ISSN 0306-2619. doi: 10.1016/j.apenergy. 2016.08.080. URL http://www.sciencedirect.com/science/article/pii/S0306261916311667.

[146] Netherlands Enterprise Agency. January 2019: Statistics Electric Vehicles and Charging in The Netherlands, February 2019. URL https://www.rvo.nl/file/statistics-electric-vehicles-and-charging-netherlands-and-including-january-2019.

[147] EV Database. Electric Vehicle Database, February 2019. URL https://ev-database.nl/.

[148] M. H. Amini and A. Islam. Allocation of electric vehicles' parking lots in distribution network. In *ISGT 2014*, pages 1–5, February 2014. doi: 10.1109/ISGT.2014.6816429.

[149] Louise Bunce, Margaret Harris, and Mark Burgess. Charge up then charge out? Drivers' perceptions and experiences of electric vehicles in the UK. *Transportation Research Part A: Policy and Practice*, 59:278–287, January 2014. ISSN 0965-8564. doi: 10.1016/j.tra.2013.12.001. URL http://www.sciencedirect.com/science/article/pii/S0965856413002395.

[150] Thomas Franke and Josef F. Krems. Understanding charging behaviour of electric vehicle users. *Transportation Research Part F: Traffic Psychology and Behaviour*, 21:75–89, November 2013. ISSN 13698478. doi: 10.1016/j.trf.2013.09.002. URL http://linkinghub.elsevier.com/retrieve/pii/S1369847813000776.

[151] Kaiyuan Li and King Jet Tseng. Energy efficiency of lithium-ion battery used as energy storage devices in micro-grid. In *IECON 2015 - 41st Annual Conference of the IEEE Industrial Electronics Society*, pages 005235–005240, Yokohama, November 2015. IEEE. ISBN 978-1-4799-1762-4. doi: 10.1109/IECON.2015. 7392923. URL http://ieeexplore.ieee.org/document/7392923/.

[152] Elpiniki Apostolaki-Iosifidou, Paul Codani, and Willett Kempton. Measurement of power loss during electric vehicle charging and discharging. *Energy*, 127:730–742, May 2017. ISSN 0360-5442. doi: 10.1016/j.energy.2017.03.015. URL http://www.sciencedirect.com/science/article/pii/S0360544217303730.

[153] Siemens. SINAMICS DCP: The innovative DC-DC converter for industry and smart grid applications, 2016. URL https://w3app.siemens.com/mcms/infocenter/dokumentencenter/ld/InfocenterLanguagePacks/sinamics-dcp/sinamics-dcp-en.pdf.

[154] N. K. Noyanbayev, A. J. Forsyth, and T. Feehally. Efficiency analysis for a grid-connected battery energy storage system. *Materials Today: Proceedings*, 5(11, Part 1):22811–22818, January 2018. ISSN 2214-7853. doi: 10.1016/j.matpr.2018.07.095. URL http://www.sciencedirect.com/science/article/pii/S2214785318318947.

[155] Michael Schimpe, Maik Naumann, Nam Truong, Holger C. Hesse, Shriram Santhanagopalan, Aron Saxon, and Andreas Jossen. Energy efficiency evaluation of a stationary lithium-ion battery container storage system via electro-thermal modeling and detailed component analysis. *Applied Energy*, 210:211–229, January 2018. ISSN 0306-2619. doi: 10.1016/j.apenergy.2017.10.129. URL http://www.sciencedirect.com/science/article/pii/S0306261917315696.

[156] Bruce R. Kinzey, Michael Myer, Michael P. Royer, and Greg P. Sullivan. Use of Occupancy Sensors in LED Parking Lot and Garage Applications: Early Experiences. Technical Report PNNL-21923, Pacific Northwest National Lab. (PNNL), Richland, WA (United States), November 2012. URL https://www.osti.gov/biblio/1057365.

[157] NEN. NEN 2443: Parkeergarages en parkeerterreinen. Technical report, Nederlands Normalisatie-instituut, March 2013. URL https://www.nen.nl/NEN-Shop/Bouwnieuwsberichten/NEN-2443-Parkeergarages-en-parkeerterreinen.htm.

[158] Paul Morgan Pattison, Monica Hansen, and Jeffrey Y. Tsao. LED lighting efficacy: Status and directions. *Comptes Rendus Physique*, 19(3):134–145, March 2018. ISSN 1631-0705. doi: 10.1016/j.crhy.2017.10.013. URL http://www.sciencedirect.com/science/article/pii/S1631070517300932.

[159] Paul J. Littlefair. The luminous efficacy of daylight: a review. *Lighting Research & Technology*, 17(4):162–182, December 1985. ISSN 0024-3426. doi: 10.1177/14771535850170040401. URL https://doi.org/10.1177/14771535850170040401.

[160] A. Bemporad, W. P. M. H. Heemels, and B. De Schutter. On hybrid systems and closed-loop MPC systems. *IEEE Transactions on Automatic Control*, 47(5):863–869, May 2002. ISSN 0018-9286. doi: 10.1109/TAC.2002.1000287.

[161] Samira S. Farahani, Sadegh Soudjani, Rupak Majumdar, and Carlos Ocampo-Martinez. Formal controller synthesis for wastewater systems with signal temporal logic constraints: The Barcelona case study. *Journal of Process Control*, 69:179–191, September 2018. ISSN 0959-1524. doi: 10.1016/j.jprocont.2018.05.011. URL http://www.sciencedirect.com/science/article/pii/S0959152418301148.

[162] D. Q. Mayne, J. B. Rawlings, C. V. Rao, and P. O. M. Scokaert. Constrained model predictive control: Stability and optimality. *Automatica*, 36(6):789–814, June 2000. ISSN 0005-1098. doi: 10.1016/S0005-1098(99)00214-9. URL http://www.sciencedirect.com/science/article/pii/S0005109899002149.

[163] Alberto Bemporad and Manfred Morari. Control of systems integrating logic, dynamics, and constraints. *Automatica*, 35(3):407–427, March 1999. ISSN 0005-1098. doi: 10.1016/S0005-1098(98)00178-2. URL http://www.sciencedirect.com/science/article/pii/S0005109898001782.

[164] Gurobi Optimization, LLC. Gurobi Optimizer, 2018. URL http://www.gurobi.com.

[165] A. Bemporad, F. Borrelli, and M. Morari. Model predictive control based on linear programming - the explicit solution. *IEEE Transactions on Automatic Control*, 47(12):1974–1985, December 2002. ISSN 0018-9286, 1558-2523. doi: 10.1109/TAC.2002.805688. URL http://ieeexplore.ieee.org/document/1137550/.

[166] P. J. Campo and M. Morari. Robust Model Predictive Control. In *1987 American Control Conference*, pages 1021–1026, June 1987. doi: 10.23919/ACC.1987.4789462.

[167] Vivek Dua and Efstratios N. Pistikopoulos. An Algorithm for the Solution of Multiparametric Mixed Integer Linear Programming Problems. *Annals of Operations Research*, 99(1):123–139, December 2000. ISSN 1572-9338. doi: 10.1023/A:1019241000636. URL https://doi.org/10.1023/A: 1019241000636.

[168] S. S. Farahani, Z. Lukszo, T. Keviczky, B. De Schutter, and R. M. Murray. Robust model predictive control for an uncertain smart thermal grid. In *2016 European Control Conference (ECC)*, pages 1195–1200, June 2016. doi: 10.1109/ECC.2016.7810452.

[169] Farid Alavi, Esther Park Lee, Nathan van de Wouw, Bart De Schutter, and Zofia Lukszo. Fuel cell cars in a microgrid for synergies between hydrogen and electricity networks. *Applied Energy*, 192:296–304, April 2017. ISSN 0306-2619. doi: 10.1016/j.apenergy.2016.10.084. URL http://www.sciencedirect. com/science/article/pii/S0306261916315288.

[170] M. N. Zeilinger, M. Morari, and C. N. Jones. Soft Constrained Model Predictive Control With Robust Stability Guarantees. *IEEE Transactions on Automatic Control*, 59(5):1190–1202, May 2014. ISSN 0018-9286. doi: 10.1109/TAC.2014.2304371.

[171] G. E. P. Box. Robustness in the Strategy of Scientific Model Building. In ROBERT L. Launer and GRAHAM N. Wilkinson, editors, *Robustness in Statistics*, pages 201–236. Academic Press, January 1979. ISBN 9780124381506. doi: 10.1016/B978-0-12-438150-6.50018-2. URL http://www.sciencedirect.com/ science/article/pii/B9780124381506500182.